



POLITECNICO DI MILANO

Facoltà di Ingegneria Industriale
Corso di Laurea Magistrale in Ingegneria Spaziale

Tesi Di Laurea

Phase-B Thermal Control Subsystem Design for the ESEO Satellite

Laureando

Michel Jean-Louis Chris Poucet

Matricola 735515

Relatore

Prof. Alfonso Niro

Tutor Aziendale

Ing. Marco Molina

Anno Accademico 2011/2012

Contents

Contents	I
List of Figures	IV
Acknowledgements	i
Abstract	iii
Riassunto	iv
1 Introduction	1
2 ESEO Project	3
1 What is ESEO	3
1.1 ESEO Project Network	3
2 Mission Objectives	4
2.1 Mission Requirements & Technical Data	6
3 ESEO Mission Phase & Activities	7
3.1 Mission Phases	7
4 Spacecraft Operational Activities	10
5 ESEO Mission Analysis	12
5.1 Launch Window	12
5.2 Target Orbits	12
3 Thermal Control Subsystem	13
1 The TCS Subsystem	13

2	Thermal Environment	14
3	Relationship to Other Subsystems	15
4	Thermal Analysis	16
1	Lumped Thermal Modelling	16
2	MiniTAN	18
3	ESATAN-TMS	21
3.1	ESATAN Modules	22
3.2	ESATAN Results	24
5	ESEO Thermal Model Development	25
1	ESEO Model - Geometry	26
1.1	External Geometry	26
1.2	Internal Geometry	28
2	ESEO Model - Optical Data & Nodal Dispostion	30
2.1	Optical Data	30
2.2	Nodal Disposition	31
3	ESEO Model - Thermal Conductance	33
3.1	Through-Thickness Conductance	33
3.2	Intra-Shell Conductors	33
3.3	Inter-Shell Conductors	33
3.4	Radiative Conductance	36
4	Boundary Conditions - Internal Heat Dissipation	37
5	Radiative Case	39
6	Results & Margins	42
1	Creating Analyses Case and Result Files	42
2	ESATAN Results Tool	46
3	First Analysis - Single Modes	47
3.1	Sun-Pointing Heat Results	48
3.2	Nadir-Pointing Heat Results	51
3.3	Hot & Cold Case	54

4	Operative Case	66
4.1	Radiative Results	66
4.2	Passive Thermal Results	70
4.3	Heater Modelling	80
4.4	Active Thermal Results	81
5	Margin Philosophy	86
6	Margin Results	87
7	Phase-A Minitan Results vs. Phase-B ESATAN Results	90
7	Conclusions	93
	Bibliography	95

List of Figures

2.1	ESEO Teams	4
2.2	Operational Modes	10
2.3	Operative Phase - Cyclic Modes	11
2.4	Keplerian Parameters for the Operative Orbit	12
4.1	Nodal Discretization	17
4.2	MiniTAN Input File - Node Example	20
4.3	MiniTAN Input File - Conductors	20
4.4	ESATAN Geometry Definition (L), Orbit (C) & Thermal Results (R)	21
4.5	ESATAN GEOMETRY DEFINITION	23
5.1	ESEO Final Design	25
5.2	ESEO External Panel Properties	27
5.3	ESEO External Panel Properties	28
5.4	ESEO Component Properties	29
5.5	ESEO Geometry	30
5.6	ESEO External Optical Properties	30
5.7	ESEO Nodal Breakdown	31
5.8	ESEO Nodal Breakdown	32
5.9	ESEO Fillers	34
5.10	ESEO Deployment System	34
5.11	Inter-Shell Conductivities	35
5.12	Possible Boundary Conditions	37
5.13	Boundary Conditions	38

5.14	Dissipated Power Modes 1-13	38
5.15	Dissipated Power Modes 14-26	39
5.16	Orbital Parameters	40
5.17	Radiative Case	41
6.1	Thermal Model Analyses Case	44
6.2	Thermal Model Analyses Case	45
6.3	Thermal Model Analyses Case	46
6.4	ESATAN Results Tools - Main Window	46
6.5	ESATAN Results Tools - Modes & Comonents	47
6.6	Node 10 Heat Results	48
6.7	Node 20 Heat Results	48
6.8	Node 200 Heat Results	48
6.9	Node 30 Heat Results	49
6.10	Node 300 Heat Results	49
6.11	Node 40 Heat Results	49
6.12	Node 50 Heat Results	49
6.13	Node 60 Heat Results	50
6.14	Node 70 Heat Results	50
6.15	Node 80 Heat Results	50
6.16	Node 90 Heat Results	50
6.17	Node 10 Heat Results	51
6.18	Node 20 Heat Results	51
6.19	Node 200 Heat Results	51
6.20	Node 30 Heat Results	52
6.21	Node 300 Heat Results	52
6.22	Node 40 Heat Results	52
6.23	Node 50 Heat Results	52
6.24	Node 60 Heat Results	53
6.25	Node 70 Heat Results	53
6.26	Node 80 Heat Results	53
6.27	Node 90 Heat Results	53

6.28	Hot Case - Sun Pointing Results 1	55
6.29	Hot Case - Sun Pointing Results 2	56
6.30	Cold Case - Sun Pointing Results 1	57
6.31	Cold Case - Sun Pointing Results 2	58
6.32	Hot Case - Nadir Pointing Results 1	59
6.33	Hot Case - Nadir Pointing Results 2	60
6.34	Cold Case - Nadir Pointing Results 1	61
6.35	Cold Case - Nadir Pointing Results 2	62
6.36	Node 10 Heat Results	67
6.37	Node 20 Heat Results	67
6.38	Node 200 Heat Results	67
6.39	Node 30 Heat Results	67
6.40	Node 300 Heat Results	68
6.41	Node 40 Heat Results	68
6.42	Node 50 Heat Results	68
6.43	Node 60 Heat Results	69
6.44	Node 70 Heat Results	69
6.45	Node 80 Heat Results	69
6.46	Node 90 Heat Results	69
6.47	Passive Operative Hot Case Results 1	71
6.48	Passive Operative Hot Case Results 2	72
6.49	Passive Operative Cold Case Results 1	73
6.50	Passive Operative Cold Case Results 2	74
6.51	EPS Batteries (A) & Gyro Box (B) Heat Results	76
6.52	Reaction Wheels 1-4 (A) & Reaction Wheel +Y(B) Heat Results	77
6.53	EPS PEB (A) & OBDH (B) Heat Results	78
6.54	Magnetometer 1 & 2 (A) & Ucam (B) Heat Results	79
6.55	EPS Battery Heater	81
6.56	EPS Batteries (A) & Gyro Box (B) Heat Results	82
6.57	Reaction Wheels 1-4 (A) & Reaction Wheel +Y(B) Heat Results	83
6.58	EPS PEB (A) & OBDH (B) Heat Results	84

6.59 Magnetometer 1 & 2 (A) & Ucam (B) Heat Results	85
6.60 EPS Batteries Nominal Results	87
6.61 EPS Batteries 90% Margin (T) & 110% Margin (B) Results	88
6.62 SYSTEMA(A) & ESATAN (B) NODE 10 Heat Flux Results	90
6.63 MiniTAN (A) & ESATAN (B) EPS Batteries Thermal Results	91
6.64 MiniTAN (A) & ESATAN (B) Reaction Wheel Thermal Results	91

Acknowledgements

With this huge goal ends an entire cycle of my life which has formed me and made me who I am. Along the road which has led me to this destination there have been many obstacles which I was able to overcome thanks to those close to me. For this I would like to thank my parents André & Yvette who have always supported me and allowed me to make my own free choices. Together with them I thank my two older brothers Philippe and Christophe in whose footsteps I walk proud, hoping only to achieve a part of what they have done.

I would like to thank Barbara, Roberto and the whole Ferrarin family who were always willing enough to allow me into their homes and who were always there for a chat whenever times were difficult, or even after periods where I had not been very present.

I thank Prof. Niro, Prof. Bernelli and Ing. Molina for helping in completing this final dissertation and for their patience. I would like to thank Professoressa Finzi who always found a way to put a smile on your face even when some exams didn't go as expected. Together with her I have to thank all the Professors of the Politecnico di Milano with whom I may not always have agreed but each and everyone has added a piece into this final puzzle which brought to my degree.

Thanks to Manu, Paolo, Ricky, Dimpo, Ottone, Spino, Willy, Prove and Maio who have been my buddies in all these tough years at PoliMi. Thank you Joakim, Germano, Giuseppe and Cata who remained in touch with me even though the distance.

I must thank all the guys at Marvy who have kept me company in all those mornings I did not feel like going to lesson and who have accompanied me through the years. Thanks to them I was able to meet a person to whom I am most thankful.

Giulia, Babe, Orange! Thank you! I doubt I would've made it until the end had you not been there. You inspired me to give more and you accompanied me in those long nights before exams together with a cup of tea and a Redbull. It is my duty now to accompany you to this same goal as mine as I owe it to you for all you have done. Thank you babe, and thank you to your family Gianpaolo, Roberta and Francesco who have allowed me so many times to come into their home.

I believe that the most important thing is not what I receive at the end of this voyage but what I have learned and the people I have met along the way. These are the memories and experiences which I will bring into my future and allow me to go forward.

Thank You All

Michel Poucet

Abstract

The objective of this thesis work is the Phase-B design of the thermal control subsystem on the ESEO satellite. The ESEO project is a mission created by the Education Satellite programme of the European Space Agency (ESA). The ESEO project is an opportunity created by ESA to allow students from various European universities to collaborate and get a hands on experience on developing and doing actual feasibility studies on a satellite.

The initial part of this work is relevant to the nature of the ESEO project and gives a brief description of its requirements, mission phases and payloads. Afterwards the mathematical model used for the thermal model are studied because these are the foundations of the thermal softwares used to model ESEO. The two main tools used for the creation of the thermal model are MiniTAN and ESATAN with its important radiative module ESARAD.

The second phase consists of the hypothesis taken and the materials and data used in order to create a proper model. The design steps are described and the satellite is then inserted into its orbit so as to create a simulation of the actual thermal heat fluxes it is exposed to.

Once properly designed the results were analyzed and the model was adjusted in matter to satisfy all thermal requirements. The model was then margined and the results listed.

Riassunto

In questo lavoro di tesi verrà discussa la modellazione e la progettazione della Fase-B del sottosistema termico del progetto ESEO. Quest'ultimo è una missione dell'Education Satellite Program dell'ESA atta a far svolgere a studenti universitari le analisi di fattibilità, la modellazione, la progettazione e la costruzione di un satellite. L'ESA ha dunque effettuato il bando per trovare il primary contractor per la gestione e lo sviluppo di questo progetto, bando che è stato vinto dalla CGSpace.

Prima di procedere alla descrizione del sottosistema termico si illustrerà lo stato globale del progetto ESEO insieme a tutte le varie caratteristiche dei diversi sottosistemi e alle fasi di missione. Il satellite ESEO è un satellite polare ad orbita bassa con a bordo diversi payload per andare a soddisfare tre obiettivi.

Il primo è quello di effettuare delle fotografie terrestri e di altri corpi celesti, il che sarà ottenuto mediante una μ -cam. Il secondo è misurare le radiazioni che un satellite incontra in un'orbita bassa terrestre (con un dosimetro chiamato Tritel-S) e rilevare le caratteristiche del plasma (utilizzando il Langmuir Probe, LMP). Il terzo invece è quello di testare nuove tecnologie per eventuali future missioni educative dell'ESA, più precisamente si tratta di un rilevatore di stelle e una ruota di reazione, che se validati verranno utilizzati nella missione sorella di ESEO, ESMO.

Per soddisfare tali scopi il satellite deve effettuare due tipi di assetto durante la sua vita operativa. Il primo, chiamato Nadir-Pointing, prevede l'asse z orientato verso il centro della Terra (ovvero Nadir), l'asse x allineato con il vettore velocità orbitale e l'asse y di conseguenza, essendo una terna destrorsa. Il secondo assetto viene invece chiamato Sun-Pointing e ha l'asse y rivolto verso il Sole, l'asse x verso il polo nord celeste e l'asse z di conseguenza (terna destrorsa).

Una volta noti i dettagli e i requisiti del progetto si è proceduto alla modellazione del sottosistema termico, continuando il lavoro effettuato dall'Ing. Canistro, che si è occupato del Phase-A design tramite il software MiniTAN. Per poter realizzare delle analisi più precise e creare un modello più rappresentativo è stato usato il solutore ESATAN che, analogamente a MiniTAN, si basa sulla modellazione a parametri concentrati.

Validato il solutore del modello, è stato possibile ricostruire il modello geometrico del satellite in ESATAN. Mentre con MiniTAN era necessario affidarsi ai calcoli effettuati dal sottosistemista termico, con l'uso dell'interfaccia grafica, si possono invece calcolare tutti i flussi termici del sottosistema termico in modo più preciso, modellando correttamente la geometria del satellite e inserendo i vari parametri termo-ottici (l'emissività, assorbività, proprietà del materiale e dissipazioni termiche). Le uniche incognite che rimangono sono le condizioni al contorno, più precisamente i parametri dell'orbita e dell'assetto del satellite.

Il modulo ESARAD all'interno di ESATAN, data l'orbita di riferimento, permette di calcolare i flussi termici provenienti dal sole, dalla terra e dagli scambi termici con lo spazio. Esso calcola anche tutti i fattori di vista interni che poi permettono di calcolare i flussi termici radiativi tra i vari componenti.

Come primo target per il dimensionamento del sottosistema termico si è deciso di modellare un controllo passivo. Le prime analisi sono state effettuate per trovare le fasi operative che corrispondono ai casi limite di temperatura massima e minima (hot & cold case). Successivamente si è deciso di osservare il comportamento termico del satellite durante la sua vita operativa. Essendo quest'ultima composta da diversi cicli di 28 orbite, si è scelto di prendere in considerazione 56 orbite in modo da trovare i componenti critici e vedere il comportamento termico del sistema.

Con i risultati ottenuti sono stati fatti degli interventi sul sottosistema termico in modo da migliorare i range di temperature ottenute nei vari componenti. Purtroppo i due assetti che il satellite effettua nel ciclo operativo creano due condizioni termiche molto differenti tra di loro pertanto non è possibile modellare un controllo termico di tipo passivo in quanto le batterie all'interno del satellite dispongono di un range termico molto limitato. E' stato dunque modellato un heater all'interno del sistema con una legge specifica che minimizza la potenza necessaria.

Utilizzando un'opportuna legge per l'heater è stato possibile creare un modello termico completo che soddisfi i range termici richiesti. Purtroppo non tutti i valori dei parametri utilizzati per il dimensionamento termico sono assoluti ma alcuni cambiano con la temperatura mentre altri variano attorno ad un valore medio. Pertanto è stato necessario marginare il modello termico variando le caratteristiche termiche del $\pm 10\%$ così da tenere conto di queste variazioni.

Queste due analisi hanno fornito risultati soddisfacenti per tutti i componenti in esame eccetto che per le batterie, sempre per il problema della limitata banda di temperature operative (0-15°C). Dal momento che tale limite non era superabile marginando il sistema, si è deciso di ritenere accettabile il modello termico siffatto mantenendo però il componente critico sotto osservazione nelle fasi successive del progetto (Fase C/D). Successivamente infatti, bisognerà modificare opportunamente il modello per crearne uno correlato ai dati ottenuti dai test sperimentali effettuati in camera termovuota. Non è stato però possibile effettuare quest'ultima fase poichè la CGSpace ha deciso di chiudere il progetto ESEO al termine della final review del Phase-B design per mancanza di fondi.

Chapter 1

Introduction

This dissertation project was created thanks to the collaboration between the Politecnico di Milano, the European Space Agency (ESA) and CGSpace. The ESEO project is an opportunity created by ESA to allow students from various European universities to collaborate and get a hands on experience on developing and doing actual feasibility studies on a satellite.

This work focuses on designing the Phase-B thermal model of the satellite ESEO. Previous Phase-A studies were done on the ESEO satellite which led to a reduced thermal model which was created in MiniTAN with various approximations. In this project the model was enlarged and remodelled in ESATAN in order to create a more complete thermal representation of the ESEO satellite. The model was then fully inserted into various scenarios giving different results. This entire project has been divided into the following chapters.

Chapter 2: ESEO Project This initial chapter describes the origin and development of the ESEO satellite and its current configuration. A general review of the satellite's requirements and technical data, including payloads, is given together with various details on mission phases, mission windows and operational activities.

Chapter 3: Thermal Control Subsystem This chapter describes what the thermal control subsystem (TCS) does and its importance. It further describes how every other subsystem is related to the TCS and how every action a subsystem does leads to a

reaction in the thermal subsystem. Together with this there is an explanation of what kind of different thermal environments and heat sources the satellite encounters during its operative lifetime and what responsibilities the TCS has.

Chapter 4: Thermal Analysis In this chapter the mathematical theories behind the ESATAN and MiniTAN softwares are explained. This consists in the lumped thermal model analysis. In this same chapter the mathematical solvers used for creating the thermal model are explained together with how the mathematical theories are used in them.

Chapter 5: Thermal Model Development Here we have an explanation of how our satellite was modeled together with all the approximation taken. Starting from the geometry and the thermo-optical characteristics the model is developed and subdivided into a rational discretization. All other thermal characteristics are also described and listed including intra and inter component conductivity.

Chapter 6: Results & Margin Various different models were made before achieving the final model. An initial passive model was used to calculate hot & cold case results. Which then lead to an operative life analysis and to an eventual active model. This model was then margined with two different philosophies. This chapter describes the various analyses and shows the various results and how they lead to the final active thermal model.

Chapter 7: Conclusion A brief analysis is done on the results and model obtained and they're reliability. Along with this is a brief description of the subsequent phases the ESEO project must go through.

Chapter 2

ESEO Project

1 What is ESEO

The European Student Earth Orbiter (ESEO) is a Low Earth Orbit micro-satellite mission. It is currently being developed by students of different European Universities as part of the ESA Education Office.

ESEO primary task will be to orbit the Earth whilst taking pictures, measuring radiation levels and testing technologies for future education satellite missions.

ESEO together with the ESMO (European Student Moon Orbiter) was created in order to provide students with valuable experience in space mission designs in order to fully develop their capabilities as future space system engineers.

ESEO is the third mission within ESA's Education programme using previous experiences gained with SSETI Express and YES2 tether and re-entry capsule experiment. At the present time about 100 students are actively involved in the ESEO project originating from 13 universities across all Europe.

ESEO satellite is being developed to be launched into Low Earth Orbit in 2012 and is candidate for launch with one of the VEGA VERTA flights.

1.1 ESEO Project Network

In order to organize and manage the ESEO project the ESA contracted Industrial System Prime Contractor (Carlo Gavazzi Space, CGS) to provide system-level and specialist

technical support to the university student teams during the execution of the project. The students obtain training and benefit from access to the CGS and ESA in-house expertise and can use Industry and ESTEC facilities for spacecraft assembly, integration and testing. The student teams are expected to provide most of the spacecraft subsystems, payload and ground support systems in coordination with their universities and European space industry in order to deliver their elements of the mission as part of their academic studies.

Team call sign	Team Name	Country	City	University
EPS	Electrical Power Supply	Hungary	Budapest	Budapest University of Technology and Economics
TriTel P/L	Tridimensional Telescope Dosimeter			
LMP P/L	Langmuir Plasma Diagnostic Probe			
uCAM P/L	Microcamera	Denmark	Lyngby	Danmarks Tekniske Universitet
AIV	Assembly, Integration and Verification	Italy	Milano	Politecnico di Milano
TCS	Termal Control Subsystem			
STT P/L	Star Tracker	France	Toulouse	ISAE (Institut supérieur de l'aéronautique et de l'espace)
ACS	Attitude Control Subsystem	Portugal	Lisboa	Universidade Técnica de Lisboa
RW P/L	Reaction Wheel			
GS1	Ground Station 1	Germany	Munich	Technische Universität München
GS2	Ground Station 2	New Zealand	Wellington	Massey University
STR	Structure Subsystem	Romania	Bucharest	POLITEHNICA University from Bucharest
MIAS	Mission Analysis	Spain	Zaragoza	University of Zaragoza
FDS	Flight Dynamic System			
CONF.	Configuration	Poland	Warsaw	Warsaw University of Technology
OBDAH	On Board Data Handling Subsystem			
OPER.	Operations			
MCC	Mission Control Center			
TMTC MAIN	Main Communication Subsystem	Poland	Wroclaw	Wroclaw University of Technology
TCC	Test Control Computer	Italy	Benevento	Università Del Sannio
HRNS	Harness	UK	Glasgow	University of Glasgow
MEX	Mission Exploitation			
TMTC RED	Redundant Communication Subsystem	UK	London	AMSAT UK
AMSAT P/L	Amsat Payload			

Figure 2.1: ESEO Teams

2 Mission Objectives

The main scope of the ESEO project as mentioned earlier is to provide a hands-on experience in satellite system design. The main mission objectives for the ESEO project are:

- Take pictures of the Earth and/or other celestial bodies from Earth orbit for educational outreach purposes

- Provide dosimetry and space plasma measurement in Earth orbit and its effects on satellite components
- Test technologies for future education satellite missions

ESEO has a LEO and the spacecraft will perform its payload operations over a minimum period of six months which could be extended. The precise orbit will be Sun Synchronous, while other orbit parameters will be selected in a proper manner to ensure that the natural orbital drag will ensure re-entry within 25 years (by using purely passive means) in order to comply with the European space debris code of conduct. A maximum orbit altitude of 600 km was set.

The first objective will be achieved by the use of a micro camera (mCAM) that, operating in the visible part of the spectrum, will acquire pictures of the Earth in a 8 bit gray-scale. The acquired images will be used for educational outreach purposes. The use of a Narrow Angle Camera is also considered optional and it will further investigated.

In order to fulfill the second objective another two instruments will be operated on board:

- Plasma diagnostic probe (LMP)
- Dosimeter instrument (Tritel-S)

In particular the LMP shall measure

- Electron density
- Electron temperature

while the Tritel-S shall measure

- LET spectra
- Absorbed dose
- Equivalent Dose

In order to realize the third objective in flight testing of two ACS components will be done. More precisely these components are:

- A star tracker
- A reaction wheel

Functional and performance tests will be performed during the satellite operative phase and the results shall be examined on ground by the design team, in order to gain a full space qualification in view of their use on other educational missions (i.e. ESMO). The satellite will also carry on board a payload proposed by the AMSAT community:

- VHF Transmitter
- S-Band Transmitter
- UHF Receiver

2.1 Mission Requirements & Technical Data

- Dimensions: Within a cube of 100 x 100 x 100 cm
- Mass: < 100kg
- Expected Lifetime: Six months mission, extendable until end-of-life
- Attitude determination system: 2 sun sensors, two magnetometers, one 3-axis gyroscope
- Attitude Control System: 3 magnetotorquers and 1 momentum wheel.
- On-board Data Transfer: CAN bus
- Telemetry
 - S-Band Primary: 513 kb/s
 - S-Band/Amateur-Band Secondary: 38.4 kb/s
- Power: Body mounted solar-cell panels
 - Average: 100W
 - Peak: 180 W
- Batteries: Li-Ion, 190Wh

- Power Bus 24-32 V Unregulated
- Thermal Control: Passive MLI coating + Active heaters

3 ESEO Mission Phase & Activities

In this section mission phases, satellite operational activities, launch, and nominal orbit will be described. In addition, the mission concept is also described from the perspective of launch, space, and ground segments.

3.1 Mission Phases

The ESEO mission is divided into five main phases:

- Launch and early operations phase;
- Operational phase;
- Extended Phase;
- Post Mission Phase
- Satellite disposal.

LEOP The launch and early orbit phase (LEOP) involves a sequence of events, many of which are programmed and automatic therefore the satellite shall not be controlled or monitored until separation from the launcher has taken place and the satellite is in a communication windows of a monitoring ground station. This phase can be further divided in the following subphases.

- Launch
- Separation
- Initial Attitude Acquisition
- Commissioning

After all vital subsystems shall be switched on and the deployment devices of the solar array will be activated. The increased inertia moment will help reduce the angular velocity which will be created by the separation from the launcher. The residual velocity will be then damped by a detumbling manoeuvre, and that will align the satellite axes with the Earth's magnetic field. From this attitude the satellite will go to a sun pointing attitude to start Commissioning Phase. In this phase all on-board equipments and payloads will be activated and tested to verify that they function and perform correctly. After successful completion of these operations the satellite is definitively accepted and delivered to the customer for its use.

Operational Phase After the commissioning phase the spacecraft shall start its operational phase to meet the mission requirements and operate the payloads for at least 6 months. According to the mission requirements the satellite shall operate the following payloads:

- TriTel-S
- uCAM
- Reaction Wheel as technological payload
- Star Tracker as technological payload
- LMP ũ Langmuir Probe
- AMSAT payload

The Operational Phase has been divided into cycles of 28 orbits; each payload will be operated four times per cycle. Telemetry and Payload Data (except for AMSAT Payload) shall be downloaded to 2 different Ground Stations located in Villafranca (SPA) and Wellington (NZ), that are connected to the Mission Control Center. AMSAT payload data shall be downloaded and managed directly by the AMSAT Ground Support Center (a separated ground station controlled by radio-amateurs).

Extended Phase The Extended Phase is an optional phase in case the spacecraft operations will last longer. Performances may be degraded thus no target is ensured and the Mission and System design shall not be affected by this Phase. The Extended Phase may start if at least one payload different from AMSAT can be operated in nominal working conditions and may last at most 2 years.

Post Mission Phase The Post Mission Phase shall start at the end of Extended Phase (if performed) or at the end of the Operational Phase and shall last at least 2 years. In this phase the satellite will be used by the AMSAT community as a transponder, fully exploiting the AMSAT Payload that will remain active. In this phase the satellite will be commanded to acquire a safe configuration, allowing it to survive without control from ground. However it will be possible to restart nominal operations, if required and agreed with ESA and the University Network.

Satellite Disposal At the end of the Post Mission Phase the satellite shall be passivated and shall re-enter the atmosphere according to its natural deorbiting. In agreement with international regulations, the deorbit shall occur within 25 years starting from the end of the Post Mission Phase.

4 Spacecraft Operational Activites

All spacecraft activities shall occur according to the following operational modes. The operational modes are defined in the following table:

	Description	System Mode	Thermal	OBDH	EPS	TMTC	ACS	uCAM	TriTel-S	LMP - Langmuir Probe	Star Tracker	Reaction Wheel	AMSAT Payload
Conf 1	Launch Mode	LM	Off	Off	Off	Off	Off	Off	Off	Off	Off	Off	Off
Conf 2	Initial Activation Mode - RX	IM	On	Nominal	On	RXTX On	Initial test state	Off	Off	Off	Off	Off	Off
Conf 3	Initial Activation Mode - RXTX	IM	On	Nominal	On	RXTX On	Initial test state	Off	Off	Off	Off	Off	Off
Conf 4	Set Up Mode RX	SM	On	Nominal	On	RX On	Damping	Off	Off	Off	Off	Off	Off
Conf 5	Set Up Mode RXTX	SM	On	Data Transmission	On	RXTX On	Damping	Off	Off	Off	Off	Off	Off
Conf 6	Nominal Mode RX	NM	On	Nominal	On	RX On	Stand by	Off	Off	Off	Off	Off	Off
Conf 7	Nominal Mode RXTX	NM	On	Data Transmission	On	RXTX On	Stand by	Off	Off	Off	Off	Off	Off
Conf 8	Nominal Mode - uCAM - RX	NM	On	Data Memorization	On	RX On	Fine Pointing	On	Off	Off	Off	Off	Off
Conf 9	Nominal Mode - uCAM - RXTX	NM	On	Data Transmission	On	RXTX On	Fine Pointing	On	Off	Off	Off	Off	Off
Conf 10	Nominal Mode - TriTel-S/LMP - RX	NM	On	Data Memorization	On	RX On	Stand by	Off	On	On	Off	Off	Off
Conf 11	Nominal Mode - TriTel-S/LMP - RXTX	NM	On	Data Transmission	On	RXTX On	Stand by	Off	On	On	Off	Off	Off
Conf 12	Nominal Mode - TriTel-S/LMP/uCAM - RX	NM	On	Data Memorization	On	RX On	Fine Pointing	On	On	On	On	Off	Off
Conf 13	Nominal Mode - TriTel-S/LMP/uCAM - RXTX	NM	On	Data Memorization	On	RXTX On	Fine Pointing	On	On	On	On	Off	Off
Conf 14	Nominal Mode - Star Tracker - RX	NM	On	Data Memorization	On	RX On	Auxiliary	Off	Off	Off	On	Off	Off
Conf 15	Nominal Mode - Star Tracker - RXTX	NM	On	Data Transmission	On	RXTX On	Auxiliary	Off	Off	Off	On	Off	Off
Conf 16	Nominal Mode - RW - RX	NM	On	Data Memorization	On	RX On	Auxiliary	Off	Off	Off	Off	On	Off
Conf 17	Nominal Mode - RW - RXTX	NM	On	Data Transmission	On	RXTX On	Auxiliary	Off	Off	Off	Off	On	Off
Conf 18	Nominal Mode - AMSAT - RX	NM	On	Data Memorization	On	RX On	Stand-by	Off	Off	Off	Off	Off	On
Conf 19	Nominal Mode - AMSAT - RXTX	NM	On	Data Transmission	On	RXTX On	Stand-by	Off	Off	Off	Off	Off	On
Conf 20	Nominal - Presafe - RX	NM	On	Nominal	On	RX On	Coarse Sun	Off	Off	Off	Off	Off	Off
Conf 21	Nominal - Presafe - RXTX	NM	On	Data Transmission	On	RXTX On	Coarse Sun	Off	Off	Off	Off	Off	Off
Conf 22	Nominal - Manouvre - RX	NM	On	Nominal	On	RX On	Fine Pointing	Off	Off	Off	Off	Off	Off
Conf 23	Nominal - Manouvre - RXTX	NM	On	Data Transmission	On	RXTX On	Fine Pointing	Off	Off	Off	Off	Off	Off
Conf 24	Safe - RX	SAFEM	On	Nominal	On	RX On	Safe	Off	Off	Off	Off	Off	Off
Conf 25	Safe - RXTX	SAFEM	On	Data Transmission	On	RXTX On	Safe	Off	Off	Off	Off	Off	Off
Conf 26	Post Mission - RX	PMM	On	Nominal	On	RX On	Safe	Off	Off	Off	Off	Off	Off

Figure 2.2: Operational Modes

As mentioned before the operative phase can be divided into cycles of 28 orbits. During these 28 orbits each mode has a specific time and place.

The modal lineup for the operative phase is described in the table below:

Mode sequence	Attitude	Time [min]	Orbits (total)	Power [W]
Mode 6	Sun	60.00	0.63	100.42
Mode 14	Sun	20.00	0.84	105.22
Mode 6	Sun	15.00	1.00	100.42
Mode 16	Sun	10.00	1.11	103.72
Mode 6	Sun	50.00	1.63	100.42
Mode 6	Sun	35.00	2.00	100.42
Mode 6	Sun	52.67	2.55	100.42
Mode 7	Sun	7.33	2.63	122.02
Mode 14	Sun	20.00	2.84	105.22
Mode 7	Sun	7.33	2.92	122.02
Mode 6	Sun	7.67	3.00	100.42
Mode 22	Nadir	15.00	3.16	127.54
Mode 9	Nadir	7.33	3.24	152.74
Mode 22	Nadir	15.00	3.39	127.54
Mode 6	Sun	22.67	3.63	100.42
Mode 7	Sun	7.33	3.71	122.02
Mode 6	Sun	27.67	4.00	100.42
Mode 18	Sun	2.67	4.03	155.26
Mode 19	Sun	7.33	4.11	176.86
Mode 6	Sun	50.00	4.63	100.42
Mode 6	Sun	27.67	4.92	100.42
Mode 7	Sun	7.33	5.00	122.02
Mode 10	Sun	35.00	5.37	117.94
Mode 10	Sun	60.00	6.00	117.94
Mode 18	Sun	2.67	6.03	155.26
Mode 19	Sun	7.33	6.11	176.86
Mode 6	Sun	50.00	6.63	100.42
Mode 6	Sun	27.67	6.92	100.42
Mode 7	Sun	7.33	7.00	122.02
Mode 22	Nadir	15.00	7.16	127.54
Mode 8	Nadir	7.33	7.24	131.14
Mode 22	Nadir	15.00	7.39	127.54
Mode 6	Sun	22.67	7.63	100.42
Mode 6	Sun	35.00	8.00	100.42
Mode 16	Sun	10.00	8.11	103.72
Mode 6	Sun	50.00	8.63	100.42
Mode 6	Sun	35.00	9.00	100.42
Mode 6	Sun	60.00	9.63	100.42
Mode 6	Sun	35.00	10.00	100.42
Mode 6	Sun	60.00	10.63	100.42
Mode 6	Sun	35.00	11.00	100.42
Mode 6	Sun	52.67	11.55	100.42
Mode 7	Sun	7.33	11.63	122.02
Mode 6	Sun	27.67	11.92	100.42
Mode 7	Sun	7.33	12.00	122.02
Mode 6	Sun	52.67	12.55	100.42
Mode 7	Sun	7.33	12.63	122.02
Mode 6	Sun	27.67	12.92	100.42
Mode 7	Sun	7.33	13.00	122.02
Mode 6	Sun	60.00	13.63	100.42
Mode 6	Sun	35.00	14.00	100.42
Mode 10	Sun	60.00	14.37	117.94
Mode 10	Sun	35.00	15.00	117.94
Mode 6	Sun	60.00	15.63	100.42
Mode 6	Sun	35.00	16.00	100.42
Mode 16	Sun	10.00	16.11	103.72
Mode 6	Sun	50.00	16.63	100.42
Mode 6	Sun	35.00	17.00	100.42
Mode 6	Sun	60.00	17.63	100.42
Mode 14	Sun	20.00	17.84	105.22
Mode 6	Sun	15.00	18.00	100.42
Mode 22	Nadir	15.00	18.16	127.54
Mode 9	Nadir	7.33	18.24	152.74
Mode 22	Nadir	15.00	18.39	127.54
Mode 6	Sun	22.67	18.63	100.42
Mode 7	Sun	7.33	18.71	122.02
Mode 6	Sun	27.67	19.00	100.42
Mode 18	Sun	2.67	19.03	155.26
Mode 19	Sun	7.33	19.11	176.86
Mode 6	Sun	50.00	19.63	100.42
Mode 6	Sun	27.67	19.92	100.42
Mode 7	Sun	7.33	20.00	122.02
Mode 10	Sun	60.00	20.37	117.94
Mode 10	Sun	35.00	21.00	117.94
Mode 10	Sun	60.00	21.37	117.94
Mode 10	Sun	35.00	22.00	117.94
Mode 6	Sun	60.00	22.63	100.42
Mode 6	Sun	35.00	23.00	100.42
Mode 6	Sun	60.00	23.63	100.42
Mode 6	Sun	35.00	24.00	100.42
Mode 16	Sun	10.00	24.11	103.72
Mode 6	Sun	50.00	24.63	100.42
Mode 6	Sun	35.00	25.00	100.42
Mode 6	Sun	60.00	25.63	100.42
Mode 14	Sun	20.00	25.84	105.22
Mode 6	Sun	15.00	26.00	100.42
Mode 22	Nadir	15.00	26.16	127.54
Mode 9	Nadir	7.33	26.24	152.74
Mode 22	Nadir	15.00	26.39	127.54
Mode 6	Sun	22.67	26.63	100.42
Mode 7	Sun	7.33	26.71	122.02
Mode 6	Sun	27.67	27.00	100.42
Mode 18	Sun	2.67	27.03	155.26
Mode 19	Sun	7.33	27.11	176.86
Mode 6	Sun	50.00	27.63	100.42
Mode 6	Sun	27.67	27.92	100.42
Mode 7	Sun	7.33	28.00	122.02

Figure 2.3: Operative Phase - Cyclic Modes

5 ESEO Mission Analysis

The mission baseline is to launch the spacecraft on secondary/auxiliary/shared launch opportunity into a SSO with an altitude of 520 Km and with LTAN 10:30. The baseline launcher shall be VEGA. The spacecraft should be designed in order to be compatible with a launch occurring any day of the year. The reference date for the launch is the 01/06/2012.

5.1 Launch Window

All the launchers considered can launch any day of the year and any time of the day [RD2]. For this reason, there are two launch opportunities everyday of the year. Each of the launch opportunity corresponds to the insertion of ESEO either in the ascending or in the descending part of the SSO. One of the two opportunity could be not available due to azimuth launch restrictions related to the specific launch site.

5.2 Target Orbits

The target orbit for ESEO mission is a circular SSO 10:30 LTAN. The target orbital parameters are listed in the table below.

Keplerian orbital parameters	Symbol	Units	
Altitude	a	km	6898
Eccentricity	e	--	0
RAAN	Ω	deg	47.7 (at nominal launch date)
Argument of periapsis	ω	deg	N/A
Inclination	i	deg	97.48
Initial true anomaly	$\theta_{\text{insertion}}$	deg	Dependent on launch base

Figure 2.4: Keplerian Parameters for the Operative Orbit

Note that initial inclination, RAAN, and true anomaly do not play a major role on the mission analysis. The SSO inclination exhibits a small variation with the altitude, the initial RAAN just determines the launch window in order to be compatible with the 10:30 LTAN requirement, whereas the initial true anomaly determines if the spacecraft injection occurs in sunlight or in eclipse.

Chapter 3

Thermal Control Subsystem

1 The TCS Subsystem

The purpose of a spacecraft thermal control subsystem (TCS) is to maintain all of the elements of a spacecraft system within their temperature limits for all mission phases. These temperature ranges must be satisfied for every external environment the satellite encounters in its lifetime and for all operational modes.

In order to keep all temperatures inside the appropriate ranges the TCS must be properly modelled. The TCS must therefore be able to dissipate all power absorbed from the external environment and all power generated internally. To do this the thermal subsystem uses the following active and passive thermal elements:

- Coatings & Paintings in order to achieve the best optical setup.
- Multi Layer Insulation with low conductivity
- Thermal fillers which increases heat transfer
- Heaters with thermostats which keep temperatures up when satellite is eclipsed.

The geometry of a spacecraft is generally very complex. Therefore on a typical spacecraft project the computer usage by the thermal control group will be relatively high. However the thermal control subsystem accounts for only about 2 – 5% of the total spacecraft cost and about the same percentage of the weight.

2 Thermal Environment

The first part relative to the design of the TCS is to analyze the thermal environment in which the satellite operates. A satellite which orbits the earth suffers from 3 different external heat fluxes.

- Direct Solar Heat Flux ($\cong 1371 \text{ Wm}^{-2}$)
- Sun Albedo Heat Flux ($\cong 30 \pm 5 \%$ of Direct Solar Heat Flux)
- Planetary Infrared Heat Flux ($\cong 237 \pm 21 \text{ Wm}^{-2}$)

These heat fluxes are not constant and depend on the keplerian parameters and the orientation of the spacecraft. The thermal environment can vary from high heat fluxes when in full solar exposition to very low heat fluxes when in eclipse. It is therefore important that the thermal subsystem is designed for both conditions. This is why a thermal subsystem design is divided into a hot-case and cold-case study.

3 Relationship to Other Subsystems

The TCS is affected by all subsystems onboard a spacecraft and in result also affects most subsystems. The biggest interactions are with the power, payload and configurations subsystem. An important aspect mentioned before is that all component temperatures must be maintained inside their limits and the components of the power subsystem and payload are those with the most narrow margins. The configuration subsystem is very interested by the thermal subsystem because the positioning of various components inside the spacecraft can significantly alter thermal results. In the table below there is a brief list of the most sensible components onboard a spacecraft.

Component	Typical Temperature Range [°C]
Batteries NiCd	5 to 20
Batteries NiH	-10 to 20
Electronics	0 to 40
Solar Cells	-90 to 115
P/L	-45 to 40
OBDH	-30 to 40

Table 3.1: Typical Temperature Ranges for Onboard Components

Chapter 4

Thermal Analysis

To be able to model the ESEO spacecraft thermal control subsystem a numerical computing environment was necessary. In the initial Phase-A design of ESEO MiniTAN was used to model the thermal subsystem. Unfortunately as mentioned MiniTAN is limited to a 50 node model and does not have a graphic 3d interface. Therefore for the Phase-B design of ESEO a more accurate model solution was made by using ESATAN, a more complete thermal modeller.

The main method used in thermal modelling is the lumped parameter method which consists in discretizing a continuous model into a network of nodes. Each node will have capacitance and will be linked with conductors to the other nodes. The lumped method derives from the electric/thermal analogy here temperature is equivalent to voltage and heat flow to current.

Discrete calculations has enormous advantages in numerical analysis and eases hand and computer based solutions as a continuous must obey differential equations, while a discrete body can be described with algebraic equations. The lumped parameter method is thus an easy way to obtain a numerical solution from a differential equation.

1 Lumped Thermal Modelling

To obtain a lumped parameter equation the first thing one must do is to discretize the geometry. Here under is an example of how a metal plate would be divided.

Once divided on every node there is the following nodal heat balance:

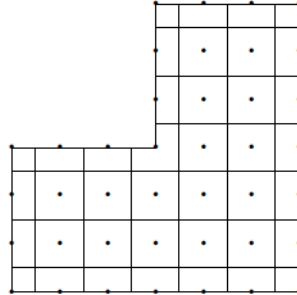


Figure 4.1: Nodal Discretization

$$C_i \frac{dT_i}{dt} = \sum_i K_{ij} (T_j - T_i) + \sum_i R_{ij} (T_j^4 - T_i^4) + Q_i \quad (4.1)$$

Where in this equation:

- T_i = Temperature of node
- T_j = Temperature of adjacent node
- Q_i = Nodal power dissipation
- K_{ij} = Conductivity between nodes
- C_i = Heat capacity of node
- R_{ij} Radiative exchange constant

This equation assumes that may be derived but do not how this can be done. In some application as in MiniTAN for example these values must be calculated manually. They are then inserted, where GL and GF linear and fluidic conductors represent K_{ij} and GR radiative condctor R_{ij} . If a steady state case is done the left side of the equation becomes equal to 0. With few nodes these calculations can be done by hand. In the case of a full thermal model the number of nodes and equations becomes very large and therefore numerical computing is necessary. Two numerical computer based solvers are ESATAN and MiniTAN, where the second is a limited version of the first.

2 MiniTAN

MiniTAN is a numerical solver which is based on a 50 node zero-dimensional modelling. MiniTAN uses lumped parameter modelling and can do both static and transient case calculations. It does not have a graphic interface but uses pre-edited text files as inputs. This text file contains all information about the discretized thermal model. Unfortunately MiniTAN only solves the lumped parameter equation and does not calculate the different thermal constants like the conductivity between nodes. Therefore the input file must be either manually created or created by another tool. Therefore in MiniTAN for every node we must explicit K_{ij} , C_i , R_{ij} and Q_i manually.

As mentioned before in MiniTAN K_{ij} is expressed as GL and GF. GL are linear conductors where $q_{ij} = h(T_i - T_j)$ and h, the heat transfer factor is the value of the GL conductance. Linear conductors are used to describe solid conductance, convection, condensation and evaporation.

The heat capacitance for every node must also be calculated. C_i is calculated by multiplying the mass of the node by the heat capacity of the node. $C = m \cdot c_p$.

A very difficult value which unfortunately is not calculated either by MiniTAN is the radiative exchange constant R_{ij} . In MiniTAN a value GR called the radiative conductor must be given.

$$q_{ij} = \sigma \epsilon_i \epsilon_j A_i F_{ij} (T_i^4 - T_j^4) = \sigma G R_{ij} (T_i^4 - T_j^4) \quad (4.2)$$

Where

- T_i = Temperature of node
- T_j = Temperature of adjacent node
- q_{ij} = Heat flux due to radiative heat between node i & j
- F_{ij} = View Factor between nodes i & j
- A_i = Area of node i
- σ = Stefan Boltzmann Constant

- ϵ_i = Node i emissivity
- ϵ_j = Node j emissivity
- GR_{ij} = Radiative conductor between node i & j

Along with these properties, the coincident heat on each node must be calculated. These can be calculated manually or using another computer based tool like Topic. Along with these heat fluxes one must also insert the heat dissipated by the node.

Once all this data is calculated it must be properly inserted into the MiniTAN input file.

```
#
$NODES
#
#   Nodes block for model SAMPLE
#
D10= 'TELESCOPE', T=20.0, C=0.5, QA=0.0, QE=0.5,   #DIFFUSION NODE
      QI=0.2, QR=1.2, QS=2.3;
#
D25, C=0.3, QS=0.11E2, T=12.0E0;
#
B30= 'NOSE CONE', T = -273.15;                    #BOUNDARY NODE
#
```

Figure 4.2: MiniTAN Input File - Node Example

In the example above DXX & BXX represent the nodes of our thermal model, but are different. BXX represents a boundary node where as DXX is a normal diffusion node. Diffusion nodes need an initial temperature, the capacitance and the heat fluxes of the node. The boundary node instead only needs its temperature as input. QA, QE, QI, QR and QS are measured in W and represent the Albedo, Planet, Internal, Other and Sun heat Sources. MiniTAN uses these 5 heat inputs, summing them together and applying a unique Q on the node.

Once all nodes have been described the different linear and radiative conductors must be inserted.

```
#
$CONDUCTORS
#
#   Conductor block for model SAMPLE
#
GL (10,20) = 0.35;
GF (20,25) = 6.80E-03;
GR (10,30) = 0.05;
```

Figure 4.3: MiniTAN Input File - Conductors

These conductors are defined by inserting $GL(II,JJ)=K_{ij}$ & $GR(II,JJ)=R_{ij}$ where II is node i, JJ node j, K_{ij} is the linear conductance and R_{ij} Radiative conductor.

Once all these parameters are defined the one must specify the type of analysis, static or transient. The input file is then run with MiniTAN. This after gives in output a text file with the results of the thermal analysis calculations.

For small or initial thermal models MiniTAN is used, but obviously if a larger thermal model must be designed a different solver must be used. For larger models ESATAN-TMS is used.

3 ESATAN-TMS

ESATAN-TMS Workbench offers advanced geometric modelling, calculation and visualisation capabilities. Where MiniTAN need a lot of user calculated information, ESATAN on the contrary once a geometry with optical and mass properties has been designed automatically calculates most thermal properties. ESARAD, the radiative module of ESATAN, in particular calculates all view factors and, if an orbit is defined, all external heat fluxes. Obviously all material properties must be initially defined.

The user must follow predefined steps in order to create a thermal model. The user must create a geometric module, insert its properties, then calculate the radiative exchange factors and heat fluxes. The user must then insert the dissipated heat of different components and if necessary include extra conductors. Once all these steps have been taken the user can finally obtain the thermal results of the model. In order to sustain these different steps ESATAN is divided into various modules.

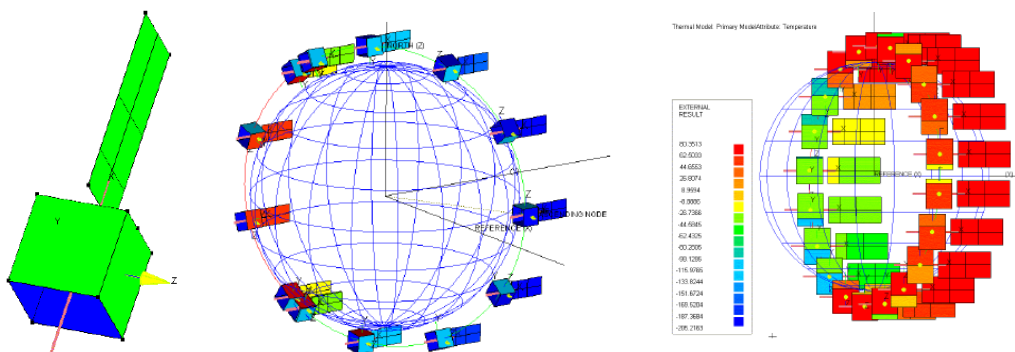


Figure 4.4: ESATAN Geometry Definition (L), Orbit (C) & Thermal Results (R)

3.1 ESATAN Modules

- Geometry Module
- Visualization Module
- Radiative Module
- Reporting Module
- Thermal Module
- Library Module

Geometry Module ESATAN-TMS geometry module allows users to load, create and edit a geometric representation of the thermal model. Once the the geometry is defined ESATAN allows the user to define the thermo-optical and mass properties. It also allows users to define the thermal mesh of the geometry created.

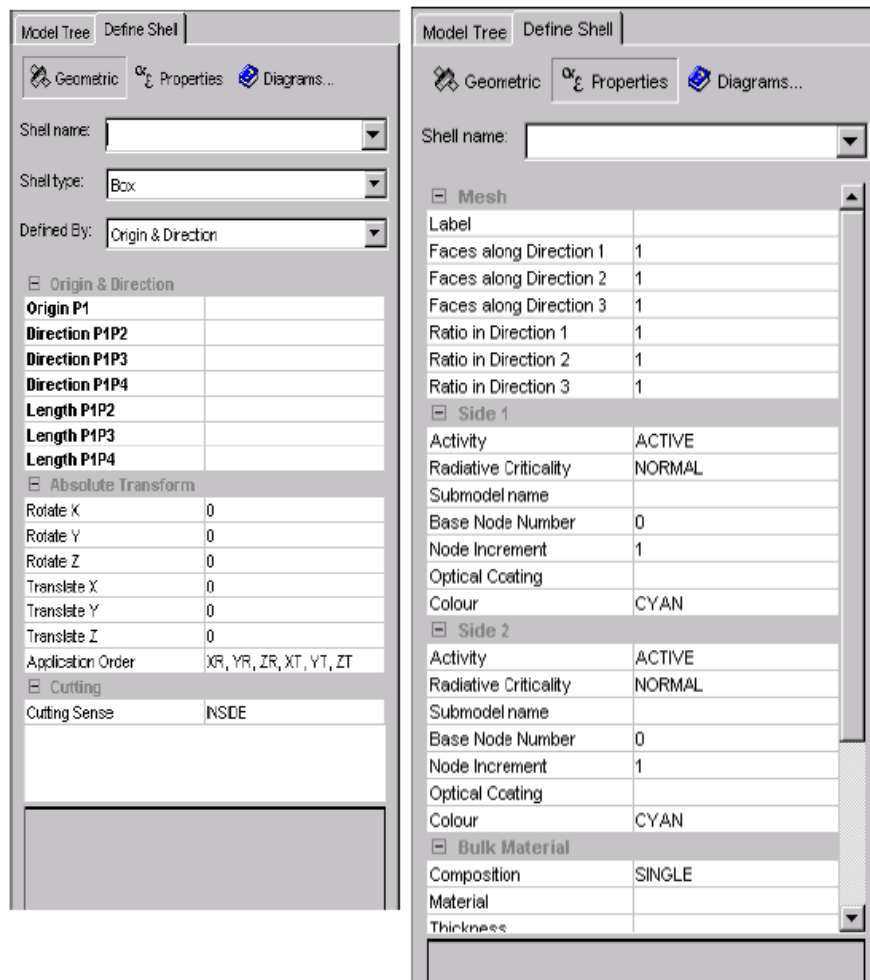


Figure 4.5: ESATAN GEOMETRY DEFINITION

Visualization Module The Visualization Module allows users to display all information relevant to the thermal model. It shows the 3D structure of the model, all results calculated by the radiative module and all post-processing results of the thermal model.

Radiative Module Once the geometry of the thermal model has been defined with its equivalent thermal model the radiative module can be used. The radiative module cal-

culates all view factors, radiative exchange factors and direct and absorbed heat fluxes. It uses the keplerian parameters to calculate the spacecraft's orbit and by defining the satellites orientation it can calculate all radiative heat fluxes.

Reporting Module This module allows the users to create reports about any information relevant to the thermal model. It also permits users to export files to use for thermal post-processing.

Thermal Module This allows users to create various thermal cases. The thermal module allows users to choose different boundary conditions, change thermal and orbit parameters in order to obtain a thermal analysis of all possible cases a spacecraft might encounter.

Library Module This module contains all various independant functions and variables like optical and bulk properties. It is used to export this data to other modules.

3.2 ESATAN Results

ESATAN results can be obtained graphically or in report format. A .GFF file readable with any text reader reports all heat and temperature results of every node. Results can be obtained for different settings using the Thermal Module. For example a satellite simple thermal study can divide e satellite into two modes, safe mode and operational mode. In safe mode most components are switched off and do not dissipate power, while in operational mode many components dissipate heat. The thermal conditions are therefore very different for these two cases and it is necessary to study two different scenarios.

Chapter 5

ESEO Thermal Model Development

The ESEO satellite during the design phase underwent various changes. The original design consisted in a 60 cm cubic satellite with bodymounted solar panels. This was later converted to a 80 cm cubic satellite, again with bodymounted solar panels. Finally the ESEO was again redesigned into a cuboid shape with deployable solar panels.

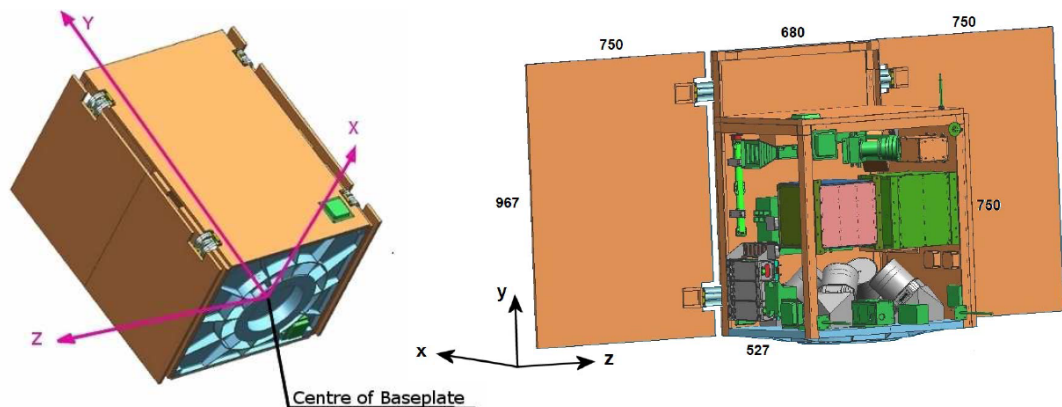


Figure 5.1: ESEO Final Design

In this section we will breakdown and explain all design choices and properties used to model the ESEO thermal control subsystem.

1 ESEO Model - Geometry

The entire ESEO satellite was modelled using ESATAN-TMS. In order to model the satellite properly a geometrical representation was created. The external geometry shown in ES as previously mentioned is a cuboid with three solar panels of which two are deployable and one fixed. The internal components also shown in ES and are of various shapes and forms and will therefore suffer some approximations during modelling.

While modelling the geometry the properties of each component must be attributed in order to have a model which not only represents ESEO geometrically but also in its thermal and structural characteristics.

1.1 External Geometry

The external solar and structural panels were designed by creating a box geometry to represent the satellite's shell and three rectangles to represent the solar panels. The external panels are made of two different materials.

- Honeycomb in Aluminum
- Aluminum Panels

Honeycomb panels were used for all external panels except the baseplate -Y and on structural side +X / -X.

Another difference subsists between the honeycomb panels used for the solar panels and those used on the main structure. Both panels have two 0.3 mm skins with a different core thickness. The solar panels have a core thickness of 13 mm giving the panels a total thickness of 13.6 mm. The structural panels instead have a core thickness of 20 mm which leads to a 20.6 mm total thickness. For design reasons also the aluminum panels have a thickness of 20.6 mm.

Once drawn an artificial density was created in order to be able to include additional masses. Together with this the specific heat used for each panel was 921 J/kgK which is the equivalent of pure aluminum. The conductivity used for the aluminum panels was 155 W/mK, coincident with Al 2024, while for the honeycomb a value of 97.86 W/mK was obtained with the following equation:

$$k = \frac{8}{3} \cdot \bar{k} \frac{\delta}{S} [2] \quad (5.1)$$

Where:

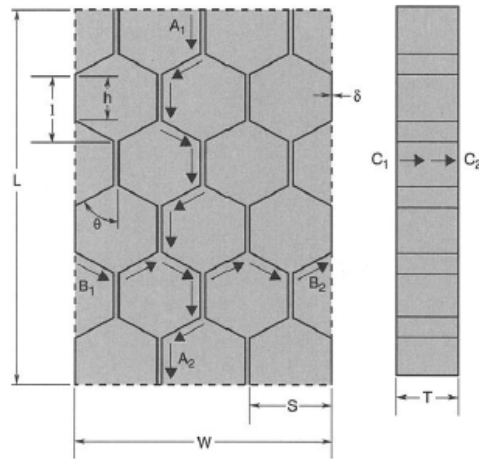


Figure 5.2: ESEO External Panel Properties

- $\bar{k} = 137 \text{ W/mK}$ is the conductivity of Al 5052
- $\delta = 3/16$ is the Ribbon Thickness
- $S = 0.0007 \text{ inch}$ is the Cell Size

The thermal and structural properties used for the external panels are therefore:

STRUCTURAL DATA	DENSITY [kg/m ³]	MATERIAL	Cp [J/kg K]	Conductivity [W/K m]
STRUCTURE +X	522,8782122	ALUMINUM	921	155
STRUCTURE -X	541,2919248	ALUMINUM	921	155
STRUCTURE +Y	725,7010054	HONEYCOMB	921	97,85714
STRUCTURE -Y	1177,373448	ALUMINUM	921	155
STRUCTURE +Z OSR	895,0646136	HONEYCOMB	921	97,85714
STRUCTURE +Z MLI	791,0739885	HONEYCOMB	921	97,85714
STRUCTURE -Z	707,1233157	HONEYCOMB	921	97,85714
SOLAR DATA	DENSITY [kg/m ³]	MATERIAL	Cp [J/kg K]	Conductivity [W/K m]
SOLAR +X	537,1630363	HONEYCOMB	921	97,85714
SOLAR -Z	503,9533274	HONEYCOMB	921	97,85714
SOLAR +Z	503,9533274	HONEYCOMB	921	97,85714

Figure 5.3: ESEO External Panel Properties

1.2 Internal Geometry

In order to properly create a thermal model of the internal components some hypothesis and simplifications were made. The first consists in the shape of each component. In the ESATAN geometrical model all components were approximated with cylindrical or box shapes. The second approximation consists in giving each component a virtual thickness of 5 mm. This was done in order to have a certain volume with which, knowing the mass of each component, a fictitious density could be calculated. The last approximation was that of considering a heat capacity of $C_p = 921$ J/KgK and conductivity of $k = 155$ W/mK which approximates all components to aluminium.

A summary of every component is listed below:

COMPONENT	SHAPE	Thickness [M]	MASS [kg]	VOLUME [m3]	DENSITY [kg/m3]
AMSAT BOX	BOX	0,005	0,72	0,000695	1035,971223
TMTC REDUNDANT	BOX	0,005	4,61	0,000836	5514,354067
TMTCR PATCH +X	BOX	0,005	0,12	0,00019812	605,6935191
OBDH	BOX	0,005	12	0,00144531	8302,717064
EPS PEB	BOX	0,005	8,4	0,0014915	5631,91418
STAR TRACKER INSIDE	BOX	0,005	2,06	0,000341472	6032,701247
STAR TRACKER OUTSIDE	CYLINDER	0,005	2,06	0,000151872	6032,701247
TMTCR PATCH -X	BOX	0,005	0,12	0,00019812	605,6935191
REACTION WHEEL	BOX	0,005	0,96	0,00261725	366,7972108
UCAM	BOX	0,005	0,72	0,000222405	3237,33729
MAGNETO-TORQUER +Y	CYLINDER	0,005	1,44	0,000124056	11607,66142
TMTCR PATCH +Y	BOX	0,005	0,12	0,00019812	605,6935191
REACTION WHEEL 1	BOX	0,005	1,8	0,00097775	1840,961391
REACTION WHEEL 2	BOX	0,005	1,8	0,00097775	1840,961391
REACTION WHEEL 3	BOX	0,005	1,8	0,00097775	1840,961391
REACTION WHEEL 4	BOX	0,005	1,8	0,00097775	1840,961391
MAGNETO-TORQUER -Y	CYLINDER	0,005	1,44	0,000124056	11607,66142
TRITEL S	BOX	0,005	1,44	0,00011039	13044,65984
TMTCR PATCH -Y	BOX	0,005	0,12	0,00019812	605,6935191
TMTC BOX	BOX	0,005	4,61	0,000836	5514,354067
GYRO BOX	BOX	0,005	1,8	0,00038632	4659,349762
MAGNETOMETER 1	BOX	0,005	0,07	0,00007275	962,1993127
MAGNETOMETER 2	BOX	0,005	0,07	0,00007275	962,1993127
TMTCR PATCH +Z	BOX	0,005	0,12	0,00019812	605,6935191
EPS BATTERY	BOX	0,005	7,98	0,006035	1322,286661
LMP LCB	CUBE	0,005	0,96	0,000192	5000
MAGNETO-TORQUER -Z	CYLINDER	0,005	1,44	0,000124056	11607,66142
TMTCR PATCH -Z	BOX	0,005	0,12	0,00019812	605,6935191

Figure 5.4: ESEO Component Properties

The final geometrical model obtained in ESATAN is:

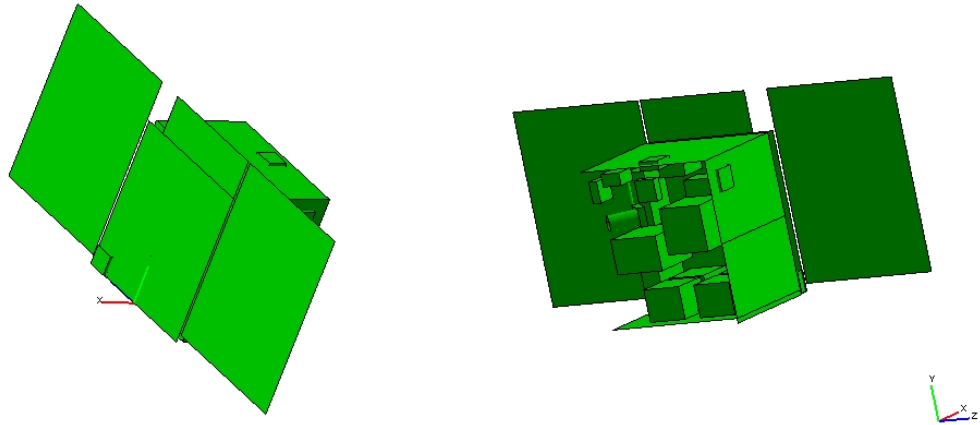


Figure 5.5: ESEO Geometry

2 ESEO Model - Optical Data & Nodal Disposition

Once the geometry and material characteristics are modelled, the thermo-optical properties of each component must be defined.

2.1 Optical Data

The thermo-optical properties used on the external structure of the ESEO satellite are mentioned below:

MATERIAL	TYPE	α	ϵ	PANEL
MLI	INSULATION	0.55	0.78	STRUCTURAL: +X,+Y,-Y,+Z (50 %),-Z
AZW-LA-II	COATING	0.09	0.91	STRUCTURAL: +Z (50%)
SILVER TEFLON	TAPE	0.08	0.78	SOLAR: FRONTSIDE
SOLAR CELLS	CELLS	0.92	0.85	SOLAR: FRONTSIDE
AMJ-750-LSBU	COATING	0.76	0.81	SOLAR: BACKSIDE
BRILLIANT ALLUMINUM	COATING	0.3	0.31	STRUCTURAL: -X

Figure 5.6: ESEO External Optical Properties

As shown in the table above most panels are covered with MLI, this together with its optical properties also insulates. Internally all panels are also covered with a layer of MLI. The solar panels are made of solar cells put inside a silver teflon frame. The properties of each material are listed in the table. Solar cells have a 60% packaging factor. A mean value for absorptance and emissivity were calculated to represent this.

$$\cdot \alpha = 0.92 \cdot 0.6 + 0.13 \cdot 0.4 = 0.604$$

$$\cdot \epsilon = 0.85 \cdot 0.6 + 0.75 \cdot 0.4 = 0.81$$

Internal components on the other hand were not covered with coating and all components have the optical properties of polished aluminum:

$$\cdot \alpha = 0.15$$

$$\cdot \epsilon = 0.05$$

2.2 Nodal Disposition

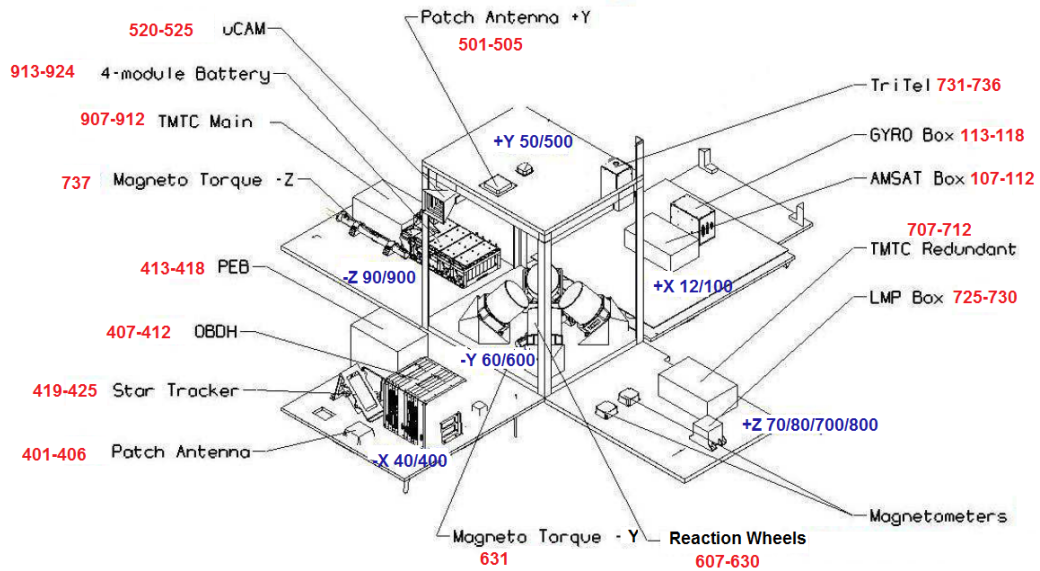


Figure 5.7: ESEO Nodal Breakdown

Together with defining the geometry and its characteristics in order to create the thermal model each structural component must be divided into nodes.

All panels except for -Z are subdivided into two nodes, one node for the external side and one for the internal side. -Z panel was divide into four nodes seeing it has two different optical properties. Every part with a different optical property was divided into two nodes again internally and externally. The external parts of panels were subject to a two digit identification while external parts to a three digit identification. The first digit of each internal/external subdivision is the same. The lateral solar panels are divided in a similar fashion where the external part is considered to be the side with the solar cells. The central solar panel was divided into four nodes all with a two digit identification.

Internal components were divided into six nodes if of box shape and a single node if cylindrical. All component nodes have a three digit identification and the first digiti represents the internal panel the component is attached to. This nodal breakdown leads to a thermal model of 172 nodes.

A summary of the nodal disposition is listed below:

COMPONENT	NODE NUMBER	COMPONENT	NODE NUMBER	COMPONENT	NODE NUMBER
AMSAT BOX	107-112	REACTION WHEEL 2	613-618	MAGNETO-TORQUER -Z	737
TMTC REDUNDANT	707-712	REACTION WHEEL 3	619-624	TMTCR PATCH -Z	901-906
TMTCR PATCH +X	101-106	REACTION WHEEL 4	625-630	STRUCTURE +X	12/100
OBDH	407-412	MAGNETO-TORQUER -Y	631	STRUCTURE -X	40/400
EPS PEB	413-418	TRITEL S	731-736	STRUCTURE +Y	50/500
STAR TRACKER INSIDE	419-424	TMTCR PATCH -Y	601-606	STRUCTURE -Y	60/600
STAR TRACKER OUTSIDE	425	TMTC BOX	907-912	STRUCTURE +Z OSR	70/700
TMTCR PATCH -X	401-406	GYRO BOX	113-118	STRUCTURE +Z MLI	80/800
REACTION WHEEL	507-512	MAGNETOMETER 1	713-718	STRUCTURE -Z	90/901
UCAM	520-525	MAGNETOMETER 2	719-724	SOLAR +X	10/13/14/15
MAGNETO-TORQUER +Y	519	TMTCR PATCH +Z	701-706	SOLAR -Z	20/200
TMTCR PATCH +Y	501-506	EPS BATTERY	913-924	SOLAR +Z	30/300
REACTION WHEEL 1	607-612	LMP LCB	725-730		

Figure 5.8: ESEO Nodal Breakdown

3 ESEO Model - Thermal Conductance

Now that the properties of all nodes have been described the relationship that link the nodes together must be added. We must therefore described all conductances between each node. There are different types of conductances that exist between various nodes.

3.1 Through-Thickness Conductance

This represents the conductance between the nodes on two sides of a panel. In other words this is the conductance which passes through a panel. In our model earlier we defined the thickness, size and conductivity of our panels, therefore ESATAN automatically calculates this conductance.

3.2 Intra-Shell Conductors

This represents the conductance between different panels or different side of a component and again seeing that all properties were previously defined this is automatically calculated.

3.3 Inter-Shell Conductors

Thir represent the conductance between different components. Three inter-shell conductors cases exist and for each case the value was manually calculated. The first consists of the conductance between the internal structural panels and the components fitted on them.

To isolate or create thermal bridges special fillers were used in order to achieve specific heat fluxes between each component and the panel it is fixed to. Three different thermal fillers were chosen:

Not existing a node representing the thermal filler a manual conductance was included. The conductance becomes therefore:

$$GL = \frac{k}{s} \cdot A \quad (5.2)$$

Where A is the contact area between the panel and the component.

FILLER	k [W/mK]	thickness [mm]	k/s [W/m2K]
HALA TGF-C0500-SI	1.5	2 mm	750
HALA TGF-C2000-SI	1.5	0.5 mm	3000
Alfatec Softtherm 86/20	1	5 mm	200

Figure 5.9: ESEO Fillers

The second inter-shell conductor is that relative between the three solar panels. The two lateral solar panels are connected to the central panel with a two hinges relative to the deployment system. Each hinge is made of three metal strips and therefore there are six bridges between the central panel and each solar panel. The conductance therefore is.

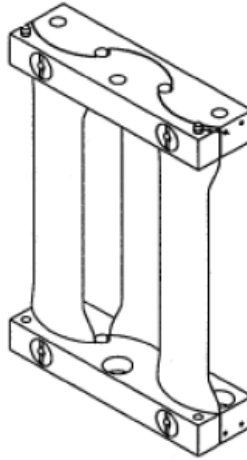


Figure 5.10: ESEO Deployment System

$$GL = 0.5 \cdot 6 \left(\frac{k}{s} \cdot A \right) \quad (5.3)$$

Where:

- $A = \text{Area of one strip} = 0.03 \cdot 0.001 = 0.00003 \text{ m}^2$

- $L = \text{Length of one strip} = 0.105 \text{ m}$

- $k = \text{Conductivity} = 25 \text{ W/mK}$;

The 0.5 factor accounts for the fact that the conductance is split equally between the front and rear node while the 6 accounts for the thermal bridges.

The last inter-shell conductor is that between the central solar panel and the structural panel to which it is attached. The central solar panel is coupled to the main structure of ESEO with four cylinders. This leads to the following conductance:

$$GL = \frac{4 \cdot \pi d^2}{4L} \tag{5.4}$$

Where:

- $d = \text{Diameter of one cylinder} = 8 \text{ mm}$
- $L = \text{Length of one cylinder} = 5 \text{ mm}$
- $k = \text{Conductivity} = 21.9 \text{ W/mK}$;

A brief summary containing all inter-shell conductances is listed below:

COMPONENTS			
SIDE A	SIDE B	k/s	Conductive Area
TMTC	BODY -Z	750	0,068
EPS BAT	BODY -Z	200	0,054
MAGNETORQUER_ZM	BODY -Z	750	0,28
PEB	BODY -X	750	0,0645
OBDH	BODY -X	750	0,0588
GYRO BOX	BODY +X	200	0,0125
AMSAT BOX	BODY +X	750	0,0105
MAGNETORQUER_XP	BODY +X	750	0,028
TMTC_RED	BODY +Z	750	0,068
LMP_LCB	BODY +Z	750	0,0064
TRITEL	BODY +Z	750	0,009
MAGNETOMETER_1	BODY +Z	750	0,0039
MAGNETOMETER_2	BODY +Z	750	0,0039
UCAM	BODY +Y	750	0,0105
REACTION_YP	BODY +Y	750	0,021
REACTION_1	BODY -Y	3000	0,0226
REACTION_2	BODY -Y	3000	0,0226
REACTION_3	BODY -Y	3000	0,0226
REACTION_4	BODY -Y	3000	0,0226
MAGNETORQUER_YM	BODY -Y	750	0,028

PANELS			
SIDE A	SIDE B	k	SHAPE FACTOR
BODY +X	PANEL +Z	21,9	0,040212386
PANEL +Z	PANEL +Z	25	0,000857143
PANEL +Z	PANEL +Y	26	0,000857143

Figure 5.11: Inter-Shell Conductivities

3.4 Radiative Conductance

The last conductance which exists is the radiative coupling which exists between all internal components and that between different sides of each components. It also includes the radiative conductance between the components and the internal structural walls. There are also radiative exchanges between the solar panels and the satellite body together with the conductance between the external panels and deep space. These are automatically calculated by ESATAN which calculates all view factors and by knowing the optical properties of all components calculates the radiative conductance.

Once all conductances have been inserted the thermal model is complete. The only data missing now are the boundary conditions which is the radiative case that includes the solar and planetary heat fluxes, radiative conductances and deep-space boundary conditions. In ESATAN it is possible to represent this dissipated heat by creating a boundary condition.

4 Boundary Conditions - Internal Heat Dissipation

Another parameter that must be inserted into our thermal model is the heat dissipation of each component. Most components when switched on dissipate heat. This heat contributes to the thermal model and is very important for the thermal control subsystem.

During the entire ESEO mission the satellite has different mission phases. In each phase the satellite has different operating modes in which a certain amount of components are switched or in standby. In every mode each component will have a different heat dissipation. It is therefore important to create a boundary condition for every component in every mode.

Different boundary conditions can be implemented as shown in the following table:

Type of Boundary Condition	Allocation	Units
Initial Temperature	The given initial temperature is assigned to each thermal node defined by the reference.	°C
Temperature	The given temperature is assigned to each thermal node defined by the reference, and the thermal node is set to be a boundary.	°C
Heat Load/Unit Area	A heat load is assigned to each face defined by the reference as the given value multiplied by the face's area.	W/m ²
Heat Load/Face	The given heat load is assigned to each of the faces defined by the reference.	Watts
Total Heat Load	If applied to a region including more than one thermal node, the specified heat load is divided between the nodes in proportion to the area of the faces that make up each node.	Watts

Figure 5.12: Possible Boundary Conditions

To insert heat dissipations the last type is chosen. Once the type of boundary condition is selected the nodes on which applied must be selected in the reference bar and the boundary condition value must be inserted. We will see later on that two types of boundary conditions were created for every component. One consists in a constant boundary condition and this is created by inserting a value while the other consists in inserting a time dependant variable in order to change the boundary condition with time. For the second case instead of inserting a value a function must be created and then this function must be inserted into the value bar.

This data is inserted in the following window in ESATAN.

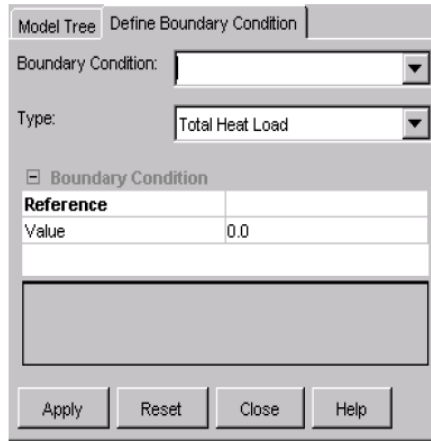


Figure 5.13: Boundary Conditions

A summary of the heat dissipation modelled of every component for every mode is listed below:

COMPONENT/MODE	MODE 1	MODE 2	MODE 3	MODE 4	MODE 5	MODE 6	MODE 7	MODE 8	MODE 9	MODE 10	MODE 11	MODE 12	MODE 13
AMSAT BOX	0	0	0	0	0	0	0	0	0	0	0	0	0
TMTC RED	0	0	0	0	0	0	0	0	0	0	0	0	0
TMTCR PATCH +X	0	0	0	0	0	0	0	0	0	0	0	0	0
OBDAH	0	30	30	30	30	30	30	30	30	30	30	30	30
EPS PEB	0	12	12	12	12	12	12	12	12	12	12	12	12
STARTRACKER	0	0	0	0	0	0	0	0	0	0	0	0	0
TMTCR PATCH -X	0	0	0	0	0	0	0	0	0	0	0	0	0
REACTION WHEEL	0	0	0	0	0	0	0	0	0	0	0	0	0
UCAM	0	0	0	0	0	0	0	3,6	3,6	0	0	3,6	3,6
MAGNETOTORQUER +Y	0	1,2	1,2	3	3	2,16	2,16	0	0	0	0	0	0
TMTCR PATCH +Y	0	0	0	0	0	0	0	0	0	0	0	0	0
REACTION 1	0	0	0	0	0	6	6	14,4	14,4	8,4	8,4	14,4	14,4
REACTION 2	0	0	0	0	0	6	6	14,4	14,4	8,4	8,4	14,4	14,4
REACTION 3	0	0	0	0	0	6	6	14,4	14,4	8,4	8,4	14,4	14,4
REACTION 4	0	0	0	0	0	6	6	14,4	14,4	8,4	8,4	14,4	14,4
MAGNETOTORQUER -Y	0	1,2	1,2	3	3	2,16	2,16	0	0	0	0	0	0
TRITELS	0	0	0	0	0	0	0	0	8,4	8,4	8,4	8,4	8,4
TMTCR PATCH -Y	0	0	0	0	0	0	0	0	0	0	0	0	0
TMTC BOX	0	12	33,6	12	33,6	12	33,6	12	33,6	12	33,6	12	33,6
GYRO BOX	0	0	0	0	0	13,2	13,2	13,2	13,2	13,2	13,2	13,2	13,2
MAGNETOMETER 1	0	1,44	1,44	1,44	1,44	1,44	1,44	1,44	1,44	1,44	1,44	1,44	1,44
MAGNETOMETER 2	0	1,44	1,44	1,44	1,44	1,44	1,44	1,44	1,44	1,44	1,44	1,44	1,44
TMTCR PATCH +Z	0	0	0	0	0	0	0	0	0	0	0	0	0
EPS BATTERIES	0	0	0	0	0	0	0	0	0	0	0	0	0
LMP LCB	0	0	0	0	0	0	0	0	6	6	6	6	6
MAGNETOTORQUER -Z	0	1,2	1,2	3	3	2,16	2,16	0	0	0	0	0	0
TMTCR PATCH -Z	0	0	0	0	0	0	0	0	0	0	0	0	0

Figure 5.14: Dissipated Power Modes 1-13

COMPONENT/MODE	MODE 14	MODE 15	MODE 16	MODE 17	MODE 18	MODE 19	MODE 20	MODE 21	MODE 22	MODE 23	MODE 24	MODE 25	MODE 26
AMSAT BOX	0	0	0	0	54,84	54,84	0	0	0	0	0	0	54,84
TMTC RED	0	0	0	0	0	0	0	0	0	0	0	0	0
TMTCR PATCH +X	0	0	0	0	0	0	0	0	0	0	0	0	0
OBDH	30	30	30	30	30	30	30	30	30	30	30	30	30
EPS PEB	12	12	12	12	12	12	12	12	12	12	12	12	12
STARTRACKER	4,8	4,8	0	0	0	0	0	0	0	0	0	0	0
TMTCR PATCH -X	0	0	0	0	0	0	0	0	0	0	0	0	0
REACTION WHEEL	0	0	3,3	3,3	0	0	0	0	0	0	0	0	0
UCAM	0	0	0	0	0	0	0	0	0	0	0	0	0
MAGNETOTORQUER +Y	2,16	2,16	2,16	2,16	2,16	2,16	2,16	2,16	0	0	1,08	1,08	1,08
TMTCR PATCH +Y	0	0	0	0	0	0	0	0	0	0	0	0	0
REACTION 1	6	6	6	6	6	6	12	12	14,4	14,4	0	0	0
REACTION 2	6	6	6	6	6	6	12	12	14,4	14,4	0	0	0
REACTION 3	6	6	6	6	6	6	0	0	14,4	14,4	0	0	0
REACTION 4	6	6	6	6	6	6	0	0	14,4	14,4	0	0	0
MAGNETOTORQUER -Y	2,16	2,16	2,16	2,16	2,16	2,16	2,16	2,16	0	0	1,08	1,08	1,08
TRITEL S	0	0	0	0	0	0	0	0	0	0	0	0	0
TMTCR PATCH -Y	0	0	0	0	0	0	0	0	0	0	0	0	0
TMTC BOX	12	33,6	12	33,6	12	33,6	12	33,6	12	33,6	12	33,6	0
GYRO BOX	13,2	13,2	13,2	13,2	13,2	13,2	0	0	13,2	13,2	0	0	0
MAGNETOMETER 1	1,44	1,44	1,44	1,44	1,44	1,44	1,44	1,44	1,44	1,44	1,44	1,44	1,44
MAGNETOMETER 2	1,44	1,44	1,44	1,44	1,44	1,44	1,44	1,44	1,44	1,44	1,44	1,44	1,44
TMTCR PATCH +Z	0	0	0	0	0	0	0	0	0	0	0	0	0
EPS BATTERIES	0	0	0	0	0	0	0	0	0	0	0	0	0
LMP LCB	0	0	0	0	0	0	0	0	0	0	0	0	0
MAGNETOTORQUER -Z	2,16	2,16	2,16	2,16	2,16	2,16	2,16	2,16	0	0	1,08	1,08	1,08
TMTCR PATCH -Z	0	0	0	0	0	0	0	0	0	0	0	0	0

Figure 5.15: Dissipated Power Modes 14-26

5 Radiative Case

Once the thermal model is completed it must be inserted inside the proper orbit in order to calculate all radiative conditions. In ESATAN the radiative view factors and heat fluxes can be obtained directly by inserting the planetary data, orbital parameters and pointing data. The orbit is first defined by choosing the attractor of the orbit, in this case the earth.

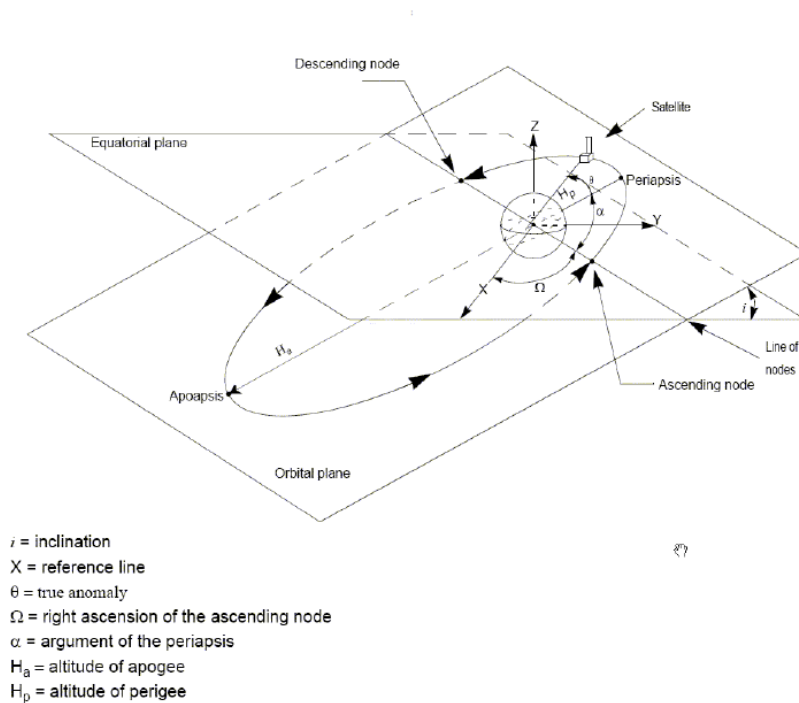


Figure 5.16: Orbital Parameters

This data must be inserted in the following fields.

All planet data is already included in ESATAN but can be manually changed (Left Table).

Afterwards the orbital parameters are inserted, as mentioned before the mission is based on a 6898 km LEOP orbit with an inclination of 97.48° with an eccentricity $e=0$ (Center Table).

The third data (Right Table) necessary is that relative to the satellite pointing. In order to describe the satellite's pointing two vectors must be defined. For the ESEO mission there are two pointing directions, SUN & NADIR pointing. In order to define these satellite orientations the following vectors were given:

- SUN POINTING = The x-axis points the Sun and the y-axis the North Celestial Pole
- NADIR POINTING = The -z-axis points the Earth and the y-axis follows the

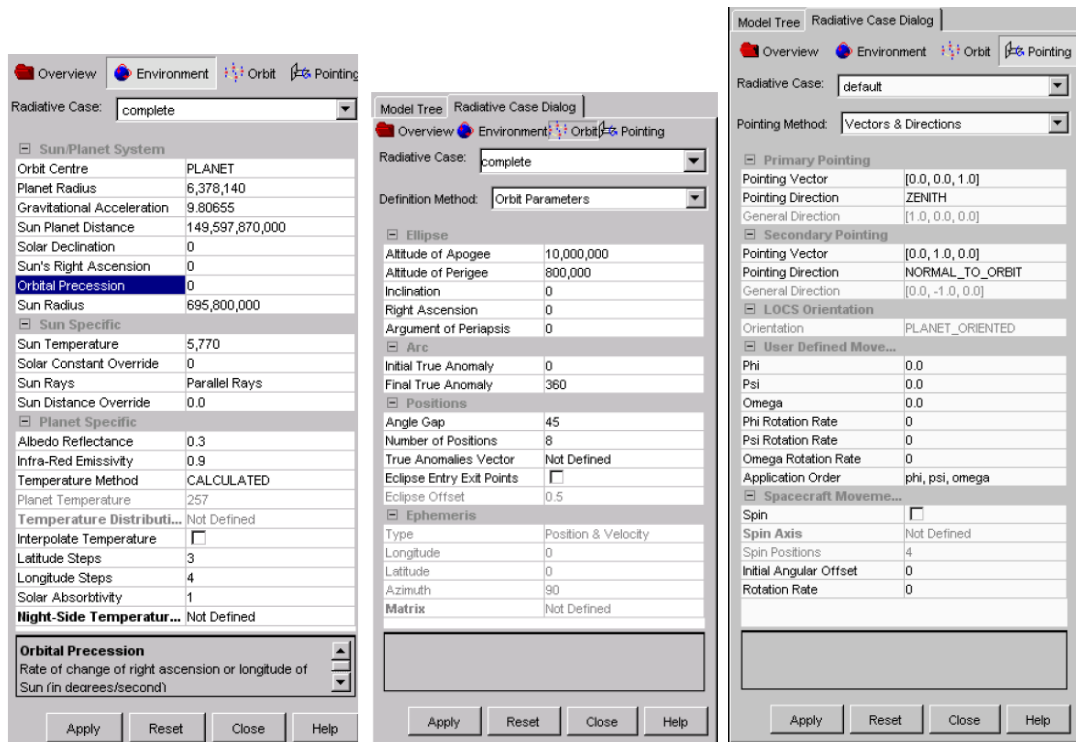


Figure 5.17: Radiative Case

velocity vector.

Chapter 6

Results & Margins

Once the satellite was properly modelled a series of studies were done in order to verify and if necessary modify the TCS. Initially a passive approach was considered and modelled. To study the thermal attitude of the satellite the thermal model was inserted into 52 different boundary condition for one orbit in order to be able to study all modes in both Nadir & Sun pointing. Afterwards the model was inserted in a single boundary condition over an arc of 56 orbits. In these 56 orbits the satellite will perform two operative mode cycles.

Unfortunately a passive TCS was not able to keep all components inside there thermal ranges and therefore a active TCS ws modelled. Heaters were modelled and inserted into the thermal model. Afterwards the thermal model was inserted into the 56 orbit operative modes cycle boundary condition.

Once the active TCS was properly modelled the satellite was further tested in order to be margined. The thermal model was again inserted into the 56 orbit operative modes cycle boundary condition. This time though the model was tested considering that all modelled values must be margined appropriately seeing these values inserted are nominal values which will never be respected.

1 Creating Analyses Case and Result Files

To create a thermal case in ESATAN the following parameters must be inserted:

-
- Analysis File Name
 - Radiative Case: Sun/Nadir Pointing
 - Boundary Conditions
 - Type of Solution Transient/Steady State
 - Tolerance Level and Iteration Number

Once the model name is inserted the radiative case is chosen. There are two ways to insert the radiative case, the first consists in choosing the radiative case name (Sun-Pointing or Nadir-Pointing). This analyses only studies a single orbit. The second instead consists in ticking chained radiative cases and connecting different radiative cases together. This option will be discussed later when we explain the operative orbits.

These parameters are inserted in the following window:

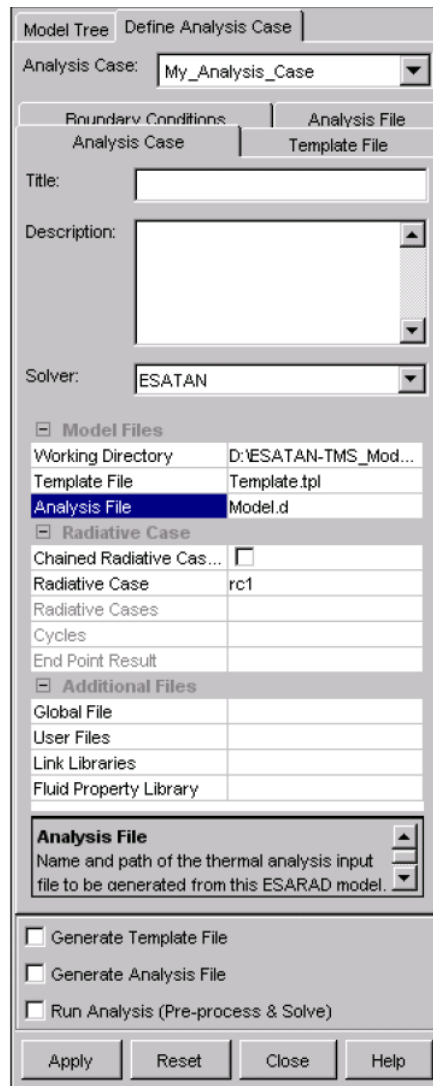


Figure 6.1: Thermal Model Analyses Case

Once the radiative case is defined the boundary conditions must be inserted by clicking the boundary conditions tab. This leads to a new window where the boundary conditions previously created necessary for each analysis case can be selected. Boundary conditions consist in imposed temperatures or imposed heat. In our case our boundary conditions all consist in dissipated heat.

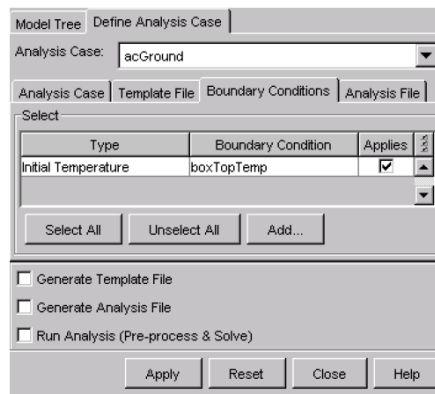


Figure 6.2: Thermal Model Analyses Case

Now that the thermal model has been perfectly locked into the boundary conditions we must select the type of analyses we want to consider. Our goal is to study how the temperature of our components vary in an entire orbit and therefore a transient analyses was necessary with a tolerance level of 0.0001 and a 1000 number of maximum iterations. In a transient analysis a thermal solution for every requested time step. In this analysis an entire orbit was analysed and divided into 100 elements with a time step of approximately 57 seconds.

Now that the analyses case is entirely defined the thermal input file is created and solved by ESATAN. ESATAN first calculates the radiative model heat fluxes one each node for every time step. Afterwards calculating internal view factors and heat fluxes together with calculating the heat fluxes between the satellite and its external environment ESATAN is able to calculate the temperature of each node in every time step. All this data is stored on an external output file which can be read with any note reader.

The data in this output file can be reopened in ESATAN in order to have only a visual contour representation of the temperatures and heat fluxes on each node.

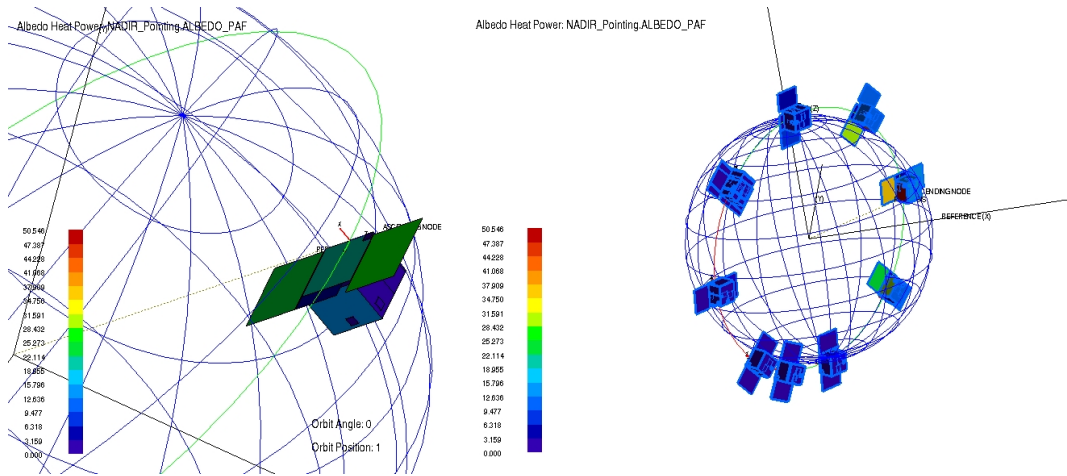


Figure 6.3: Thermal Model Analyses Case

Unfortunately to obtain numerical and graphical results another software called THERMNV is necessary. This software is licensed and was not available therefore a tool in matlab was created in order to retrieve the appropriate thermal data from the ESATAN output files.

2 ESATAN Results Tool

The tool created was necessary to extrapolate all Temperatures and Sun, Albedo and Planetary IR powers for every node in order to analyse how these parameters vary during orbit. The tool's main window is shown below:

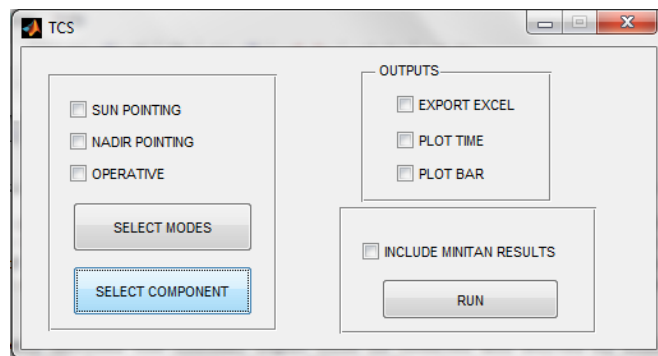


Figure 6.4: ESATAN Results Tools - Main Window

In the top left side of the main window the type of analysis can be chosen. By selecting either the Sun Pointing or Nadir Pointing option the tool will automatically calculate a single orbit single mode boundary condition. By selecting the operative option the tool calculates the 56 orbit boundary condition. If one of the two first options is chosen the tool allows the user to choose which modes he wants to analyse. Once the type of pointing is ticked and modes are chosen or the operative case is ticked the user can decide which components he wants to analyse.

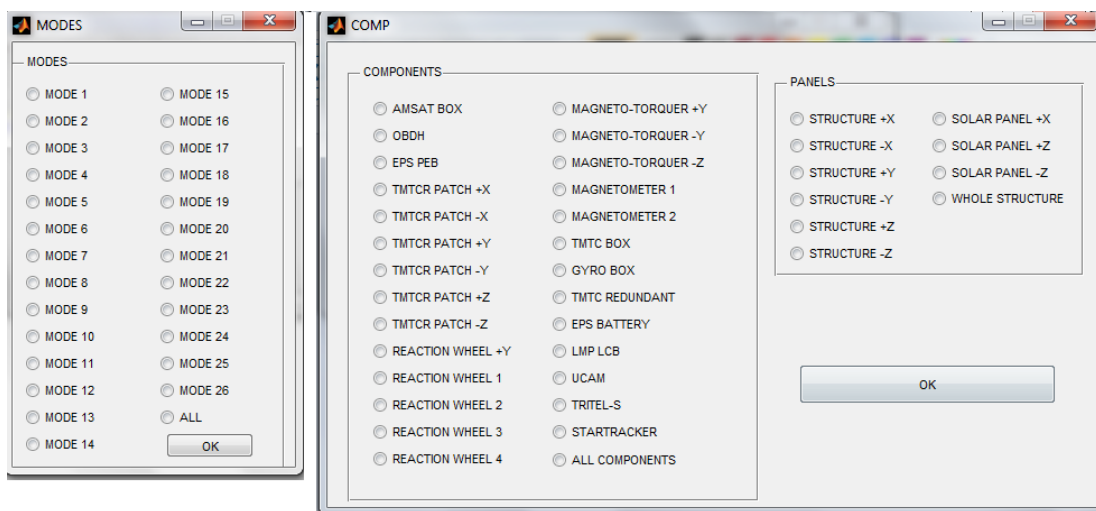


Figure 6.5: ESATAN Results Tools - Modes & Components

Once the components, modes and analysis type are chosen the type of output can be selected. The tool allows user to export data into EXCEL files, create a normal graph or to create a bar graph. All data exported can also be varified with earlier MiniTAN models created by the previous TCS engineer.

3 First Analysis - Single Modes

As previously mentioned the first analysis consisted in analyzing every distinctive mode in both pointing directions. The boundary conditions where thereful constant and non chained radiative cases were studied. The sun, albedo and planetary IR heat results obtained for both pointing directions for all external panels are illustrated below.

3.1 Sun-Pointing Heat Results

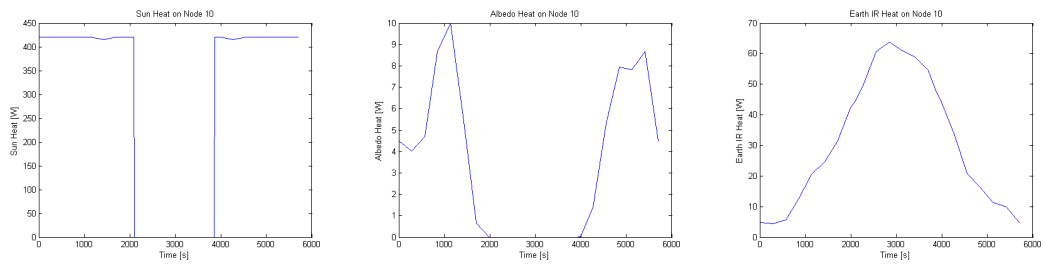


Figure 6.6: Node 10 Heat Results

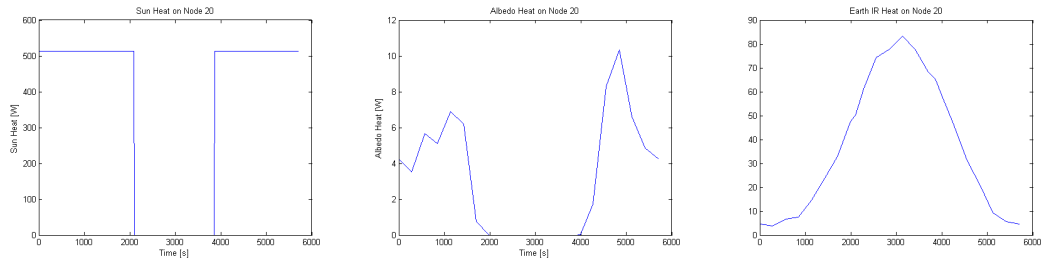


Figure 6.7: Node 20 Heat Results

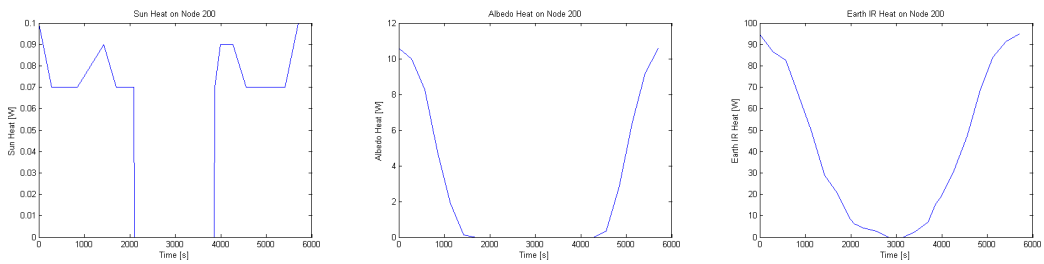


Figure 6.8: Node 200 Heat Results

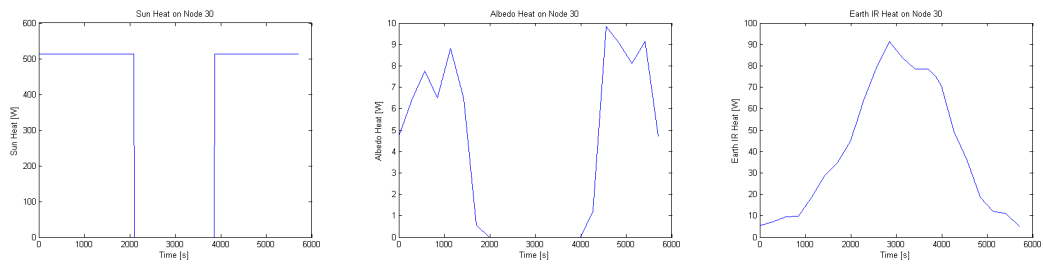


Figure 6.9: Node 30 Heat Results

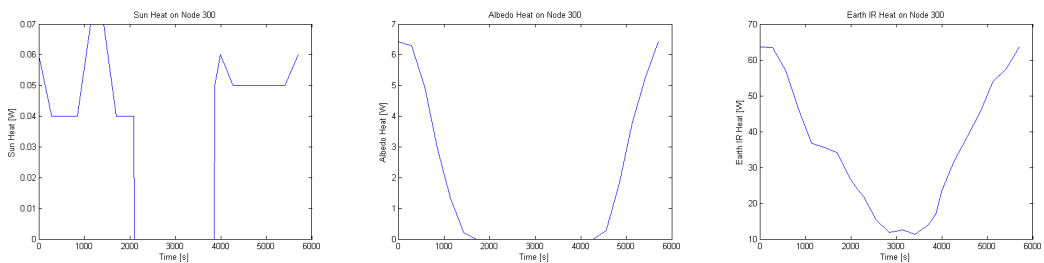


Figure 6.10: Node 300 Heat Results

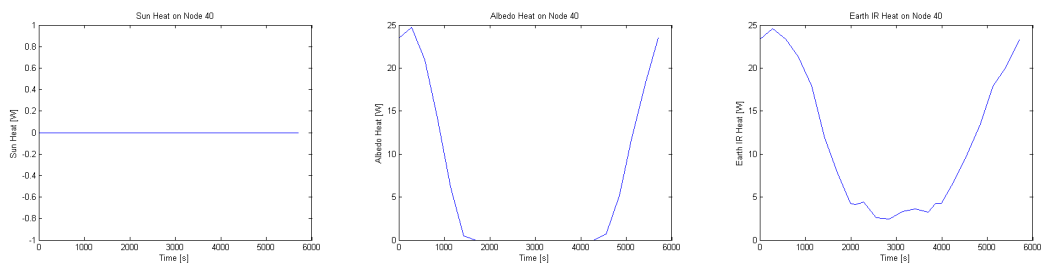


Figure 6.11: Node 40 Heat Results

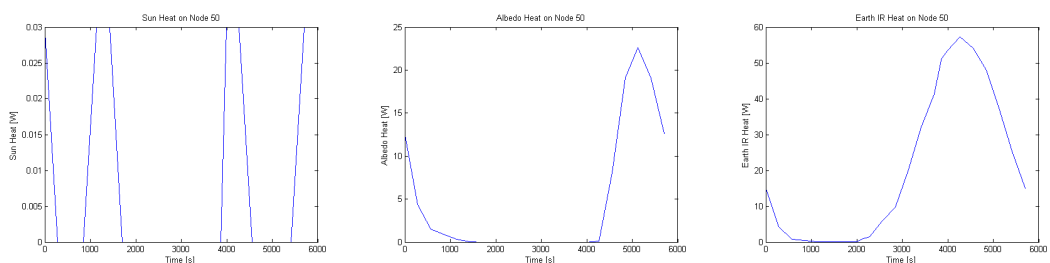


Figure 6.12: Node 50 Heat Results

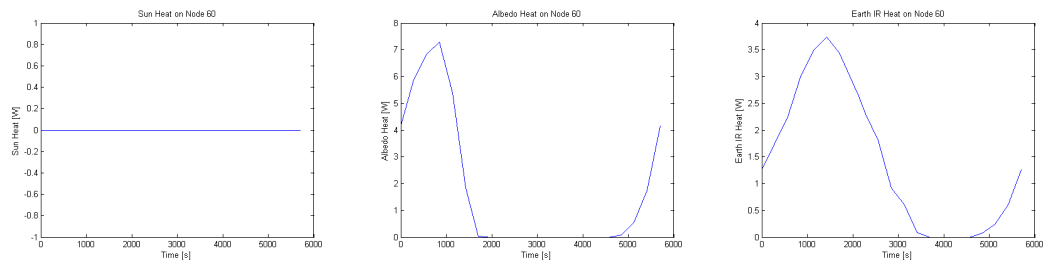


Figure 6.13: Node 60 Heat Results

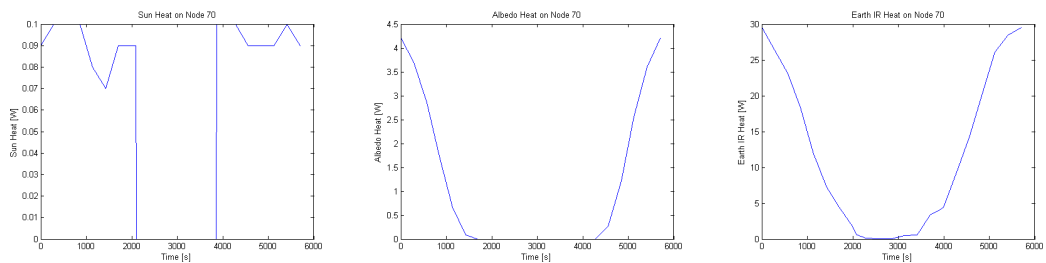


Figure 6.14: Node 70 Heat Results

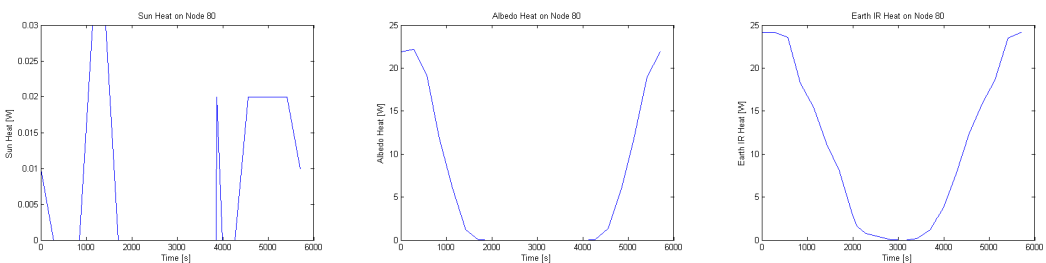


Figure 6.15: Node 80 Heat Results

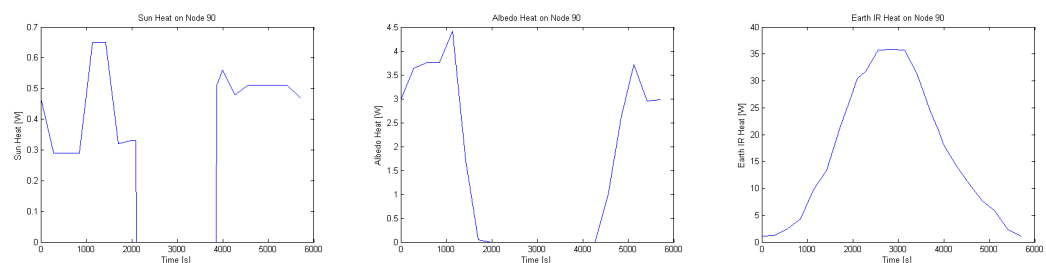


Figure 6.16: Node 90 Heat Results

3.2 Nadir-Pointing Heat Results

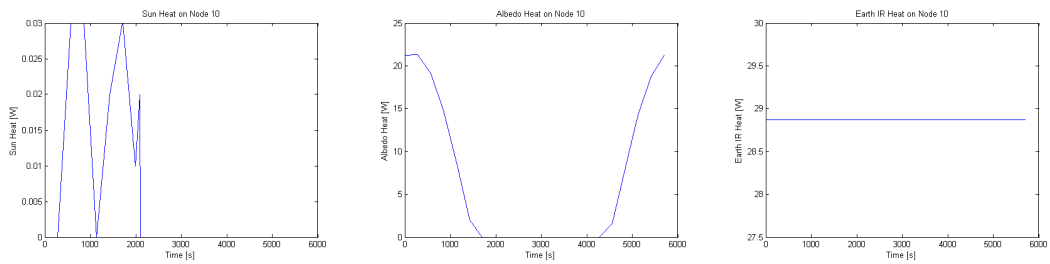


Figure 6.17: Node 10 Heat Results

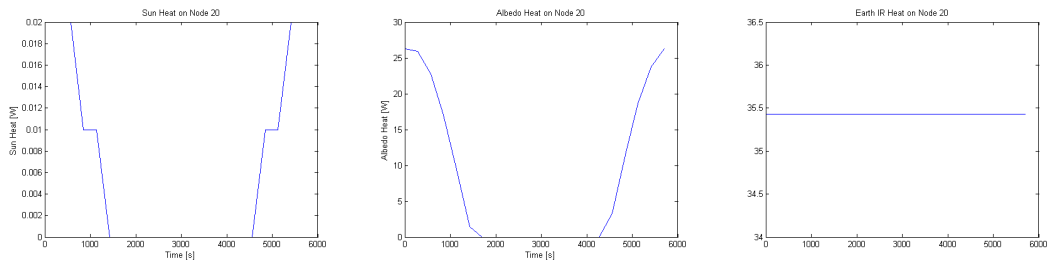


Figure 6.18: Node 20 Heat Results

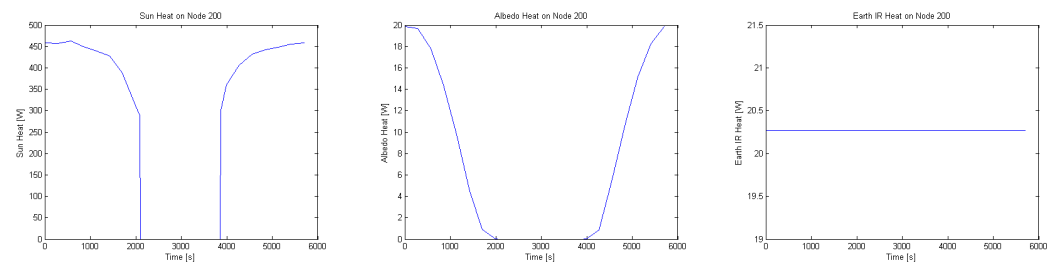


Figure 6.19: Node 200 Heat Results

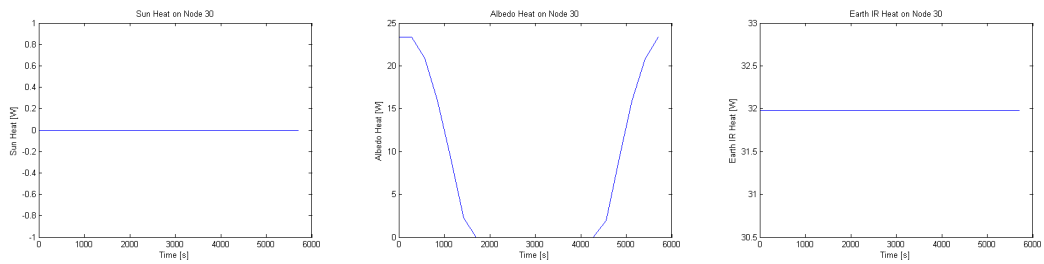


Figure 6.20: Node 30 Heat Results

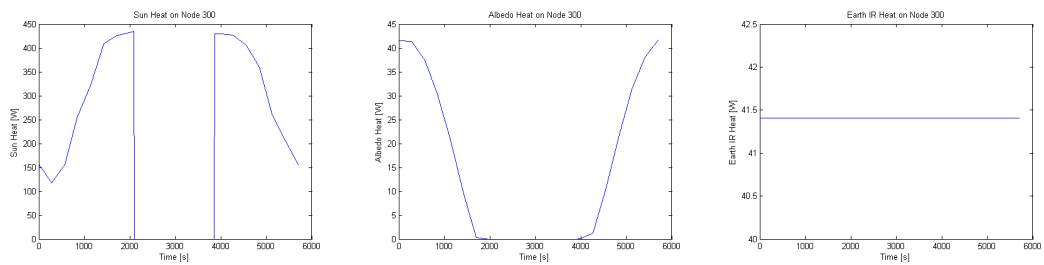


Figure 6.21: Node 300 Heat Results

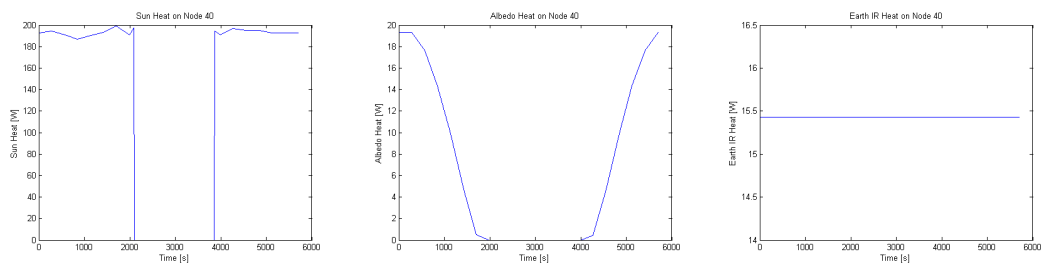


Figure 6.22: Node 40 Heat Results

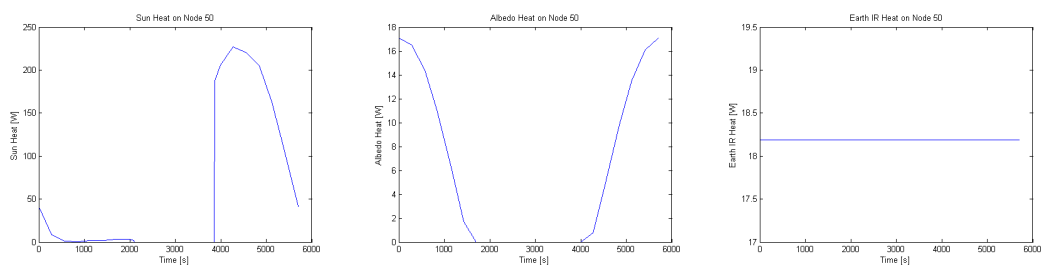


Figure 6.23: Node 50 Heat Results

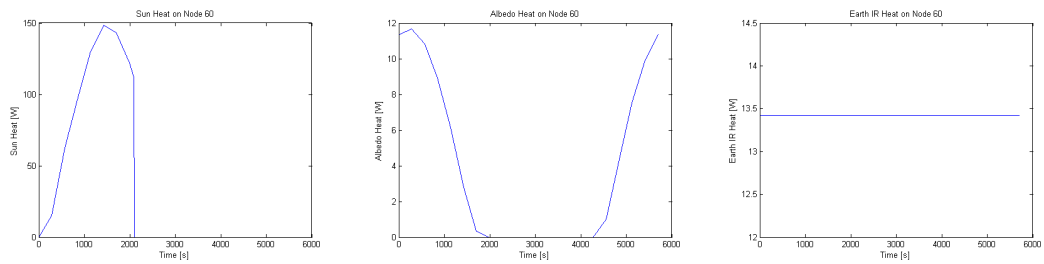


Figure 6.24: Node 60 Heat Results

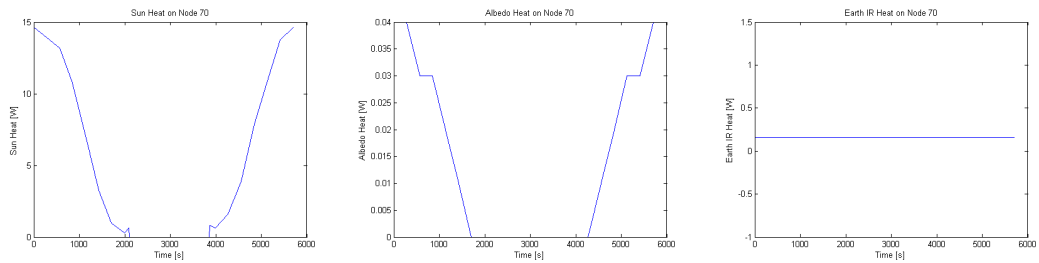


Figure 6.25: Node 70 Heat Results

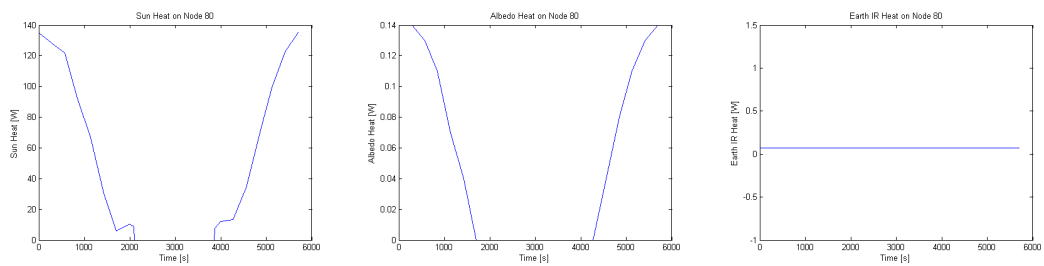


Figure 6.26: Node 80 Heat Results

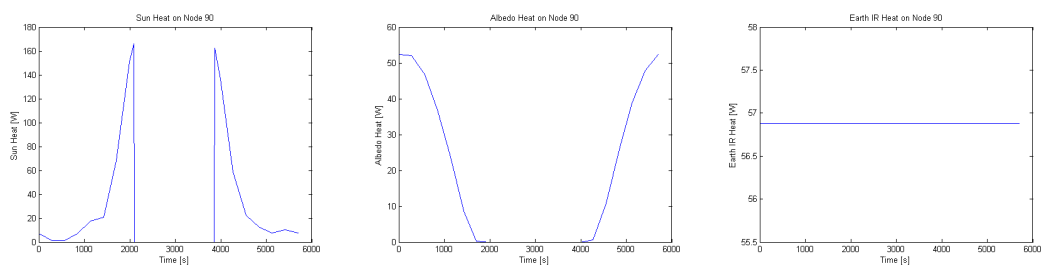


Figure 6.27: Node 90 Heat Results

These results do not vary if different modes are chosen.

3.3 Hot & Cold Case

As previously mentioned all modes were studied for both pointings. This leads to a large amount of results for every component. In order to prioritize critical components for each pointing case an excel sheet was created with a summarized version of all information obtained from all components for all modes. The ESATAN results tool extrapolates the minimum and maximum temperature of every component in each mode. It then confronts these temperature and saves the minimum and maximum value inside the excel sheet together with its associated mode. In this way instead of having to analyze all results manually, the ESATAN results tool automatically gives the hot and cold case of every component. The results obtained are shown in the following representation of the ESATAN results tool excel sheet.

Unit	Node Number	Max Calculated	Max Uncertainty	Max Predicted	Max Allowable Op	Max Margin Op	Max Allowable Fa	Max Margin Fa	Max Mode
COMPONENTS	ID	°C	°C	°C	°C	°C	°C	°C	N°
SOLAR +X	10	59.82	10	69.82	115	45.18	115	45.18	19
SOLAR +X	11	59.77	10	69.77	115	45.23	115	45.23	19
STRUCTURE +X	12	22.96	10	32.96	50	17.04	50	17.04	19
SOLAR +X	13	54.4	10	64.4	115	50.6	115	50.6	19
SOLAR +X	14	54.36	10	64.36	115	50.64	115	50.64	19
SOLAR -Z	20	51.4	10	61.4	115	53.6	115	53.6	19
SOLAR +Z	30	47.86	10	57.86	115	57.14	115	57.14	19
STRUCTURE -X	40	0.59	10	10.59	50	39.41	50	39.41	19
STRUCTURE +Y	50	0.68	10	10.68	50	39.32	50	39.32	19
STRUCTURE -Y	60	11.53	10	21.53	50	28.47	50	28.47	13
STRUCTURE +Z OSR	70	4.12	10	14.12	50	35.88	50	35.88	19
STRUCTURE +Z MLI	80	4.61	10	14.61	50	35.39	50	35.39	19
STRUCTURE -Z	90	-2.29	10	7.71	50	42.29	50	42.29	19
STRUCTURE +X	100	22.95	10	32.95	50	17.05	50	17.05	19
TMTCR PATCH +X	101	83.81	10	93.81	120	26.19	165	71.19	19
TMTCR PATCH +X	102	83.57	10	93.57	120	26.43	165	71.43	19
TMTCR PATCH +X	103	83.58	10	93.58	120	26.42	165	71.42	19
TMTCR PATCH +X	104	83.58	10	93.58	120	26.42	165	71.42	19
TMTCR PATCH +X	105	83.56	10	93.56	120	26.44	165	71.44	19
TMTCR PATCH +X	106	83.49	10	93.49	120	26.51	165	71.51	19
AMSAT BOX	107	34.81	10	44.81	65	20.19	100	55.19	19
AMSAT BOX	108	34.24	10	44.24	65	20.66	100	55.66	19
AMSAT BOX	109	28.17	10	38.17	65	26.83	100	61.83	19
AMSAT BOX	110	34.24	10	44.24	65	20.66	100	55.66	19
AMSAT BOX	111	36.78	10	46.78	65	18.22	100	53.22	19
AMSAT BOX	112	34.81	10	44.81	65	20.19	100	55.19	19
GYRO BOX	113	26.37	10	36.37	40	3.63	60	23.63	19
GYRO BOX	114	26.28	10	36.28	40	3.72	60	23.72	19
GYRO BOX	115	23.92	10	33.92	40	6.08	60	26.08	19
GYRO BOX	116	26.28	10	36.28	40	3.72	60	23.72	19
GYRO BOX	117	26.71	10	36.71	40	3.29	60	23.29	19
GYRO BOX	118	26.37	10	36.37	40	3.63	60	23.63	19
SOLAR -Z	200	51.35	10	61.35	115	53.65	115	53.65	18
SOLAR +Z	300	47.8	10	57.8	115	57.2	115	57.2	19
STRUCTURE -X	400	0.59	10	10.59	50	39.41	50	39.41	19
TMTCR PATCH -X	401	-3.16	10	6.84	120	113.16	165	158.16	19
TMTCR PATCH -X	402	-3.16	10	6.84	120	113.16	165	158.16	19
TMTCR PATCH -X	403	-3.17	10	6.83	120	113.17	165	158.17	19
TMTCR PATCH -X	404	-3.17	10	6.83	120	113.17	165	158.17	19
TMTCR PATCH -X	405	-3.17	10	6.83	120	113.17	165	158.17	19
TMTCR PATCH -X	406	-3.17	10	6.83	120	113.17	165	158.17	19
OBDAH	407	6.03	10	16.03	40	23.97	70	53.97	19
OBDAH	408	6.03	10	16.03	40	23.97	70	53.97	19
OBDAH	409	7.19	10	17.19	40	22.81	70	52.81	19
OBDAH	410	6.02	10	16.02	40	23.98	70	53.98	19
OBDAH	411	1.03	10	11.03	40	28.97	70	58.97	19
OBDAH	412	6.03	10	16.03	40	23.97	70	53.97	19
EPS PEB	413	2.72	10	12.72	40	27.28	50	37.28	19
EPS PEB	414	2.66	10	12.66	40	27.34	50	37.34	19
EPS PEB	415	3.11	10	13.11	40	26.89	50	36.89	19
EPS PEB	416	2.66	10	12.66	40	27.34	50	37.34	19
EPS PEB	417	0.73	10	10.73	40	29.27	50	39.27	19
EPS PEB	418	2.7	10	12.7	40	27.3	50	37.3	19
STAR TRACKER INSIDE	419	-1.39	10	8.61	50	41.39	70	61.39	19
STAR TRACKER INSIDE	420	-1.39	10	8.61	50	41.39	70	61.39	19
STAR TRACKER INSIDE	421	-1.39	10	8.61	50	41.39	70	61.39	19
STAR TRACKER INSIDE	422	-1.39	10	8.61	50	41.39	70	61.39	19
STAR TRACKER INSIDE	423	-1.4	10	8.6	50	41.4	70	61.4	19
STAR TRACKER INSIDE	424	-1.39	10	8.61	50	41.39	70	61.39	19
STAR TRACKER OUTSIDE	425	-13.62	10	-3.62	50	53.62	70	73.62	19
STRUCTURE +Y	500	0.69	10	10.69	50	39.31	50	39.31	19
TMTCR PATCH +Y	501	-5.94	10	4.06	120	115.94	165	160.94	19
TMTCR PATCH +Y	502	-5.94	10	4.06	120	115.94	165	160.94	19
TMTCR PATCH +Y	503	-5.94	10	4.06	120	115.94	165	160.94	19
TMTCR PATCH +Y	504	-5.93	10	4.07	120	115.93	165	160.93	19
TMTCR PATCH +Y	505	-5.94	10	4.06	120	115.94	165	160.94	19
TMTCR PATCH +Y	506	-5.94	10	4.06	120	115.94	165	160.94	19
REACTION WHEEL	507	0.68	10	10.68	45	34.32	60	49.32	19
REACTION WHEEL	508	0.68	10	10.68	45	34.32	70	59.32	19
REACTION WHEEL	509	0.69	10	10.69	45	34.31	60	49.31	19
REACTION WHEEL	510	0.69	10	10.69	45	34.31	60	49.31	19
REACTION WHEEL	511	0.68	10	10.68	45	34.32	60	49.32	19
REACTION WHEEL	512	0.68	10	10.68	45	34.32	60	49.32	19
MAGNETO-TORQUER +Y	519	0.72	10	10.72	45	34.28	55	44.28	19
UCAM	520	0.5	10	10.5	55	44.5	80	69.5	19
UCAM	521	0.46	10	10.46	55	44.54	80	69.54	19
UCAM	522	0.5	10	10.5	55	44.5	80	69.5	19
UCAM	523	0.62	10	10.62	55	44.38	80	69.38	19
UCAM	524	0.5	10	10.5	55	44.5	80	69.5	19
UCAM	525	0.5	10	10.5	55	44.5	80	69.5	19
STRUCTURE -Y	600	11.55	10	21.55	50	28.45	50	28.45	13
TMTCR PATCH -Y	601	3.01	10	13.01	120	106.99	165	151.99	13
TMTCR PATCH -Y	602	3.02	10	13.02	120	106.98	165	151.98	13
TMTCR PATCH -Y	603	3.02	10	13.02	120	106.98	165	151.98	13
TMTCR PATCH -Y	604	3.02	10	13.02	120	106.98	165	151.98	13
TMTCR PATCH -Y	605	3.02	10	13.02	120	106.98	165	151.98	13
TMTCR PATCH -Y	606	3.02	10	13.02	120	106.98	165	151.98	13
REACTION WHEEL 1	607	14.44	10	24.44	45	20.56	60	35.56	13

Figure 6.28: Hot Case - Sun Pointing Results 1

Unit	Node Number	Max Calculated	Max Uncertainty	Max Predicted	Max Allowable Op	Max Margin Op	Max Allowable Fa	Max Margin Fa	Max Mode
COMPONENTS	ID	°C	°C	°C	°C	°C	°C	°C	N°
REACTION WHEEL 1	608	12,14	10	22,14	45	22,86	60	37,86	13
REACTION WHEEL 1	609	14,44	10	24,44	45	20,56	60	35,56	13
REACTION WHEEL 1	610	15,02	10	25,02	45	19,98	60	34,98	13
REACTION WHEEL 1	611	14,43	10	24,43	45	20,57	60	35,57	13
REACTION WHEEL 1	612	14,43	10	24,43	45	20,57	60	35,57	13
REACTION WHEEL 2	613	14,41	10	24,41	45	20,59	60	35,59	13
REACTION WHEEL 2	614	12,14	10	22,14	45	22,86	60	37,86	13
REACTION WHEEL 2	615	14,42	10	24,42	45	20,58	60	35,58	13
REACTION WHEEL 2	616	15	10	25	45	20	60	35	13
REACTION WHEEL 2	617	14,42	10	24,42	45	20,58	60	35,58	13
REACTION WHEEL 2	618	14,42	10	24,42	45	20,58	60	35,58	13
REACTION WHEEL 3	619	14,44	10	24,44	45	20,56	60	35,56	13
REACTION WHEEL 3	620	12,14	10	22,14	45	22,86	60	37,86	13
REACTION WHEEL 3	621	14,43	10	24,43	45	20,57	60	35,57	13
REACTION WHEEL 3	622	15,01	10	25,01	45	19,99	60	34,99	13
REACTION WHEEL 3	623	14,42	10	24,42	45	20,58	60	35,58	13
REACTION WHEEL 3	624	14,43	10	24,43	45	20,57	60	35,57	13
REACTION WHEEL 4	625	14,43	10	24,43	45	20,57	60	35,57	13
REACTION WHEEL 4	626	12,13	10	22,13	45	22,87	60	37,87	13
REACTION WHEEL 4	627	14,43	10	24,43	45	20,57	60	35,57	13
REACTION WHEEL 4	628	15	10	25	45	20	60	35	13
REACTION WHEEL 4	629	14,41	10	24,41	45	20,59	60	35,59	13
REACTION WHEEL 4	630	14,43	10	24,43	45	20,57	60	35,57	13
MAGNETO-TORQUER -Y	631	11,54	10	21,54	45	23,46	55	33,46	13
STRUCTURE +Z OSR	700	4,13	10	14,13	50	35,87	50	35,87	19
TMTR PATCH +Z	701	16,49	10	26,49	120	93,51	165	138,51	19
TMTR PATCH +Z	702	16,49	10	26,49	120	93,51	165	138,51	19
TMTR PATCH +Z	703	16,57	10	26,57	120	93,43	165	138,43	19
TMTR PATCH +Z	704	16,49	10	26,49	120	93,51	165	138,51	19
TMTR PATCH +Z	705	16,48	10	26,48	120	93,52	165	138,52	19
TMTR PATCH +Z	706	16,49	10	26,49	120	93,51	165	138,51	19
TMTC REDUNDANT	707	4,22	10	14,22	60	45,78	70	55,78	19
TMTC REDUNDANT	708	3,86	10	13,86	60	46,14	70	56,14	19
TMTC REDUNDANT	709	3,88	10	13,88	60	46,12	70	56,12	19
TMTC REDUNDANT	710	3,86	10	13,86	60	46,14	70	56,14	19
TMTC REDUNDANT	711	3,87	10	13,87	60	46,13	70	56,13	19
TMTC REDUNDANT	712	3,83	10	13,83	60	46,17	70	56,17	19
MAGNETOMETER 1	713	4,99	10	14,99	65	50,01	80	65,01	19
MAGNETOMETER 1	714	5,18	10	15,18	65	49,82	80	64,82	19
MAGNETOMETER 1	715	5,18	10	15,18	65	49,82	80	64,82	19
MAGNETOMETER 1	716	5,18	10	15,18	65	49,82	80	64,82	19
MAGNETOMETER 1	717	5,18	10	15,18	65	49,82	80	64,82	19
MAGNETOMETER 1	718	5,24	10	15,24	65	49,76	80	64,76	19
MAGNETOMETER 2	719	4,99	10	14,99	65	50,01	80	65,01	19
MAGNETOMETER 2	720	5,18	10	15,18	65	49,82	80	64,82	19
MAGNETOMETER 2	721	5,18	10	15,18	65	49,82	80	64,82	19
MAGNETOMETER 2	722	5,18	10	15,18	65	49,82	80	64,82	19
MAGNETOMETER 2	723	5,18	10	15,18	65	49,82	80	64,82	19
MAGNETOMETER 2	724	5,24	10	15,24	65	49,76	80	64,76	19
LMP LCB	725	3,97	10	13,97	60	46,03	80	66,03	19
LMP LCB	726	3,97	10	13,97	60	46,03	80	66,03	19
LMP LCB	727	3,97	10	13,97	60	46,03	80	66,03	19
LMP LCB	728	3,97	10	13,97	60	46,03	80	66,03	19
LMP LCB	729	3,97	10	13,97	60	46,03	80	66,03	19
LMP LCB	730	3,98	10	13,98	60	46,02	80	66,02	19
TRITEL S	731	3,97	10	13,97	20	6,03	70	56,03	19
TRITEL S	732	3,98	10	13,98	20	6,02	70	56,02	19
TRITEL S	733	3,98	10	13,98	20	6,02	70	56,02	19
TRITEL S	734	3,98	10	13,98	20	6,02	70	56,02	19
TRITEL S	735	3,98	10	13,98	20	6,02	70	56,02	19
TRITEL S	736	3,99	10	13,99	20	6,01	70	56,01	19
MAGNETO-TORQUER -Z	737	-2,21	10	7,79	45	37,21	55	47,21	19
STRUCTURE +Z MLI	800	4,61	10	14,61	50	35,39	50	35,39	19
STRUCTURE -Z	900	-2,27	10	7,73	50	42,27	50	42,27	19
TMTR PATCH -Z	901	2,94	10	12,94	120	107,06	165	152,06	19
TMTR PATCH -Z	902	2,94	10	12,94	120	107,06	165	152,06	19
TMTR PATCH -Z	903	2,99	10	12,99	120	107,01	165	152,01	19
TMTR PATCH -Z	904	2,93	10	12,93	120	107,07	165	152,07	19
TMTR PATCH -Z	905	2,93	10	12,93	120	107,07	165	152,07	19
TMTR PATCH -Z	906	2,93	10	12,93	120	107,07	165	152,07	19
TMTC BOX	907	3,53	10	13,53	60	46,47	70	56,47	19
TMTC BOX	908	2,37	10	12,37	60	47,63	70	57,63	19
TMTC BOX	909	2,11	10	12,11	60	47,89	70	57,89	19
TMTC BOX	910	2,36	10	12,36	60	47,64	70	57,64	19
TMTC BOX	911	2,1	10	12,1	60	47,9	70	57,9	19
TMTC BOX	912	-1,81	10	8,19	60	51,81	70	61,81	19
EPS BATTERY	913	-2,27	10	7,73	15	7,27	20	12,27	19
EPS BATTERY	914	-2,31	10	7,69	15	7,31	20	12,31	19
EPS BATTERY	915	-2,28	10	7,72	15	7,28	20	12,28	19
EPS BATTERY	916	-2,3	10	7,7	15	7,3	20	12,3	19
EPS BATTERY	917	-2,3	10	7,7	15	7,3	20	12,3	19
EPS BATTERY	918	-2,27	10	7,73	15	7,27	20	12,27	19
EPS BATTERY	919	1,29	10	11,29	15	3,71	20	8,71	19
EPS BATTERY	920	1,29	10	11,29	15	3,71	20	8,71	19
EPS BATTERY	921	1,29	10	11,29	15	3,71	20	8,71	19
EPS BATTERY	922	1,29	10	11,29	15	3,71	20	8,71	19
EPS BATTERY	923	1,29	10	11,29	15	3,71	20	8,71	19
EPS BATTERY	924	1,29	10	11,29	15	3,71	20	8,71	19

Figure 6.29: Hot Case - Sun Pointing Results 2

Unit	Node Number	Min Calculated	Min Uncertainty	Min Predicted	Min Allowable Op	Min Margin Op	Min Allowable Fa	Max Margin Fa	Min Mode
COMPONENTS	ID	°C	°C	°C	°C	°C	°C	°C	N°
SOLAR +X	10	-8.61	-10	-18.61	-90	71.39	-90	71.39	24
SOLAR +X	11	-8.6	-10	-18.6	-90	71.4	-90	71.4	24
STRUCTURE +X	12	-9.67	-10	-19.67	-30	10.33	-30	10.33	24
SOLAR +X	13	-13.61	-10	-23.61	-90	66.39	-90	66.39	24
SOLAR +X	14	-13.61	-10	-23.61	-90	66.39	-90	66.39	24
SOLAR -Z	20	-30.49	-10	-40.49	-90	49.51	-90	49.51	24
SOLAR +Z	30	-32.27	-10	-42.27	-90	47.73	-90	47.73	24
STRUCTURE -X	40	-13.45	-10	-23.45	-30	6.55	-30	6.55	24
STRUCTURE +Y	50	-14.07	-10	-24.07	-30	5.93	-30	5.93	24
STRUCTURE -Y	60	-31.19	-10	-41.19	-30	-11.19	-30	-11.19	24
STRUCTURE +Z OSR	70	-14.32	-10	-24.32	-30	5.68	-30	5.68	24
STRUCTURE +Z MLI	80	-14.46	-10	-24.46	-30	5.54	-30	5.54	24
STRUCTURE -Z	90	-17.26	-10	-27.26	-30	2.74	-30	2.74	24
STRUCTURE +X	100	-9.67	-10	-19.67	-30	10.33	-30	10.33	24
TMTCR PATCH +X	101	53.51	-10	43.51	-100	143.51	-155	198.51	24
TMTCR PATCH +X	102	53.23	-10	43.23	-100	143.23	-155	198.23	24
TMTCR PATCH +X	103	53.24	-10	43.24	-100	143.24	-155	198.24	24
TMTCR PATCH +X	104	53.35	-10	43.35	-100	143.35	-155	198.35	24
TMTCR PATCH +X	105	53.24	-10	43.24	-100	143.24	-155	198.24	24
TMTCR PATCH +X	106	53.15	-10	43.15	-100	143.15	-155	198.15	24
AMSAT BOX	107	-8.95	-10	-18.95	-40	21.05	-50	31.05	24
AMSAT BOX	108	-8.98	-10	-18.98	-40	21.02	-50	31.02	24
AMSAT BOX	109	-9.27	-10	-19.27	-40	20.63	-50	30.63	24
AMSAT BOX	110	-8.98	-10	-18.98	-40	21.02	-50	31.02	24
AMSAT BOX	111	-8.81	-10	-18.81	-40	21.19	-50	31.19	24
AMSAT BOX	112	-8.95	-10	-18.95	-40	21.05	-50	31.05	24
GYRO BOX	113	-8.14	-10	-18.14	-5	-13.14	-25	6.86	24
GYRO BOX	114	-8.13	-10	-18.13	-5	-13.13	-25	6.87	24
GYRO BOX	115	-8.74	-10	-18.74	-5	-13.74	-25	6.26	24
GYRO BOX	116	-8.13	-10	-18.13	-5	-13.13	-25	6.87	24
GYRO BOX	117	-8.16	-10	-18.16	-5	-13.16	-25	6.84	24
GYRO BOX	118	-8.14	-10	-18.14	-5	-13.14	-25	6.86	24
SOLAR -Z	200	-30.5	-10	-40.5	-90	49.5	-90	49.5	24
SOLAR +Z	300	-32.27	-10	-42.27	-90	47.73	-90	47.73	24
STRUCTURE -X	400	-13.44	-10	-23.44	-30	6.56	-30	6.56	24
TMTCR PATCH -X	401	-15.63	-10	-25.63	-100	74.37	-155	129.37	24
TMTCR PATCH -X	402	-15.64	-10	-25.64	-100	74.36	-155	129.36	24
TMTCR PATCH -X	403	-15.63	-10	-25.63	-100	74.37	-155	129.37	24
TMTCR PATCH -X	404	-15.63	-10	-25.63	-100	74.37	-155	129.37	24
TMTCR PATCH -X	405	-15.63	-10	-25.63	-100	74.37	-155	129.37	24
TMTCR PATCH -X	406	-15.64	-10	-25.64	-100	74.36	-155	129.36	24
OSDH	407	-5.9	-10	-15.9	-20	4.1	-35	19.1	24
OSDH	408	-5.91	-10	-15.91	-20	4.09	-35	19.09	24
OSDH	409	-4.66	-10	-14.66	-20	5.34	-35	20.34	24
OSDH	410	-5.91	-10	-15.91	-20	4.09	-35	19.09	24
OSDH	411	-12.84	-10	-22.84	-20	-2.84	-35	12.16	24
OSDH	412	-5.9	-10	-15.9	-20	4.1	-35	19.1	24
EPS PEB	413	-9.52	-10	-19.52	-20	0.48	-30	10.48	24
EPS PEB	414	-9.59	-10	-19.59	-20	0.41	-30	10.41	24
EPS PEB	415	-9.07	-10	-19.07	-20	0.93	-30	10.93	24
EPS PEB	416	-9.58	-10	-19.58	-20	0.42	-30	10.42	24
EPS PEB	417	-13.18	-10	-23.18	-20	-3.18	-30	6.82	24
EPS PEB	418	-9.53	-10	-19.53	-20	0.47	-30	10.47	24
STAR TRACKER INSIDE	419	-10.83	-10	-20.83	-20	-0.83	-40	19.17	24
STAR TRACKER INSIDE	420	-10.83	-10	-20.83	-20	-0.83	-40	19.17	24
STAR TRACKER INSIDE	421	-10.83	-10	-20.83	-20	-0.83	-40	19.17	24
STAR TRACKER INSIDE	422	-10.83	-10	-20.83	-20	-0.83	-40	19.17	24
STAR TRACKER INSIDE	423	-10.83	-10	-20.83	-20	-0.83	-40	19.17	24
STAR TRACKER INSIDE	424	-10.83	-10	-20.83	-20	-0.83	-40	19.17	24
STAR TRACKER OUTSIDE	425	-21.18	-10	-31.18	-20	-11.18	-40	8.82	24
STRUCTURE +Y	500	-14.07	-10	-24.07	-30	5.93	-30	5.93	24
TMTCR PATCH +Y	501	-17.69	-10	-27.69	-100	72.31	-155	127.31	24
TMTCR PATCH +Y	502	-17.7	-10	-27.7	-100	72.3	-155	127.3	24
TMTCR PATCH +Y	503	-17.7	-10	-27.7	-100	72.3	-155	127.3	24
TMTCR PATCH +Y	504	-17.7	-10	-27.7	-100	72.3	-155	127.3	24
TMTCR PATCH +Y	505	-17.7	-10	-27.7	-100	72.3	-155	127.3	24
TMTCR PATCH +Y	506	-17.7	-10	-27.7	-100	72.3	-155	127.3	24
REACTION WHEEL	507	-14.05	-10	-24.05	-20	-4.05	-25	0.95	24
REACTION WHEEL	508	-14.05	-10	-24.05	-20	-4.05	-25	0.95	24
REACTION WHEEL	509	-14.05	-10	-24.05	-20	-4.05	-25	0.95	24
REACTION WHEEL	510	-14.06	-10	-24.06	-20	-4.06	-25	0.94	24
REACTION WHEEL	511	-14.05	-10	-24.05	-20	-4.05	-25	0.95	24
REACTION WHEEL	512	-14.05	-10	-24.05	-20	-4.05	-25	0.95	24
MAGNETO-TORQUER +Y	519	-13.99	-10	-23.99	-30	6.01	-40	16.01	24
UCAM	520	-13.96	-10	-23.96	-20	-3.96	-45	21.04	24
UCAM	521	-13.94	-10	-23.94	-20	-3.94	-45	21.06	24
UCAM	522	-13.96	-10	-23.96	-20	-3.96	-45	21.04	24
UCAM	523	-14.03	-10	-24.03	-20	-4.03	-45	20.97	24
UCAM	524	-13.96	-10	-23.96	-20	-3.96	-45	21.04	24
UCAM	525	-13.96	-10	-23.96	-20	-3.96	-45	21.04	24
STRUCTURE -Y	600	-31.19	-10	-41.19	-30	-11.19	-30	-11.19	24
TMTCR PATCH -Y	601	-26.25	-10	-36.25	-100	63.75	-155	118.75	24
TMTCR PATCH -Y	602	-26.26	-10	-36.26	-100	63.74	-155	118.74	24
TMTCR PATCH -Y	603	-26.25	-10	-36.25	-100	63.75	-155	118.75	24
TMTCR PATCH -Y	604	-26.25	-10	-36.25	-100	63.75	-155	118.75	24
TMTCR PATCH -Y	605	-26.25	-10	-36.25	-100	63.75	-155	118.75	24
TMTCR PATCH -Y	606	-26.26	-10	-36.26	-100	63.74	-155	118.74	24
REACTION WHEEL 1	607	-30.93	-10	-40.93	-20	-20.93	-25	-15.93	24

Figure 6.30: Cold Case - Sun Pointing Results 1

Unit	Node Number	Min Calculated	Min Uncertainty	Min Predicted	Min Allowable Op	Min Margin Op	Min Allowable Fa	Max Margin Fa	Min Mode
COMPONENTS	ID	°C	°C	°C	°C	°C	°C	°C	N°
REACTION WHEEL 1	608	-31.15	-10	-41.15	-20	-21.15	-25	-16.15	24
REACTION WHEEL 1	609	-30.92	-10	-40.92	-20	-20.92	-25	-15.92	24
REACTION WHEEL 1	610	-30.86	-10	-40.86	-20	-20.86	-25	-15.86	24
REACTION WHEEL 1	611	-30.94	-10	-40.94	-20	-20.94	-25	-15.94	24
REACTION WHEEL 1	612	-30.93	-10	-40.93	-20	-20.93	-25	-15.93	24
REACTION WHEEL 2	613	-30.93	-10	-40.93	-20	-20.93	-25	-15.93	24
REACTION WHEEL 2	614	-31.15	-10	-41.15	-20	-21.15	-25	-16.15	24
REACTION WHEEL 2	615	-30.92	-10	-40.92	-20	-20.92	-25	-15.92	24
REACTION WHEEL 2	616	-30.86	-10	-40.86	-20	-20.86	-25	-15.86	24
REACTION WHEEL 2	617	-30.94	-10	-40.94	-20	-20.94	-25	-15.94	24
REACTION WHEEL 2	618	-30.93	-10	-40.93	-20	-20.93	-25	-15.93	24
REACTION WHEEL 3	619	-30.97	-10	-40.97	-20	-20.97	-25	-15.97	24
REACTION WHEEL 3	620	-31.16	-10	-41.16	-20	-21.16	-25	-16.16	24
REACTION WHEEL 3	621	-30.98	-10	-40.98	-20	-20.98	-25	-15.98	24
REACTION WHEEL 3	622	-30.92	-10	-40.92	-20	-20.92	-25	-15.92	24
REACTION WHEEL 3	623	-30.97	-10	-40.97	-20	-20.97	-25	-15.97	24
REACTION WHEEL 3	624	-30.98	-10	-40.98	-20	-20.98	-25	-15.98	24
REACTION WHEEL 4	625	-30.95	-10	-40.95	-20	-20.95	-25	-15.95	24
REACTION WHEEL 4	626	-31.15	-10	-41.15	-20	-21.15	-25	-16.15	24
REACTION WHEEL 4	627	-30.96	-10	-40.96	-20	-20.96	-25	-15.96	24
REACTION WHEEL 4	628	-30.89	-10	-40.89	-20	-20.89	-25	-15.89	24
REACTION WHEEL 4	629	-30.95	-10	-40.95	-20	-20.95	-25	-15.95	24
REACTION WHEEL 4	630	-30.95	-10	-40.95	-20	-20.95	-25	-15.95	24
MAGNETO-TORQUER -Y	631	-31.17	-10	-41.17	-30	-11.17	-40	-1.17	24
STRUCTURE +Z OSR	700	-14.21	-10	-24.21	-30	5.69	-30	5.69	24
TMTR PATCH +Z	701	1.85	-10	-8.15	-100	91.85	-155	146.85	24
TMTR PATCH +Z	702	1.86	-10	-8.14	-100	91.86	-155	146.86	24
TMTR PATCH +Z	703	1.97	-10	-8.03	-100	91.97	-155	146.97	24
TMTR PATCH +Z	704	1.86	-10	-8.14	-100	91.86	-155	146.86	24
TMTR PATCH +Z	705	1.85	-10	-8.15	-100	91.85	-155	146.85	24
TMTR PATCH +Z	706	1.87	-10	-8.13	-100	91.87	-155	146.87	24
TMTC REDUNDANT	707	-14.3	-10	-24.3	-25	0.7	-35	10.7	24
TMTC REDUNDANT	708	-13.42	-10	-23.42	-25	1.58	-35	11.58	24
TMTC REDUNDANT	709	-13.48	-10	-23.48	-25	1.52	-35	11.52	24
TMTC REDUNDANT	710	-13.42	-10	-23.42	-25	1.58	-35	11.58	24
TMTC REDUNDANT	711	-13.48	-10	-23.48	-25	1.52	-35	11.52	24
TMTC REDUNDANT	712	-13.51	-10	-23.51	-25	1.49	-35	11.49	24
MAGNETOMETER 1	713	-14.11	-10	-24.11	-20	-4.11	-40	15.89	24
MAGNETOMETER 1	714	-13.94	-10	-23.94	-20	-3.94	-40	16.06	24
MAGNETOMETER 1	715	-13.94	-10	-23.94	-20	-3.94	-40	16.06	24
MAGNETOMETER 1	716	-13.94	-10	-23.94	-20	-3.94	-40	16.06	24
MAGNETOMETER 1	717	-13.94	-10	-23.94	-20	-3.94	-40	16.06	24
MAGNETOMETER 1	718	-13.88	-10	-23.88	-20	-3.88	-40	16.12	24
MAGNETOMETER 2	719	-14.11	-10	-24.11	-20	-4.11	-40	15.89	24
MAGNETOMETER 2	720	-13.94	-10	-23.94	-20	-3.94	-40	16.06	24
MAGNETOMETER 2	721	-13.94	-10	-23.94	-20	-3.94	-40	16.06	24
MAGNETOMETER 2	722	-13.94	-10	-23.94	-20	-3.94	-40	16.06	24
MAGNETOMETER 2	723	-13.94	-10	-23.94	-20	-3.94	-40	16.06	24
MAGNETOMETER 2	724	-13.88	-10	-23.88	-20	-3.88	-40	16.12	24
LMP LCB	725	-14.23	-10	-24.23	-25	0.77	-45	20.77	24
LMP LCB	726	-14.1	-10	-24.1	-25	0.9	-45	20.9	24
LMP LCB	727	-14.1	-10	-24.1	-25	0.9	-45	20.9	24
LMP LCB	728	-14.1	-10	-24.1	-25	0.9	-45	20.9	24
LMP LCB	729	-14.1	-10	-24.1	-25	0.9	-45	20.9	24
LMP LCB	730	-14.06	-10	-24.06	-25	0.94	-45	20.94	24
TRITEL S	731	-14.24	-10	-24.24	-30	5.76	-40	15.76	24
TRITEL S	732	-14.13	-10	-24.13	-30	5.87	-40	15.87	24
TRITEL S	733	-14.13	-10	-24.13	-30	5.87	-40	15.87	24
TRITEL S	734	-14.13	-10	-24.13	-30	5.87	-40	15.87	24
TRITEL S	735	-14.13	-10	-24.13	-30	5.87	-40	15.87	24
TRITEL S	736	-14.06	-10	-24.06	-30	5.94	-40	15.94	24
MAGNETO-TORQUER -Z	737	-17.19	-10	-27.19	-30	2.81	-40	12.81	24
STRUCTURE +Z MLI	800	-14.46	-10	-24.46	-30	5.54	-30	5.54	24
STRUCTURE -Z	900	-17.25	-10	-27.25	-30	2.75	-30	2.75	24
TMTR PATCH -Z	901	-8.4	-10	-18.4	-100	81.6	-155	136.6	24
TMTR PATCH -Z	902	-8.41	-10	-18.41	-100	81.59	-155	136.59	24
TMTR PATCH -Z	903	-8.34	-10	-18.34	-100	81.66	-155	136.66	24
TMTR PATCH -Z	904	-8.41	-10	-18.41	-100	81.59	-155	136.59	24
TMTR PATCH -Z	905	-8.42	-10	-18.42	-100	81.58	-155	136.58	24
TMTR PATCH -Z	906	-8.42	-10	-18.42	-100	81.58	-155	136.58	24
TMTC BOX	907	-14.82	-10	-24.82	-25	0.18	-35	10.18	24
TMTC BOX	908	-15.31	-10	-25.31	-25	-0.31	-35	9.69	24
TMTC BOX	909	-15.41	-10	-25.41	-25	-0.41	-35	9.59	24
TMTC BOX	910	-15.31	-10	-25.31	-25	-0.31	-35	9.69	24
TMTC BOX	911	-15.42	-10	-25.42	-25	-0.42	-35	9.58	24
TMTC BOX	912	-17.03	-10	-27.03	-25	-2.03	-35	7.97	24
EPS BATTERY	913	-17.2	-10	-27.2	0	-27.2	-5	-22.2	24
EPS BATTERY	914	-17.23	-10	-27.23	0	-27.23	-5	-22.23	24
EPS BATTERY	915	-17.2	-10	-27.2	0	-27.2	-5	-22.2	24
EPS BATTERY	916	-17.21	-10	-27.21	0	-27.21	-5	-22.21	24
EPS BATTERY	917	-17.22	-10	-27.22	0	-27.22	-5	-22.22	24
EPS BATTERY	918	-17.23	-10	-27.23	0	-27.23	-5	-22.23	24
EPS BATTERY	919	-8.9	-10	-18.9	0	-18.9	-5	-13.9	24
EPS BATTERY	920	-8.9	-10	-18.9	0	-18.9	-5	-13.9	24
EPS BATTERY	921	-8.9	-10	-18.9	0	-18.9	-5	-13.9	24
EPS BATTERY	922	-8.9	-10	-18.9	0	-18.9	-5	-13.9	24
EPS BATTERY	923	-8.9	-10	-18.9	0	-18.9	-5	-13.9	24
EPS BATTERY	924	-8.9	-10	-18.9	0	-18.9	-5	-13.9	24

Figure 6.31: Cold Case - Sun Pointing Results 2

Unit	Node Number	Max Calculated	Max Uncertainty	Max Predicted	Max Allowable Op	Max Margin Op	Max Allowable Fa	Max Margin Fa	Max Mode
COMPONENTS	ID	°C	°C	°C	°C	°C	°C	°C	N°
SOLAR +X	10	-1,87	10	8,13	115	106,87	115	106,87	19
SOLAR +X	11	-1,85	10	8,15	115	106,85	115	106,85	19
STRUCTURE +X	12	21,46	10	31,46	50	18,54	50	18,54	19
SOLAR +X	13	15,88	10	25,88	115	89,12	115	89,12	19
SOLAR +X	14	15,94	10	25,94	115	89,06	115	89,06	19
SOLAR -Z	20	36,24	10	46,24	115	68,76	115	68,76	3
SOLAR +Z	30	20,07	10	30,07	115	84,93	115	84,93	19
STRUCTURE -X	40	34,87	10	44,87	50	5,13	50	5,13	19
STRUCTURE +Y	50	26,98	10	36,98	50	13,02	50	13,02	19
STRUCTURE -Y	60	39,73	10	49,73	50	0,27	50	0,27	13
STRUCTURE +Z OSR	70	22,33	10	32,33	50	17,67	50	17,67	19
STRUCTURE +Z MLI	80	24,56	10	34,56	50	15,44	50	15,44	19
STRUCTURE -Z	90	29,02	10	39,02	50	10,98	50	10,98	19
STRUCTURE +X	100	21,48	10	31,48	50	18,52	50	18,52	19
TMTR PATCH +X	101	13,45	10	23,45	120	96,55	165	141,55	19
TMTR PATCH +X	102	13,58	10	23,58	120	96,42	165	141,42	19
TMTR PATCH +X	103	13,47	10	23,47	120	96,53	165	141,53	19
TMTR PATCH +X	104	13,45	10	23,45	120	96,55	165	141,55	19
TMTR PATCH +X	105	13,46	10	23,46	120	96,54	165	141,54	19
TMTR PATCH +X	106	13,5	10	23,5	120	96,5	165	141,5	19
AMSAT BOX	107	33,2	10	43,2	65	21,8	100	56,8	19
AMSAT BOX	108	32,73	10	42,73	65	22,27	100	57,27	19
AMSAT BOX	109	26,68	10	36,68	65	28,32	100	63,32	19
AMSAT BOX	110	32,73	10	42,73	65	22,27	100	57,27	19
AMSAT BOX	111	35,15	10	45,15	65	19,85	100	54,85	19
AMSAT BOX	112	33,2	10	43,2	65	21,8	100	56,8	19
GYRO BOX	113	24,91	10	34,91	40	5,09	60	25,09	19
GYRO BOX	114	24,82	10	34,82	40	5,18	60	25,18	19
GYRO BOX	115	22,48	10	32,48	40	7,52	60	27,52	19
GYRO BOX	116	24,82	10	34,82	40	5,18	60	25,18	19
GYRO BOX	117	25,28	10	35,28	40	4,72	60	24,72	19
GYRO BOX	118	24,91	10	34,91	40	5,09	60	25,09	19
SOLAR -Z	200	36,3	10	46,3	115	68,7	115	68,7	3
SOLAR +Z	300	20,11	10	30,11	115	84,89	115	84,89	19
STRUCTURE -X	400	34,85	10	44,85	50	5,15	50	5,15	19
TMTR PATCH -X	401	76,65	10	86,65	120	33,35	165	78,35	19
TMTR PATCH -X	402	76,76	10	86,76	120	33,24	165	78,24	19
TMTR PATCH -X	403	76,72	10	86,72	120	33,28	165	78,28	19
TMTR PATCH -X	404	76,71	10	86,71	120	33,29	165	78,29	19
TMTR PATCH -X	405	76,72	10	86,72	120	33,28	165	78,28	19
TMTR PATCH -X	406	76,89	10	86,89	120	33,11	165	78,11	19
OBDR	407	38,72	10	48,72	40	-8,72	70	21,28	19
OBDR	408	38,73	10	48,73	40	-8,73	70	21,27	19
OBDR	409	39,54	10	49,54	40	-9,54	70	20,46	19
OBDR	410	38,71	10	48,71	40	-8,71	70	21,29	19
OBDR	411	35,15	10	45,15	40	-5,15	70	24,85	19
OBDR	412	38,73	10	48,73	40	-8,73	70	21,27	19
EPS PEB	413	35,63	10	45,63	40	-5,63	50	4,37	19
EPS PEB	414	35,59	10	45,59	40	-5,59	50	4,41	19
EPS PEB	415	35,88	10	45,88	40	-5,88	50	4,12	19
EPS PEB	416	35,59	10	45,59	40	-5,59	50	4,41	19
EPS PEB	417	34,89	10	44,89	40	-4,89	50	5,11	19
EPS PEB	418	35,64	10	45,64	40	-5,64	50	4,36	19
STAR TRACKER INSIDE	419	29,26	10	39,26	50	10,74	70	30,74	19
STAR TRACKER INSIDE	420	29,26	10	39,26	50	10,74	70	30,74	19
STAR TRACKER INSIDE	421	29,26	10	39,26	50	10,74	70	30,74	19
STAR TRACKER INSIDE	422	29,26	10	39,26	50	10,74	70	30,74	19
STAR TRACKER INSIDE	423	29,26	10	39,26	50	10,74	70	30,74	19
STAR TRACKER INSIDE	424	29,26	10	39,26	50	10,74	70	30,74	19
STAR TRACKER OUTSIDE	425	75,48	10	85,48	50	-35,48	70	-15,48	19
STRUCTURE +Y	500	26,96	10	36,96	50	13,04	50	13,04	19
TMTR PATCH +Y	501	40,79	10	50,79	120	69,21	165	114,21	19
TMTR PATCH +Y	502	40,79	10	50,79	120	69,21	165	114,21	19
TMTR PATCH +Y	503	40,8	10	50,8	120	69,2	165	114,2	19
TMTR PATCH +Y	504	40,84	10	50,84	120	69,16	165	114,16	19
TMTR PATCH +Y	505	40,85	10	50,85	120	69,15	165	114,15	19
TMTR PATCH +Y	506	40,81	10	50,81	120	69,19	165	114,19	19
REACTION WHEEL	507	26,86	10	36,86	45	8,14	60	23,14	19
REACTION WHEEL	508	26,84	10	36,84	45	8,16	60	23,16	19
REACTION WHEEL	509	26,86	10	36,86	45	8,14	60	23,14	19
REACTION WHEEL	510	26,93	10	36,93	45	8,07	60	23,07	19
REACTION WHEEL	511	26,87	10	36,87	45	8,13	60	23,13	19
REACTION WHEEL	512	26,87	10	36,87	45	8,13	60	23,13	19
MAGNETO-TORQUER +Y	519	26,85	10	36,85	45	8,15	55	18,15	19
UCAM	520	26,17	10	36,17	55	18,83	80	43,83	19
UCAM	521	26,29	10	36,29	55	18,71	80	43,71	19
UCAM	522	26,17	10	36,17	55	18,83	80	43,83	19
UCAM	523	26,67	10	36,67	55	18,33	80	43,33	19
UCAM	524	26,17	10	36,17	55	18,83	80	43,83	19
UCAM	525	26,17	10	36,17	55	18,83	80	43,83	19
STRUCTURE -Y	600	39,75	10	49,75	50	0,25	50	0,25	13
TMTR PATCH -Y	601	55,92	10	65,92	120	54,08	165	99,08	13
TMTR PATCH -Y	602	55,94	10	65,94	120	54,06	165	99,06	13
TMTR PATCH -Y	603	55,94	10	65,94	120	54,06	165	99,06	13
TMTR PATCH -Y	604	55,94	10	65,94	120	54,06	165	99,06	13
TMTR PATCH -Y	605	55,94	10	65,94	120	54,06	165	99,06	13
TMTR PATCH -Y	606	55,95	10	65,95	120	54,05	165	99,05	13
REACTION WHEEL 1	607	42,57	10	52,57	45	-7,57	60	7,43	13

Figure 6.32: Hot Case - Nadir Pointing Results 1

Unit	Node Number	Max Calculated	Max Uncertainty	Max Predicted	Max Allowable Op	Max Margin Op	Max Allowable Fa	Max Margin Fa	Max Mode
COMPONENTS	ID	°C	°C	°C	°C	°C	°C	°C	N°
REACTION WHEEL 1	608	40,38	10	50,38	45	-5,38	60	9,62	13
REACTION WHEEL 1	609	42,55	10	52,55	45	-7,55	60	7,45	13
REACTION WHEEL 1	610	43,01	10	53,01	45	-8,01	60	6,99	13
REACTION WHEEL 1	611	42,59	10	52,59	45	-7,59	60	7,41	13
REACTION WHEEL 1	612	42,57	10	52,57	45	-7,57	60	7,43	13
REACTION WHEEL 2	613	42,56	10	52,56	45	-7,56	60	7,44	13
REACTION WHEEL 2	614	40,38	10	50,38	45	-5,38	60	9,62	13
REACTION WHEEL 2	615	42,55	10	52,55	45	-7,55	60	7,45	13
REACTION WHEEL 2	616	43,01	10	53,01	45	-8,01	60	6,99	13
REACTION WHEEL 2	617	42,58	10	52,58	45	-7,58	60	7,42	13
REACTION WHEEL 2	618	42,57	10	52,57	45	-7,57	60	7,43	13
REACTION WHEEL 3	619	42,7	10	52,7	45	-7,7	60	7,3	13
REACTION WHEEL 3	620	40,4	10	50,4	45	-5,4	60	9,6	13
REACTION WHEEL 3	621	42,69	10	52,69	45	-7,69	60	7,31	13
REACTION WHEEL 3	622	43,16	10	53,16	45	-8,16	60	6,84	13
REACTION WHEEL 3	623	42,69	10	52,69	45	-7,69	60	7,31	13
REACTION WHEEL 3	624	42,7	10	52,7	45	-7,7	60	7,3	13
REACTION WHEEL 4	625	42,64	10	52,64	45	-7,64	60	7,36	13
REACTION WHEEL 4	626	40,39	10	50,39	45	-5,39	60	9,61	13
REACTION WHEEL 4	627	42,65	10	52,65	45	-7,65	60	7,35	13
REACTION WHEEL 4	628	43,11	10	53,11	45	-8,11	60	6,89	13
REACTION WHEEL 4	629	42,65	10	52,65	45	-7,65	60	7,35	13
REACTION WHEEL 4	630	42,67	10	52,67	45	-7,67	60	7,33	13
MAGNETO-TORQUER -Y	631	40,04	10	50,04	45	-5,04	55	4,96	13
STRUCTURE +Z OSR	700	22,26	10	32,26	50	17,64	50	17,64	19
TMTCR PATCH +Z	701	61,31	10	71,31	120	48,69	165	93,69	19
TMTCR PATCH +Z	702	61,37	10	71,37	120	48,63	165	93,63	19
TMTCR PATCH +Z	703	61,25	10	71,25	120	48,75	165	93,75	19
TMTCR PATCH +Z	704	61,24	10	71,24	120	48,76	165	93,76	19
TMTCR PATCH +Z	705	61,3	10	71,3	120	48,7	165	93,7	19
TMTCR PATCH +Z	706	61,23	10	71,23	120	48,77	165	93,77	19
TMTC REDUNDANT	707	22,94	10	32,94	60	27,06	70	37,06	19
TMTC REDUNDANT	708	21,98	10	31,98	60	28,02	70	38,02	19
TMTC REDUNDANT	709	21,95	10	31,95	60	28,05	70	38,05	19
TMTC REDUNDANT	710	21,97	10	31,97	60	28,03	70	38,03	19
TMTC REDUNDANT	711	21,95	10	31,95	60	28,05	70	38,05	19
TMTC REDUNDANT	712	22,04	10	32,04	60	27,96	70	37,96	19
MAGNETOMETER 1	713	24,78	10	34,78	65	30,22	80	45,22	19
MAGNETOMETER 1	714	24,97	10	34,97	65	30,03	80	45,03	19
MAGNETOMETER 1	715	24,97	10	34,97	65	30,03	80	45,03	19
MAGNETOMETER 1	716	24,97	10	34,97	65	30,03	80	45,03	19
MAGNETOMETER 1	717	24,97	10	34,97	65	30,03	80	45,03	19
MAGNETOMETER 1	718	25,04	10	35,04	65	29,96	80	44,96	19
MAGNETOMETER 2	719	24,78	10	34,78	65	30,22	80	45,22	19
MAGNETOMETER 2	720	24,97	10	34,97	65	30,03	80	45,03	19
MAGNETOMETER 2	721	24,97	10	34,97	65	30,03	80	45,03	19
MAGNETOMETER 2	722	24,97	10	34,97	65	30,03	80	45,03	19
MAGNETOMETER 2	723	24,97	10	34,97	65	30,03	80	45,03	19
MAGNETOMETER 2	724	25,04	10	35,04	65	29,96	80	44,96	19
LMP LCB	725	22,14	10	32,14	60	27,86	80	47,86	19
LMP LCB	726	21,82	10	31,82	60	28,18	80	48,18	19
LMP LCB	727	21,82	10	31,82	60	28,18	80	48,18	19
LMP LCB	728	21,82	10	31,82	60	28,18	80	48,18	19
LMP LCB	729	21,82	10	31,82	60	28,18	80	48,18	19
LMP LCB	730	21,82	10	31,82	60	28,18	80	48,18	19
TRITEL S	731	22,13	10	32,13	20	-12,13	70	37,87	19
TRITEL S	732	21,87	10	31,87	20	-11,87	70	38,13	19
TRITEL S	733	21,86	10	31,86	20	-11,86	70	38,14	19
TRITEL S	734	21,87	10	31,87	20	-11,87	70	38,13	19
TRITEL S	735	21,86	10	31,86	20	-11,86	70	38,14	19
TRITEL S	736	21,85	10	31,85	20	-11,85	70	38,15	19
MAGNETO-TORQUER -Z	737	29,55	10	39,55	45	5,45	55	15,45	19
STRUCTURE +Z MLI	800	24,48	10	34,48	50	15,52	50	15,52	19
STRUCTURE -Z	900	29,05	10	39,05	50	10,95	50	10,95	19
TMTCR PATCH -Z	901	34,2	10	44,2	120	75,8	165	120,8	19
TMTCR PATCH -Z	902	34,19	10	44,19	120	75,81	165	120,81	19
TMTCR PATCH -Z	903	34,19	10	44,19	120	75,81	165	120,81	19
TMTCR PATCH -Z	904	34,19	10	44,19	120	75,81	165	120,81	19
TMTCR PATCH -Z	905	34,19	10	44,19	120	75,81	165	120,81	19
TMTCR PATCH -Z	906	34,18	10	44,18	120	75,82	165	120,82	19
TMTC BOX	907	34,37	10	44,37	60	15,63	70	25,63	19
TMTC BOX	908	33,51	10	43,51	60	16,49	70	26,49	19
TMTC BOX	909	33,29	10	43,29	60	16,71	70	26,71	19
TMTC BOX	910	33,5	10	43,5	60	16,5	70	26,5	19
TMTC BOX	911	33,3	10	43,3	60	16,7	70	26,7	19
TMTC BOX	912	29,61	10	39,61	60	20,39	70	30,39	19
EPS BATTERY	913	29,55	10	39,55	15	-24,55	20	-19,55	19
EPS BATTERY	914	29,51	10	39,51	15	-24,51	20	-19,51	19
EPS BATTERY	915	29,47	10	39,47	15	-24,47	20	-19,47	19
EPS BATTERY	916	29,51	10	39,51	15	-24,51	20	-19,51	19
EPS BATTERY	917	29,48	10	39,48	15	-24,48	20	-19,48	19
EPS BATTERY	918	29,14	10	39,14	15	-24,14	20	-19,14	19
EPS BATTERY	919	19,91	10	29,91	15	-14,91	20	-9,91	19
EPS BATTERY	920	19,91	10	29,91	15	-14,91	20	-9,91	19
EPS BATTERY	921	19,9	10	29,9	15	-14,9	20	-9,9	19
EPS BATTERY	922	19,91	10	29,91	15	-14,91	20	-9,91	19
EPS BATTERY	923	19,91	10	29,91	15	-14,91	20	-9,91	19
EPS BATTERY	924	19,91	10	29,91	15	-14,91	20	-9,91	19

Figure 6.33: Hot Case - Nadir Pointing Results 2

Unit	Node Number	Min Calculated	Min Uncertainty	Min Predicted	Min Allowable Op	Min Margin Op	Min Allowable Fa	Min Margin Fa	Min Mode
COMPONENTS	ID	°C	°C	°C	°C	°C	°C	°C	N°
SOLAR +X	10	-29,06	-10	-39,06	-90	50,94	-90	50,94	24
SOLAR +X	11	-29,04	-10	-39,04	-90	50,96	-90	50,96	24
STRUCTURE +X	12	-3,71	-10	-13,71	-30	16,29	-30	16,29	24
SOLAR +X	13	-33,68	-10	-43,68	-90	46,32	-90	46,32	24
SOLAR +X	14	-33,68	-10	-43,68	-90	46,32	-90	46,32	24
SOLAR -Z	20	-38,48	-10	-48,48	-90	41,52	-90	41,52	24
SOLAR +Z	30	-35,91	-10	-45,91	-90	44,09	-90	44,09	24
STRUCTURE -X	40	12,5	-10	2,5	-30	32,5	-30	32,5	24
STRUCTURE +Y	50	1,96	-10	-8,04	-30	21,96	-30	21,96	24
STRUCTURE -Y	60	-0,13	-10	-10,13	-30	19,87	-30	19,87	24
STRUCTURE +Z OSR	70	0,17	-10	-9,83	-30	20,17	-30	20,17	24
STRUCTURE +Z MLI	80	-0,13	-10	-10,13	-30	19,87	-30	19,87	24
STRUCTURE -Z	90	11,6	-10	1,6	-30	31,6	-30	31,6	24
STRUCTURE +X	100	-3,71	-10	-13,71	-30	16,29	-30	16,29	24
TMTCR PATCH +X	101	-4,25	-10	-14,25	-100	85,75	-155	140,75	24
TMTCR PATCH +X	102	-4,25	-10	-14,25	-100	85,75	-155	140,75	24
TMTCR PATCH +X	103	-4,24	-10	-14,24	-100	85,76	-155	140,76	24
TMTCR PATCH +X	104	-4,24	-10	-14,24	-100	85,76	-155	140,76	24
TMTCR PATCH +X	105	-4,24	-10	-14,24	-100	85,76	-155	140,76	24
TMTCR PATCH +X	106	-4,23	-10	-14,23	-100	85,77	-155	140,77	24
AMSAT BOX	107	-3,31	-10	-13,31	-40	26,69	-50	36,69	24
AMSAT BOX	108	-3,32	-10	-13,32	-40	26,68	-50	36,68	24
AMSAT BOX	109	-3,54	-10	-13,54	-40	26,46	-50	36,46	24
AMSAT BOX	110	-3,32	-10	-13,32	-40	26,68	-50	36,68	24
AMSAT BOX	111	-3,22	-10	-13,22	-40	26,78	-50	36,78	24
AMSAT BOX	112	-3,31	-10	-13,31	-40	26,69	-50	36,69	24
GYRO BOX	113	-2,86	-10	-12,86	-5	-7,86	-25	12,14	24
GYRO BOX	114	-2,86	-10	-12,86	-5	-7,86	-25	12,14	24
GYRO BOX	115	-3,23	-10	-13,23	-5	-8,23	-25	11,77	24
GYRO BOX	116	-2,86	-10	-12,86	-5	-7,86	-25	12,14	24
GYRO BOX	117	-2,88	-10	-12,88	-5	-7,88	-25	12,12	24
GYRO BOX	118	-2,86	-10	-12,86	-5	-7,86	-25	12,14	24
SOLAR -Z	200	-38,44	-10	-48,44	-90	41,56	-90	41,56	24
SOLAR +Z	300	-35,91	-10	-45,91	-90	44,09	-90	44,09	24
STRUCTURE -X	400	12,52	-10	2,52	-30	32,52	-30	32,52	24
TMTCR PATCH -X	401	50,61	-10	40,61	-100	140,61	-155	195,61	24
TMTCR PATCH -X	402	50,67	-10	40,67	-100	140,67	-155	195,67	24
TMTCR PATCH -X	403	50,71	-10	40,71	-100	140,71	-155	195,71	24
TMTCR PATCH -X	404	50,71	-10	40,71	-100	140,71	-155	195,71	24
TMTCR PATCH -X	405	50,67	-10	40,67	-100	140,67	-155	195,67	24
TMTCR PATCH -X	406	50,86	-10	40,86	-100	140,86	-155	195,86	24
OBDH	407	24,05	-10	14,05	-20	34,05	-35	49,05	24
OBDH	408	24,05	-10	14,05	-20	34,05	-35	49,05	24
OBDH	409	25,55	-10	15,55	-20	35,55	-35	50,55	24
OBDH	410	24,06	-10	14,06	-20	34,06	-35	49,06	24
OBDH	411	13,6	-10	3,6	-20	23,6	-35	38,6	24
OBDH	412	24,07	-10	14,07	-20	34,07	-35	49,07	24
EPS PEB	413	20,07	-10	10,07	-20	30,07	-30	40,07	24
EPS PEB	414	20,02	-10	10,02	-20	30,02	-30	40,02	24
EPS PEB	415	20,53	-10	10,53	-20	30,53	-30	40,53	24
EPS PEB	416	20,03	-10	10,03	-20	30,03	-30	40,03	24
EPS PEB	417	13,18	-10	3,18	-20	23,18	-30	33,18	24
EPS PEB	418	20,08	-10	10,08	-20	30,08	-30	40,08	24
STAR TRACKER INSIDE	419	19,98	-10	9,98	-20	29,98	-40	49,98	24
STAR TRACKER INSIDE	420	19,98	-10	9,98	-20	29,98	-40	49,98	24
STAR TRACKER INSIDE	421	19,98	-10	9,98	-20	29,98	-40	49,98	24
STAR TRACKER INSIDE	422	19,98	-10	9,98	-20	29,98	-40	49,98	24
STAR TRACKER INSIDE	423	19,99	-10	9,99	-20	29,99	-40	49,99	24
STAR TRACKER INSIDE	424	19,98	-10	9,98	-20	29,98	-40	49,98	24
STAR TRACKER OUTSIDE	425	68,89	-10	58,89	-20	78,89	-40	98,89	24
STRUCTURE +Y	500	1,99	-10	-8,01	-30	21,99	-30	21,99	24
TMTCR PATCH +Y	501	15,35	-10	5,35	-100	105,35	-155	160,35	24
TMTCR PATCH +Y	502	15,42	-10	5,42	-100	105,42	-155	160,42	24
TMTCR PATCH +Y	503	15,4	-10	5,4	-100	105,4	-155	160,4	24
TMTCR PATCH +Y	504	15,43	-10	5,43	-100	105,43	-155	160,43	24
TMTCR PATCH +Y	505	15,44	-10	5,44	-100	105,44	-155	160,44	24
TMTCR PATCH +Y	506	15,44	-10	5,44	-100	105,44	-155	160,44	24
REACTION WHEEL	507	2,13	-10	-7,87	-20	12,13	-25	17,13	24
REACTION WHEEL	508	2,16	-10	-7,84	-20	12,16	-25	17,16	24
REACTION WHEEL	509	2,13	-10	-7,87	-20	12,13	-25	17,13	24
REACTION WHEEL	510	2,02	-10	-7,98	-20	12,02	-25	17,02	24
REACTION WHEEL	511	2,13	-10	-7,87	-20	12,13	-25	17,13	24
REACTION WHEEL	512	2,13	-10	-7,87	-20	12,13	-25	17,13	24
MAGNETO-TORQUER +Y	519	2,25	-10	-7,75	-30	22,25	-40	32,25	24
UCAM	520	1,54	-10	-8,46	-20	11,54	-45	36,54	24
UCAM	521	1,27	-10	-8,73	-20	11,27	-45	36,27	24
UCAM	522	1,54	-10	-8,46	-20	11,54	-45	36,54	24
UCAM	523	2,28	-10	-7,72	-20	12,28	-45	37,28	24
UCAM	524	1,54	-10	-8,46	-20	11,54	-45	36,54	24
UCAM	525	1,54	-10	-8,46	-20	11,54	-45	36,54	24
STRUCTURE -Y	600	-0,12	-10	-10,12	-30	19,88	-30	19,88	24
TMTCR PATCH -Y	601	18,59	-10	8,59	-100	108,59	-155	163,59	24
TMTCR PATCH -Y	602	18,6	-10	8,6	-100	108,6	-155	163,6	24
TMTCR PATCH -Y	603	18,6	-10	8,6	-100	108,6	-155	163,6	24
TMTCR PATCH -Y	604	18,6	-10	8,6	-100	108,6	-155	163,6	24
TMTCR PATCH -Y	605	18,6	-10	8,6	-100	108,6	-155	163,6	24
TMTCR PATCH -Y	606	18,6	-10	8,6	-100	108,6	-155	163,6	24
REACTION WHEEL 1	607	0,47	-10	-9,53	-20	10,47	-25	15,47	24

Figure 6.34: Cold Case - Nadir Pointing Results 1

Unit	Node Number	Min Calculated	Min Uncertainty	Min Predicted	Min Allowable Op	Min Margin Op	Min Allowable Fa	Min Margin Fa	Min Mode
COMPONENTS	ID	°C	°C	°C	°C	°C	°C	°C	N°
REACTION WHEEL 1	608	0	-10	-10	-20	10	-25	15	24
REACTION WHEEL 1	609	0,46	-10	-9,54	-20	10,46	-25	15,46	24
REACTION WHEEL 1	610	0,59	-10	-9,41	-20	10,59	-25	15,59	24
REACTION WHEEL 1	611	0,47	-10	-9,53	-20	10,47	-25	15,47	24
REACTION WHEEL 1	612	0,47	-10	-9,53	-20	10,47	-25	15,47	24
REACTION WHEEL 2	613	0,49	-10	-9,51	-20	10,49	-25	15,49	24
REACTION WHEEL 2	614	0	-10	-10	-20	10	-25	15	24
REACTION WHEEL 2	615	0,48	-10	-9,52	-20	10,48	-25	15,48	24
REACTION WHEEL 2	616	0,6	-10	-9,4	-20	10,6	-25	15,6	24
REACTION WHEEL 2	617	0,48	-10	-9,52	-20	10,48	-25	15,48	24
REACTION WHEEL 2	618	0,48	-10	-9,52	-20	10,48	-25	15,48	24
REACTION WHEEL 3	619	0,51	-10	-9,49	-20	10,51	-25	15,51	24
REACTION WHEEL 3	620	0	-10	-10	-20	10	-25	15	24
REACTION WHEEL 3	621	0,5	-10	-9,5	-20	10,5	-25	15,5	24
REACTION WHEEL 3	622	0,63	-10	-9,37	-20	10,63	-25	15,63	24
REACTION WHEEL 3	623	0,52	-10	-9,48	-20	10,52	-25	15,52	24
REACTION WHEEL 3	624	0,51	-10	-9,49	-20	10,51	-25	15,51	24
REACTION WHEEL 4	625	0,51	-10	-9,49	-20	10,51	-25	15,51	24
REACTION WHEEL 4	626	0	-10	-10	-20	10	-25	15	24
REACTION WHEEL 4	627	0,5	-10	-9,5	-20	10,5	-25	15,5	24
REACTION WHEEL 4	628	0,63	-10	-9,37	-20	10,63	-25	15,63	24
REACTION WHEEL 4	629	0,52	-10	-9,48	-20	10,52	-25	15,52	24
REACTION WHEEL 4	630	0,51	-10	-9,49	-20	10,51	-25	15,51	24
MAGNETO-TORQUER -Y	631	0	-10	-10	-30	20	-40	30	24
STRUCTURE +Z OSR	700	0,2	-10	-9,8	-100	20,2	-30	20,2	24
TMTR PATCH +Z	701	30,87	-10	20,87	-100	120,87	-155	175,87	24
TMTR PATCH +Z	702	30,84	-10	20,84	-100	120,84	-155	175,84	24
TMTR PATCH +Z	703	30,84	-10	20,84	-100	120,84	-155	175,84	24
TMTR PATCH +Z	704	30,9	-10	20,9	-100	120,9	-155	175,9	24
TMTR PATCH +Z	705	30,93	-10	20,93	-100	120,93	-155	175,93	24
TMTR PATCH +Z	706	30,85	-10	20,85	-100	120,85	-155	175,85	24
TMTC REDUNDANT	707	0,32	-10	-9,68	-25	15,32	-35	25,32	24
TMTC REDUNDANT	708	1,36	-10	-8,64	-25	16,36	-35	26,36	24
TMTC REDUNDANT	709	1,32	-10	-8,68	-25	16,32	-35	26,32	24
TMTC REDUNDANT	710	1,36	-10	-8,64	-25	16,36	-35	26,36	24
TMTC REDUNDANT	711	1,33	-10	-8,67	-25	16,33	-35	26,33	24
TMTC REDUNDANT	712	1,59	-10	-8,41	-25	16,59	-35	26,59	24
MAGNETOMETER 1	713	0,28	-10	-9,72	-20	10,28	-40	30,28	24
MAGNETOMETER 1	714	0,47	-10	-9,53	-20	10,47	-40	30,47	24
MAGNETOMETER 1	715	0,47	-10	-9,53	-20	10,47	-40	30,47	24
MAGNETOMETER 1	716	0,47	-10	-9,53	-20	10,47	-40	30,47	24
MAGNETOMETER 1	717	0,47	-10	-9,53	-20	10,47	-40	30,47	24
MAGNETOMETER 1	718	0,54	-10	-9,46	-20	10,54	-40	30,54	24
MAGNETOMETER 2	719	0,28	-10	-9,72	-20	10,28	-40	30,28	24
MAGNETOMETER 2	720	0,47	-10	-9,53	-20	10,47	-40	30,47	24
MAGNETOMETER 2	721	0,47	-10	-9,53	-20	10,47	-40	30,47	24
MAGNETOMETER 2	722	0,47	-10	-9,53	-20	10,47	-40	30,47	24
MAGNETOMETER 2	723	0,47	-10	-9,53	-20	10,47	-40	30,47	24
MAGNETOMETER 2	724	0,54	-10	-9,46	-20	10,54	-40	30,54	24
LMP LCB	725	0,73	-10	-9,27	-25	15,73	-45	35,73	24
LMP LCB	726	0,67	-10	-9,33	-25	15,67	-45	35,67	24
LMP LCB	727	0,67	-10	-9,33	-25	15,67	-45	35,67	24
LMP LCB	728	0,67	-10	-9,33	-25	15,67	-45	35,67	24
LMP LCB	729	0,67	-10	-9,33	-25	15,67	-45	35,67	24
LMP LCB	730	0,64	-10	-9,36	-25	15,64	-45	35,64	24
TRITEL S	731	0,76	-10	-9,24	-30	20,76	-40	30,76	24
TRITEL S	732	0,65	-10	-9,35	-30	20,65	-40	30,65	24
TRITEL S	733	0,65	-10	-9,35	-30	20,65	-40	30,65	24
TRITEL S	734	0,65	-10	-9,35	-30	20,65	-40	30,65	24
TRITEL S	735	0,65	-10	-9,35	-30	20,65	-40	30,65	24
TRITEL S	736	0,6	-10	-9,4	-30	20,6	-40	30,6	24
MAGNETO-TORQUER -Z	737	11,03	-10	1,03	-30	31,03	-40	41,03	24
STRUCTURE +Z MLI	800	-0,1	-10	-10,1	-30	19,9	-30	19,9	24
STRUCTURE -Z	900	11,57	-10	1,57	-30	31,57	-30	31,57	24
TMTR PATCH -Z	901	22,09	-10	12,09	-100	112,09	-155	167,09	24
TMTR PATCH -Z	902	22,11	-10	12,11	-100	112,11	-155	167,11	24
TMTR PATCH -Z	903	22,11	-10	12,11	-100	112,11	-155	167,11	24
TMTR PATCH -Z	904	22,15	-10	12,15	-100	112,15	-155	167,15	24
TMTR PATCH -Z	905	22,18	-10	12,18	-100	112,18	-155	167,18	24
TMTR PATCH -Z	906	22,2	-10	12,2	-100	112,2	-155	167,2	24
TMTC BOX	907	13,99	-10	3,99	-25	28,99	-35	38,99	24
TMTC BOX	908	13,69	-10	3,69	-25	28,69	-35	38,69	24
TMTC BOX	909	13,6	-10	3,6	-25	28,6	-35	38,6	24
TMTC BOX	910	13,68	-10	3,68	-25	28,68	-35	38,68	24
TMTC BOX	911	13,6	-10	3,6	-25	28,6	-35	38,6	24
TMTC BOX	912	11,67	-10	1,67	-25	26,67	-35	36,67	24
EPS BATTERY	913	10,65	-10	0,65	0	0,65	-5	5,65	24
EPS BATTERY	914	10,8	-10	0,8	0	0,8	-5	5,8	24
EPS BATTERY	915	10,81	-10	0,81	0	0,81	-5	5,81	24
EPS BATTERY	916	10,77	-10	0,77	0	0,77	-5	5,77	24
EPS BATTERY	917	10,82	-10	0,82	0	0,82	-5	5,82	24
EPS BATTERY	918	11,42	-10	1,42	0	1,42	-5	6,42	24
EPS BATTERY	919	8,72	-10	-1,28	0	-1,28	-5	3,72	24
EPS BATTERY	920	8,72	-10	-1,28	0	-1,28	-5	3,72	24
EPS BATTERY	921	8,72	-10	-1,28	0	-1,28	-5	3,72	24
EPS BATTERY	922	8,72	-10	-1,28	0	-1,28	-5	3,72	24
EPS BATTERY	923	8,72	-10	-1,28	0	-1,28	-5	3,72	24
EPS BATTERY	924	8,72	-10	-1,28	0	-1,28	-5	3,72	24

Figure 6.35: Cold Case - Nadir Pointing Results 2

In each table we have first the component name with its relative node numbers. Afterwards in the third column we have the maximum and minimum temperature for each component. Each value is then margined by $\pm 10^{\circ}\text{C}$ and inserted into the fifth column. In the sixth and eighth column we have the component temperature limits while in the seventh and eighth column we have the difference between the temperature limit and the margined temperature calculated. If positive (green) the temperature limit is respected, otherwise if negative the limit is not satisfied (red).

In these tables and in all thermal analyses two limit temperature exist:

Allowable Operative Temperature The device will operate effectively within a specified temperature range which varies based on the device function and application context, and ranges from the minimum operating temperature to the maximum operating temperature (or peak operating temperature). Outside this range of safe operating temperatures the device does not respect its specified functional parameters and may fail.

Allowable Fail Temperature The device will not operate effectively outside its allowable operative temperature but if inside the fail temperature it will not fail nor break. Once the allowable fail temperature is not respected the component fails.

Unfortunately studying these results not all component temperatures remain inside their temperature ranges. Let us analyze both pointing cases:

Sun Pointing The first results we obtain are those relative to the global hot and cold cases.

- Hot Case - Mode 13 & 19
- Cold Case - Mode 24

Analyzing both mode 13 and mode 19 we can see that these modes are those where we have the most dissipated power generated by the internal components, while mode 24 is that relative to the minimum power dissipation. Analyzing the dissipated power mode table it is clear that mode 1 is that relative to the least dissipated power, but considering that this mode occurs when the satellite is still inside the launcher it was not taken into account.

The results of the hot case demonstrate that in the sun pointing attitude all component temperature remain inside their ranges. Unfortunately the cold case results are not as satisfactory and many components are not inside their temperature ranges. Considering that some components are switched off during this cold case the most critical components are:

- EPS BATTERIES
- TMTC
- MAGNETOMETERS
- EPS PEB
- REACTION WHEEL 1-4

The EPS batteries unfortunately have a very limited temperature range and are one of the most sensible components of the ESEO satellite. Unfortunately they have a minimum temperature limit of 0°C . Together with this the EPS batteries together with the TMTC are located on the -z panel (Node 90) and this panel during the sun pointing attitude is only exposed to a small amount of Earth IR heat. The reaction wheels attached to the internal -y panel also suffers the same conditions. Even though they have a larger temperature range, with a minimum temperature limit of -20°C , the reaction wheel are attached to a surface is not invested by solar heat. It only has receives a small amount of terrestrial IR heat.

The EPS Peb instead luckily is attached to the -x panel which receives terrestrial IR and albedo heat and therefore even though its -20°C minimum temperature limit only goes a few degrees under its limit. This is also only the face which is connected with the panel. Unfortunately considering these results in future studies a heater system shall be necessary.

Nadir Pointing

- Hot Case - Mode 13 & 19
- Cold Case - Mode 24

In this case again the same modes for the hot and cold case occur. Analyzing the hot case unfortunately many components are not inside their temperature ranges. Analyzing which components are switched on during this mode and those that don't satisfy their temperature ranges, the most critical components are:

- OBDH
- EPS PEB
- TRITEL-S
- REACTION WHEEL 1-4

For the Nadir Pointing we unfortunately have an excessive heat source on those side which usually are fairly cool. The OBDH and EPS PEB are both located on the -x side which with the new configuration is highly exposed to solar heat. This therefore increase the temperatures of these two components and together with their not too high maximum temperature limit causes them to exceed their temperature ranges. In the operative phase we shall see that this panel is only temporarily exposed to these heat sources seeing that the dominant attitude is sun pointing.

The reaction wheels are also on a surface which is predominantly oriented towards a cold heat source and therefore were opportunily modelled. Unfortunately when the -y panel has a larger heat source the reaction wheels temperature rises and this together with their low maximum temperature limit of 45°C cause this problem.

Analyzing the cold case we only have the EPS batteries as critical component. Again this is because of it very low temperature range.

Analyzing the operative phase (fig OP) of the satellite which is combined of 28 orbits with a sequence of modes. In this sequence of modes the nadir pointing attitude only occurs for modes 22,8 in order to point the uCam towards the Earth. Therefore these results must be furthers studied in an other analysis which takes into account this factor. This will be studied in the operative thermal case.

4 Operative Case

The first analysis was done in order to locate those components which suffered the harsh thermal conditions the satellite goes through during its lifetime. These components are therefore those that will be more thoroughly analysed in the operative case. The operative phase, as previously illustrated in fig 2.3, is composed of a cycle of 28 orbits. During this time the satellite cycles through different modes and is mostly in the sun pointing attitude. Only during 3 modes (8,9 and 22) the nadir pointing attitude is used and therefore the single mode analysis does not represent the effective thermal case.

The only difference between this analysis and the single mode analysis consists in having variable dissipated powers with time. Therefore for every component which dissipates power a function was modelled in order to represent the dissipated heat during the 56 orbits. The other difference consists in a chained radiative case analysis. Instead of inserting a single attitude as radiative case, both radiative cases were linked in order to represent the operative phase.

During the single mode analysis a lot of components suffered the extreme cold case the ESEO satellite encounters and did not remain inside their margins. Unfortunately this also occurred during the operative thermal case and a passive approach had to be discarded in favour of a active thermal control. Therefore a heater system was modelled to keep all components inside their margins.

4.1 Radiative Results

In order to fully analyze the operative phase a 56 orbit thermal case was modelled which represents two fully operative cycles. Again using the ESATAN Results Tool the Sun, albedo and Earth IR heat was extracted from the ESATAN results. The heat on the external panels is displayed in the following diagrams:

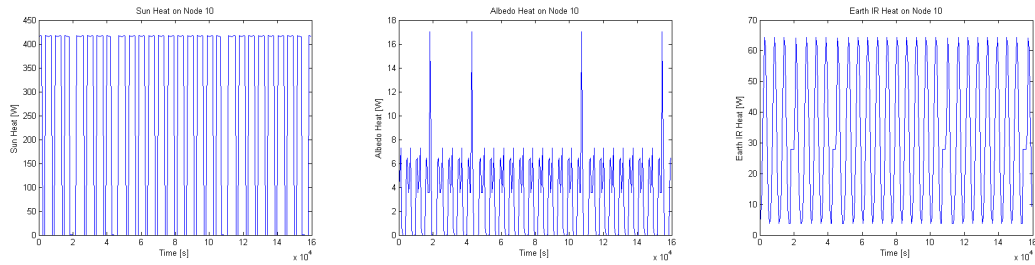


Figure 6.36: Node 10 Heat Results

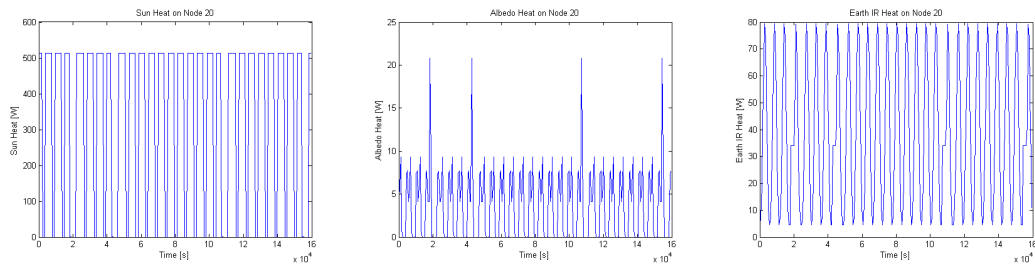


Figure 6.37: Node 20 Heat Results

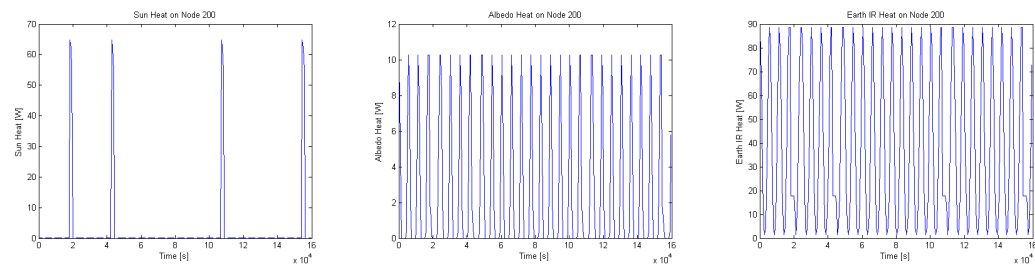


Figure 6.38: Node 200 Heat Results

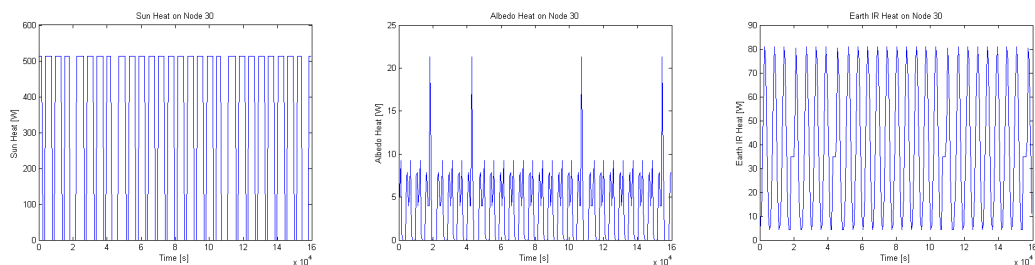


Figure 6.39: Node 30 Heat Results

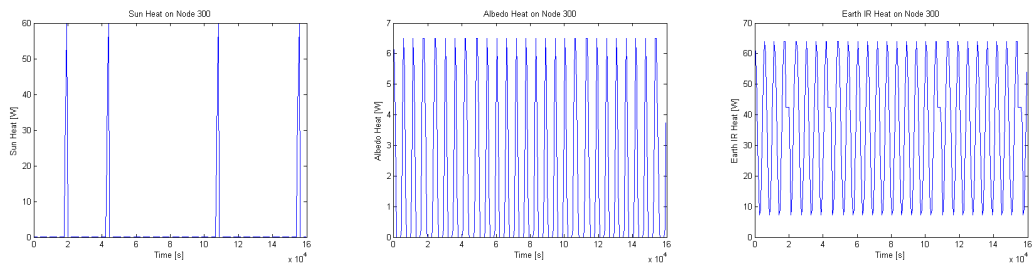


Figure 6.40: Node 300 Heat Results

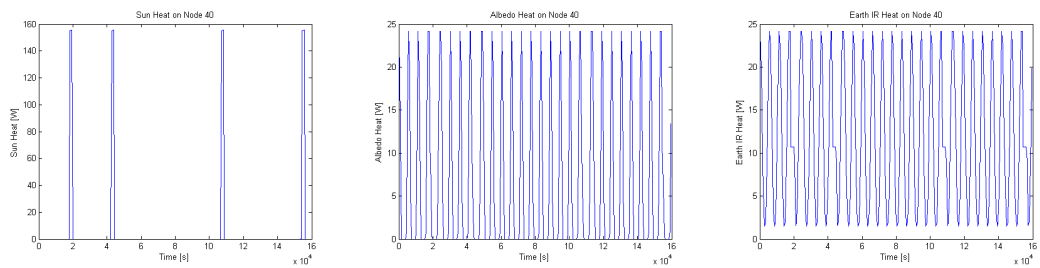


Figure 6.41: Node 40 Heat Results

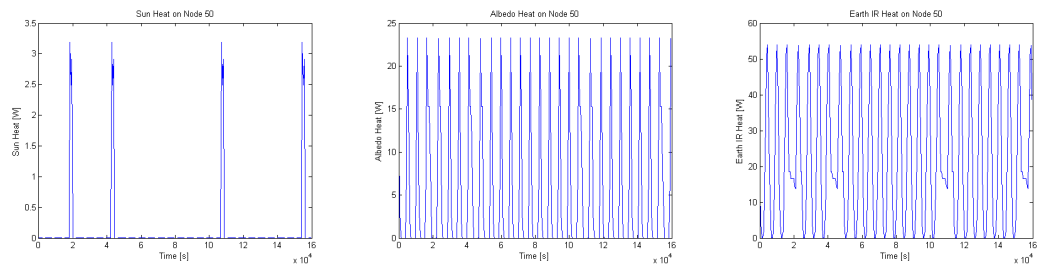


Figure 6.42: Node 50 Heat Results

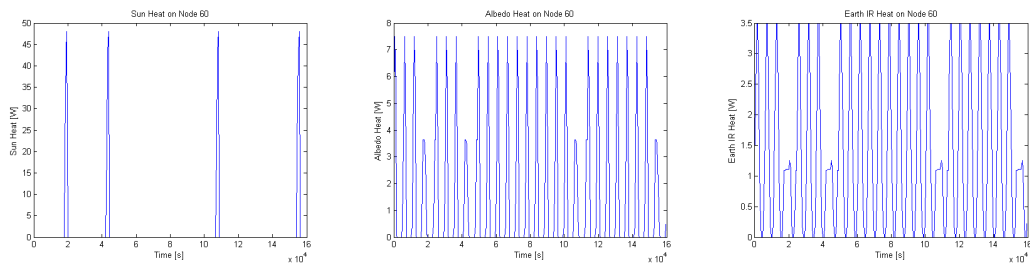


Figure 6.43: Node 60 Heat Results

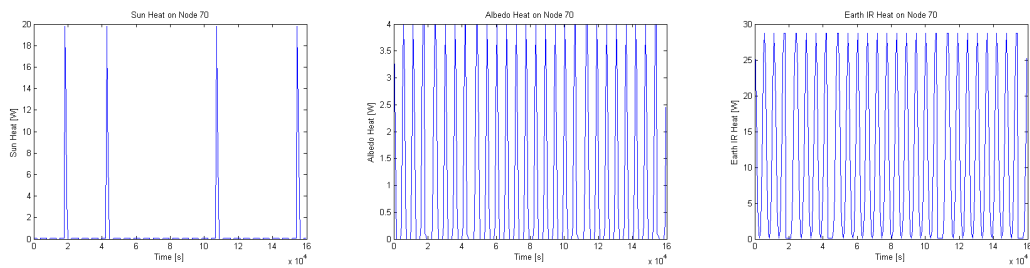


Figure 6.44: Node 70 Heat Results

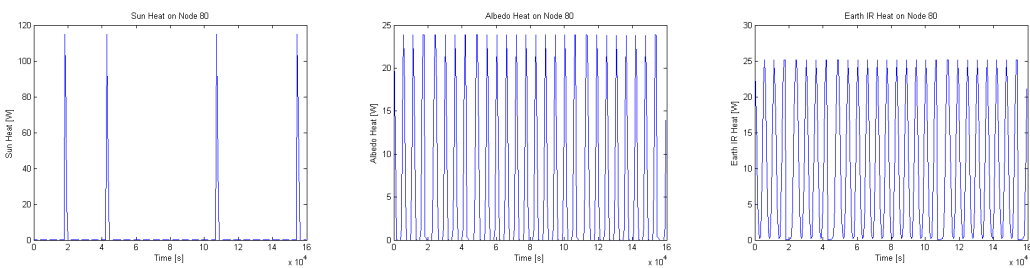


Figure 6.45: Node 80 Heat Results

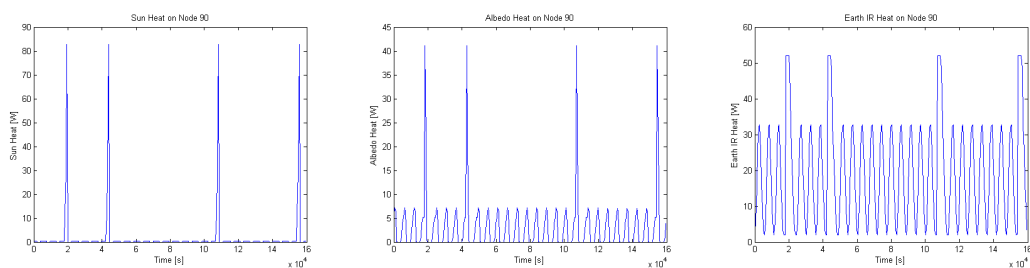


Figure 6.46: Node 90 Heat Results

Analyzing these results the attitude change can clearly be seen, especially in the albedo heat graphs. Analyzing node 90 which corresponds to the -z structural panel this is very clear. When the satellite is in its Nadir Pointing attitude the -z panel is directly pointing towards the Earth. Therefore we will have an increase in albedo and Earth IR heat. This can be seen on the node 90 results diagram, where we have 4 distinct peaks each representing the transition from Sun to Nadir Pointing attitude. Comparing these result obtained for a single orbit we can see that they overlap and that the peak in power for a single orbit coincides with this 28 orbit result. This attitude change can be seen on most graphs especially the albedo graphs.

Analyzing the solar panel which is oriented directly towards the sun (+x solar panel) we notice that during the nadir pointing attitude we have no solar heat. Analyzing the node 10 graph properly we see when the satellite eclipses at fixed periods. After 3 orbits the solar eclipse of the +x solar panel is longer. This is because the satellite is not in eclipse but after 3 orbits has changed attitude and is not pointing the sun anymore. Afterwards once it heads back into its sun pointing attitude the solar heat on the solar panel increases.

4.2 Passive Thermal Results

Initially a passive thermal control was kept to analyze which components do not respect their thermal ranges. Therefore no changes were made in the thermal model. The results obtained for this analysis are described in the following tables:

Node Number	Max Calculated	Max Uncertainty	Max Predicted	Max Allowable Op	Max Margin Op	Max Allowable Fa	Max Margin Fa
ID	°C	°C	°C	°C	°C	°C	°C
10	55,53	10	65,53	115	49,47	115	49,47
11	55,52	10	65,52	115	49,48	115	49,48
12	13,23	10	23,23	50	26,77	50	26,77
13	51,19	10	61,19	115	53,81	115	53,81
14	51,17	10	61,17	115	53,83	115	53,83
20	53,22	10	63,22	115	51,78	115	51,78
30	47,94	10	57,94	115	57,06	115	57,06
40	7,4	10	17,4	50	32,6	50	32,6
50	0	10	10	50	40	50	40
60	4,8	10	14,8	50	35,2	50	35,2
70	0,74	10	10,74	50	39,26	50	39,26
80	3,46	10	13,46	50	36,54	50	36,54
90	0,31	10	10,31	50	39,69	50	39,69
100	13,2	10	23,2	50	26,8	50	26,8
101	82,78	10	92,78	120	27,22	165	72,22
102	82,58	10	92,58	120	27,42	165	72,42
103	82,59	10	92,59	120	27,41	165	72,41
104	82,58	10	92,58	120	27,42	165	72,42
105	82,57	10	92,57	120	27,43	165	72,43
106	82,48	10	92,48	120	27,52	165	72,52
107	17,19	10	27,19	65	37,81	100	72,81
108	17	10	27	65	38	100	73
109	14,52	10	24,52	65	40,48	100	75,48
110	17	10	27	65	38	100	73
111	18,22	10	28,22	65	36,78	100	71,78
112	17,19	10	27,19	65	37,81	100	72,81
113	15,92	10	25,92	40	14,08	60	34,08
114	15,85	10	25,85	40	14,15	60	34,15
115	13,97	10	23,97	40	16,03	60	36,03
116	15,84	10	25,84	40	14,16	60	34,16
117	16,35	10	26,35	40	13,65	60	33,65
118	15,92	10	25,92	40	14,08	60	34,08
200	53,17	10	63,17	115	51,83	115	51,83
300	47,86	10	57,86	115	57,14	115	57,14
400	7,38	10	17,38	50	32,62	50	32,62
401	16,23	10	26,23	120	93,77	165	138,77
402	16,23	10	26,23	120	93,77	165	138,77
403	16,23	10	26,23	120	93,77	165	138,77
404	16,22	10	26,22	120	93,78	165	138,78
405	16,23	10	26,23	120	93,77	165	138,77
406	16,22	10	26,22	120	93,78	165	138,78
407	6,17	10	16,17	40	23,83	70	53,83
408	6,16	10	16,16	40	23,84	70	53,84
409	7,03	10	17,03	40	22,97	70	52,97
410	6,16	10	16,16	40	23,84	70	53,84
411	7,14	10	17,14	40	22,86	70	52,86
412	6,17	10	16,17	40	23,83	70	53,83
413	3,57	10	13,57	40	26,43	50	36,43
414	3,52	10	13,52	40	26,48	50	36,48
415	3,88	10	13,88	40	26,12	50	36,12
416	3,51	10	13,51	40	26,49	50	36,49
417	7	10	17	40	23	50	33
418	3,57	10	13,57	40	26,43	50	36,43
419	0,91	10	10,91	50	39,09	70	59,09
420	0,91	10	10,91	50	39,09	70	59,09
421	0,91	10	10,91	50	39,09	70	59,09
422	0,91	10	10,91	50	39,09	70	59,09
423	0,91	10	10,91	50	39,09	70	59,09
424	0,91	10	10,91	50	39,09	70	59,09
425	0,91	10	10,91	50	39,09	70	59,09
500	0	10	10	50	40	50	40
501	0	10	10	120	110	165	155
502	0	10	10	120	110	165	155
503	0	10	10	120	110	165	155
504	0	10	10	120	110	165	155
505	0	10	10	120	110	165	155
506	0	10	10	120	110	165	155
507	0	10	10	45	35	60	50
508	0	10	10	45	35	70	60
509	0	10	10	45	35	60	50
510	0	10	10	45	35	60	50
511	0	10	10	45	35	60	50
512	0	10	10	45	35	60	50
519	0	10	10	45	35	55	45
520	0	10	10	55	45	80	70
521	0	10	10	55	45	80	70
522	0	10	10	55	45	80	70
523	0	10	10	55	45	80	70
524	0	10	10	55	45	80	70
525	0	10	10	55	45	80	70
600	4,82	10	14,82	50	35,18	50	35,18
601	13,1	10	23,1	120	96,9	165	141,9
602	13,12	10	23,12	120	96,88	165	141,88
603	13,11	10	23,11	120	96,89	165	141,89
604	13,12	10	23,12	120	96,88	165	141,88
605	13,12	10	23,12	120	96,88	165	141,88
606	13,12	10	23,12	120	96,88	165	141,88
607	6,4	10	16,4	45	28,6	60	43,6

Figure 6.47: Passive Operative Hot Case Results 1

Unit	Node Number	Max Calculated	Max Uncertainty	Max Predicted	Max Allowable Op	Max Margin Op	Max Allowable Fa	Max Margin Fa
COMPONENTS	ID	°C	°C	°C	°C	°C	°C	°C
REACTION WHEEL 1	608	5,19	10	15,19	45	29,81	60	44,81
REACTION WHEEL 1	609	6,4	10	16,4	45	28,6	60	43,6
REACTION WHEEL 1	610	6,67	10	16,67	45	28,33	60	43,33
REACTION WHEEL 1	611	6,4	10	16,4	45	28,6	60	43,6
REACTION WHEEL 1	612	6,4	10	16,4	45	28,6	60	43,6
REACTION WHEEL 2	613	6,31	10	16,31	45	28,69	60	43,69
REACTION WHEEL 2	614	5,23	10	15,23	45	29,77	60	44,77
REACTION WHEEL 2	615	6,31	10	16,31	45	28,69	60	43,69
REACTION WHEEL 2	616	6,51	10	16,51	45	28,49	60	43,49
REACTION WHEEL 2	617	6,08	10	16,08	45	28,92	60	43,92
REACTION WHEEL 2	618	6,08	10	16,08	45	28,92	60	43,92
REACTION WHEEL 3	619	6,36	10	16,36	45	28,64	60	43,64
REACTION WHEEL 3	620	5,24	10	15,24	45	29,76	60	44,76
REACTION WHEEL 3	621	6,33	10	16,33	45	28,67	60	43,67
REACTION WHEEL 3	622	6,57	10	16,57	45	28,43	60	43,43
REACTION WHEEL 3	623	6,12	10	16,12	45	28,88	60	43,88
REACTION WHEEL 3	624	6,15	10	16,15	45	28,85	60	43,85
REACTION WHEEL 4	625	6,35	10	16,35	45	28,65	60	43,65
REACTION WHEEL 4	626	5,24	10	15,24	45	29,76	60	44,76
REACTION WHEEL 4	627	6,33	10	16,33	45	28,67	60	43,67
REACTION WHEEL 4	628	6,56	10	16,56	45	28,44	60	43,44
REACTION WHEEL 4	629	6,12	10	16,12	45	28,88	60	43,88
REACTION WHEEL 4	630	6,15	10	16,15	45	28,85	60	43,85
MAGNETO-TORQUER -Y	631	4,82	10	14,82	45	30,18	55	40,18
STRUCTURE +Z OSR	700	0,75	10	10,75	50	39,25	50	39,25
TMTCR PATCH +Z	701	24,14	10	34,14	120	85,86	165	130,86
TMTCR PATCH +Z	702	24,16	10	34,16	120	85,84	165	130,84
TMTCR PATCH +Z	703	24,13	10	34,13	120	85,87	165	130,87
TMTCR PATCH +Z	704	24,15	10	34,15	120	85,85	165	130,85
TMTCR PATCH +Z	705	24,17	10	34,17	120	85,83	165	130,83
TMTCR PATCH +Z	706	24,16	10	34,16	120	85,84	165	130,84
TMTC REDUNDANT	707	1,32	10	11,32	60	48,68	70	58,68
TMTC REDUNDANT	708	0,22	10	10,22	60	49,78	70	59,78
TMTC REDUNDANT	709	0,28	10	10,28	60	49,72	70	59,72
TMTC REDUNDANT	710	0,22	10	10,22	60	49,78	70	59,78
TMTC REDUNDANT	711	0,28	10	10,28	60	49,72	70	59,72
TMTC REDUNDANT	712	0,17	10	10,17	60	49,83	70	59,83
MAGNETOMETER 1	713	3,82	10	13,82	65	51,18	80	66,18
MAGNETOMETER 1	714	4,01	10	14,01	65	50,99	80	65,99
MAGNETOMETER 1	715	4,02	10	14,02	65	50,98	80	65,98
MAGNETOMETER 1	716	4,02	10	14,02	65	50,98	80	65,98
MAGNETOMETER 1	717	4,02	10	14,02	65	50,98	80	65,98
MAGNETOMETER 1	718	4,09	10	14,09	65	50,91	80	65,91
MAGNETOMETER 2	719	3,82	10	13,82	65	51,18	80	66,18
MAGNETOMETER 2	720	4,01	10	14,01	65	50,99	80	65,99
MAGNETOMETER 2	721	4,02	10	14,02	65	50,98	80	65,98
MAGNETOMETER 2	722	4,02	10	14,02	65	50,98	80	65,98
MAGNETOMETER 2	723	4,02	10	14,02	65	50,98	80	65,98
MAGNETOMETER 2	724	4,09	10	14,09	65	50,91	80	65,91
LMP LCB	725	0,72	10	10,72	60	49,28	80	69,28
LMP LCB	726	0,64	10	10,64	60	49,36	80	69,36
LMP LCB	727	0,64	10	10,64	60	49,36	80	69,36
LMP LCB	728	0,64	10	10,64	60	49,36	80	69,36
LMP LCB	729	0,64	10	10,64	60	49,36	80	69,36
LMP LCB	730	0,61	10	10,61	60	49,39	80	69,39
TRITEL S	731	0,76	10	10,76	20	9,24	70	59,24
TRITEL S	732	0,68	10	10,68	20	9,32	70	59,32
TRITEL S	733	0,68	10	10,68	20	9,32	70	59,32
TRITEL S	734	0,68	10	10,68	20	9,32	70	59,32
TRITEL S	735	0,68	10	10,68	20	9,32	70	59,32
TRITEL S	736	0,62	10	10,62	20	9,38	70	59,38
MAGNETO-TORQUER -Z	737	0,31	10	10,31	45	34,69	55	44,69
STRUCTURE +Z MLJ	800	3,42	10	13,42	50	36,58	50	36,58
STRUCTURE -Z	900	0,3	10	10,3	50	39,7	50	39,7
TMTCR PATCH -Z	901	2,1	10	12,1	120	107,9	165	152,9
TMTCR PATCH -Z	902	2,1	10	12,1	120	107,9	165	152,9
TMTCR PATCH -Z	903	2,12	10	12,12	120	107,88	165	152,88
TMTCR PATCH -Z	904	2,1	10	12,1	120	107,9	165	152,9
TMTCR PATCH -Z	905	2,11	10	12,11	120	107,89	165	152,89
TMTCR PATCH -Z	906	2,1	10	12,1	120	107,9	165	152,9
TMTC BOX	907	1,08	10	11,08	60	48,92	70	58,92
TMTC BOX	908	0,63	10	10,63	60	49,37	70	59,37
TMTC BOX	909	0,5	10	10,5	60	49,5	70	59,5
TMTC BOX	910	0,62	10	10,62	60	49,38	70	59,38
TMTC BOX	911	0,5	10	10,5	60	49,5	70	59,5
TMTC BOX	912	0,35	10	10,35	60	49,65	70	59,65
EPS BATTERY	913	0,28	10	10,28	15	4,72	20	9,72
EPS BATTERY	914	0,31	10	10,31	15	4,69	20	9,69
EPS BATTERY	915	0,33	10	10,33	15	4,67	20	9,67
EPS BATTERY	916	0,3	10	10,3	15	4,7	20	9,7
EPS BATTERY	917	0,33	10	10,33	15	4,67	20	9,67
EPS BATTERY	918	0,29	10	10,29	15	4,71	20	9,71
EPS BATTERY	919	0	10	10	15	5	20	10
EPS BATTERY	920	0	10	10	15	5	20	10
EPS BATTERY	921	0	10	10	15	5	20	10
EPS BATTERY	922	0	10	10	15	5	20	10
EPS BATTERY	923	0	10	10	15	5	20	10
EPS BATTERY	924	0	10	10	15	5	20	10

Figure 6.48: Passive Operative Hot Case Results 2

Unit	Node Number	Min Calculated	Min Uncertainty	Min Predicted	Min Allowable Op	Min Margin Op	Min Allowable Fa	Min Margin Fa
COMPONENTS	ID	°C	°C	°C	°C	°C	°C	°C
SOLAR +X	10	-22,4	-10	-32,4	-90	57,6	-90	57,6
SOLAR +X	11	-22,38	-10	-32,38	-90	57,62	-90	57,62
STRUCTURE +X	12	-6,7	-10	-16,7	-30	13,3	-30	13,3
SOLAR +X	13	-28,47	-10	-38,47	-90	51,53	-90	51,53
SOLAR +X	14	-28,45	-10	-38,45	-90	51,55	-90	51,55
SOLAR -Z	20	-32,38	-10	-42,38	-90	47,62	-90	47,62
SOLAR +Z	30	-34,1	-10	-44,1	-90	45,9	-90	45,9
STRUCTURE -X	40	-10,72	-10	-20,72	-30	9,28	-30	9,28
STRUCTURE +Y	50	-11,02	-10	-21,02	-30	8,98	-30	8,98
STRUCTURE -Y	60	-12,68	-10	-22,68	-30	7,32	-30	7,32
STRUCTURE +Z OSR	70	-11,22	-10	-21,22	-30	8,78	-30	8,78
STRUCTURE +Z MLU	80	-11,33	-10	-21,33	-30	8,67	-30	8,67
STRUCTURE -Z	90	-14,59	-10	-24,59	-30	5,41	-30	5,41
STRUCTURE +X	100	-6,72	-10	-16,72	-30	13,28	-30	13,28
TMTCR PATCH +X	101	0	-10	-10	-100	90	-155	145
TMTCR PATCH +X	102	0	-10	-10	-100	90	-155	145
TMTCR PATCH +X	103	0	-10	-10	-100	90	-155	145
TMTCR PATCH +X	104	0	-10	-10	-100	90	-155	145
TMTCR PATCH +X	105	0	-10	-10	-100	90	-155	145
TMTCR PATCH +X	106	0	-10	-10	-100	90	-155	145
AMSAT BOX	107	-6,4	-10	-16,4	-40	23,6	-50	33,6
AMSAT BOX	108	-6,4	-10	-16,4	-40	23,6	-50	33,6
AMSAT BOX	109	-6,42	-10	-16,42	-40	23,58	-50	33,58
AMSAT BOX	110	-6,4	-10	-16,4	-40	23,6	-50	33,6
AMSAT BOX	111	-6,38	-10	-16,38	-40	23,62	-50	33,62
AMSAT BOX	112	-6,4	-10	-16,4	-40	23,6	-50	33,6
GYRO BOX	113	-2,58	-10	-12,58	-5	-7,58	-25	12,42
GYRO BOX	114	-2,7	-10	-12,7	-5	-7,7	-25	12,3
GYRO BOX	115	-5,48	-10	-15,48	-5	-10,48	-25	9,52
GYRO BOX	116	-2,7	-10	-12,7	-5	-7,7	-25	12,3
GYRO BOX	117	-2,1	-10	-12,1	-5	-7,1	-25	12,9
GYRO BOX	118	-2,58	-10	-12,58	-5	-7,58	-25	12,42
SOLAR -Z	200	-32,37	-10	-42,37	-90	47,63	-90	47,63
SOLAR +Z	300	-34,09	-10	-44,09	-90	45,91	-90	45,91
STRUCTURE -X	400	-10,7	-10	-20,7	-30	9,3	-30	9,3
TMTCR PATCH -X	401	-14,53	-10	-24,53	-100	75,47	-155	130,47
TMTCR PATCH -X	402	-14,54	-10	-24,54	-100	75,46	-155	130,46
TMTCR PATCH -X	403	-14,53	-10	-24,53	-100	75,47	-155	130,47
TMTCR PATCH -X	404	-14,53	-10	-24,53	-100	75,47	-155	130,47
TMTCR PATCH -X	405	-14,53	-10	-24,53	-100	75,47	-155	130,47
TMTCR PATCH -X	406	-14,53	-10	-24,53	-100	75,47	-155	130,47
OBDH	407	-3,46	-10	-13,46	-20	6,54	-35	21,54
OBDH	408	-3,46	-10	-13,46	-20	6,54	-35	21,54
OBDH	409	-2,22	-10	-12,22	-20	7,78	-35	22,78
OBDH	410	-3,47	-10	-13,47	-20	6,53	-35	21,53
OBDH	411	-10,1	-10	-20,1	-20	-0,1	-35	14,9
OBDH	412	-3,46	-10	-13,46	-20	6,54	-35	21,54
EPS PEB	413	-7	-10	-17	-20	3	-30	13
EPS PEB	414	-7,07	-10	-17,07	-20	2,93	-30	12,93
EPS PEB	415	-6,55	-10	-16,55	-20	3,45	-30	13,45
EPS PEB	416	-7,07	-10	-17,07	-20	2,93	-30	12,93
EPS PEB	417	-10,45	-10	-20,45	-20	-0,45	-30	9,55
EPS PEB	418	-7,02	-10	-17,02	-20	2,98	-30	12,98
STAR TRACKER INSIDE	419	-1,53	-10	-11,53	-20	8,47	-40	28,47
STAR TRACKER INSIDE	420	-1,53	-10	-11,53	-20	8,47	-40	28,47
STAR TRACKER INSIDE	421	-1,53	-10	-11,53	-20	8,47	-40	28,47
STAR TRACKER INSIDE	422	-1,53	-10	-11,53	-20	8,47	-40	28,47
STAR TRACKER INSIDE	423	-1,53	-10	-11,53	-20	8,47	-40	28,47
STAR TRACKER INSIDE	424	-1,53	-10	-11,53	-20	8,47	-40	28,47
STAR TRACKER OUTSIDE	425	-1,54	-10	-11,54	-20	8,46	-40	28,46
STRUCTURE +Y	500	-11	-10	-21	-30	9	-30	9
TMTCR PATCH +Y	501	-14,32	-10	-24,32	-100	75,68	-155	130,68
TMTCR PATCH +Y	502	-14,33	-10	-24,33	-100	75,67	-155	130,67
TMTCR PATCH +Y	503	-14,32	-10	-24,32	-100	75,68	-155	130,68
TMTCR PATCH +Y	504	-14,32	-10	-24,32	-100	75,68	-155	130,68
TMTCR PATCH +Y	505	-14,32	-10	-24,32	-100	75,68	-155	130,68
TMTCR PATCH +Y	506	-14,32	-10	-24,32	-100	75,68	-155	130,68
REACTION WHEEL	507	-10,99	-10	-20,99	-20	-0,99	-25	4,01
REACTION WHEEL	508	-10,99	-10	-20,99	-20	-0,99	-25	4,01
REACTION WHEEL	509	-10,99	-10	-20,99	-20	-0,99	-25	4,01
REACTION WHEEL	510	-10,99	-10	-20,99	-20	-0,99	-25	4,01
REACTION WHEEL	511	-10,99	-10	-20,99	-20	-0,99	-25	4,01
REACTION WHEEL	512	-10,98	-10	-20,98	-20	-0,98	-25	4,02
MAGNETO-TORQUER +Y	519	-10,98	-10	-20,98	-30	9,02	-40	19,02
UCAM	520	-10,97	-10	-20,97	-20	-0,97	-45	24,03
UCAM	521	-10,96	-10	-20,96	-20	-0,96	-45	24,04
UCAM	522	-10,97	-10	-20,97	-20	-0,97	-45	24,03
UCAM	523	-10,98	-10	-20,98	-20	-0,98	-45	24,02
UCAM	524	-10,97	-10	-20,97	-20	-0,97	-45	24,03
UCAM	525	-10,97	-10	-20,97	-20	-0,97	-45	24,03
STRUCTURE -Y	600	-12,66	-10	-22,66	-30	7,34	-30	7,34
TMTCR PATCH -Y	601	-15,36	-10	-25,36	-100	74,64	-155	129,64
TMTCR PATCH -Y	602	-15,36	-10	-25,36	-100	74,64	-155	129,64
TMTCR PATCH -Y	603	-15,36	-10	-25,36	-100	74,64	-155	129,64
TMTCR PATCH -Y	604	-15,36	-10	-25,36	-100	74,64	-155	129,64
TMTCR PATCH -Y	605	-15,36	-10	-25,36	-100	74,64	-155	129,64
TMTCR PATCH -Y	606	-15,36	-10	-25,36	-100	74,64	-155	129,64
REACTION WHEEL 1	607	-11,22	-10	-21,22	-20	-1,22	-25	3,78

Figure 6.49: Passive Operative Cold Case Results 1

Unit	Node Number	Min Calculated	Min Uncertainty	Min Predicted	Min Allowable Op	Min Margin Op	Min Allowable Fa	Min Margin Fa
COMPONENTS	ID	°C	°C	°C	°C	°C	°C	°C
REACTION WHEEL 1	608	-12,36	-10	-22,36	-20	-2,36	-25	2,64
REACTION WHEEL 1	609	-11,21	-10	-21,21	-20	-1,21	-25	3,79
REACTION WHEEL 1	610	-10,93	-10	-20,93	-20	-0,93	-25	4,07
REACTION WHEEL 1	611	-11,23	-10	-21,23	-20	-1,23	-25	3,77
REACTION WHEEL 1	612	-11,22	-10	-21,22	-20	-1,22	-25	3,78
REACTION WHEEL 2	613	-11,49	-10	-21,49	-20	-1,49	-25	3,51
REACTION WHEEL 2	614	-12,37	-10	-22,37	-20	-2,37	-25	2,63
REACTION WHEEL 2	615	-11,48	-10	-21,48	-20	-1,48	-25	3,52
REACTION WHEEL 2	616	-11,32	-10	-21,32	-20	-1,32	-25	3,68
REACTION WHEEL 2	617	-11,7	-10	-21,7	-20	-1,7	-25	3,3
REACTION WHEEL 2	618	-11,69	-10	-21,69	-20	-1,69	-25	3,31
REACTION WHEEL 3	619	-11,52	-10	-21,52	-20	-1,52	-25	3,48
REACTION WHEEL 3	620	-12,37	-10	-22,37	-20	-2,37	-25	2,63
REACTION WHEEL 3	621	-11,54	-10	-21,54	-20	-1,54	-25	3,46
REACTION WHEEL 3	622	-11,35	-10	-21,35	-20	-1,35	-25	3,65
REACTION WHEEL 3	623	-11,71	-10	-21,71	-20	-1,71	-25	3,29
REACTION WHEEL 3	624	-11,69	-10	-21,69	-20	-1,69	-25	3,31
REACTION WHEEL 4	625	-11,51	-10	-21,51	-20	-1,51	-25	3,49
REACTION WHEEL 4	626	-12,37	-10	-22,37	-20	-2,37	-25	2,63
REACTION WHEEL 4	627	-11,54	-10	-21,54	-20	-1,54	-25	3,46
REACTION WHEEL 4	628	-11,34	-10	-21,34	-20	-1,34	-25	3,66
REACTION WHEEL 4	629	-11,71	-10	-21,71	-20	-1,71	-25	3,29
REACTION WHEEL 4	630	-11,68	-10	-21,68	-20	-1,68	-25	3,32
MAGNETO-TORQUER -Y	631	-12,59	-10	-22,59	-30	7,41	-40	17,41
STRUCTURE +Z OSR	700	-11,2	-10	-21,2	-30	8,8	-30	8,8
TMTCR PATCH +Z	701	0	-10	-10	-100	90	-155	145
TMTCR PATCH +Z	702	0	-10	-10	-100	90	-155	145
TMTCR PATCH +Z	703	0	-10	-10	-100	90	-155	145
TMTCR PATCH +Z	704	0	-10	-10	-100	90	-155	145
TMTCR PATCH +Z	705	0	-10	-10	-100	90	-155	145
TMTCR PATCH +Z	706	0	-10	-10	-100	90	-155	145
TMTCR REDUNDANT	707	-11,18	-10	-21,18	-25	3,82	-35	13,82
TMTCR REDUNDANT	708	-10,52	-10	-20,52	-25	4,48	-35	14,48
TMTCR REDUNDANT	709	-10,56	-10	-20,56	-25	4,44	-35	14,44
TMTCR REDUNDANT	710	-10,52	-10	-20,52	-25	4,48	-35	14,48
TMTCR REDUNDANT	711	-10,57	-10	-20,57	-25	4,43	-35	14,43
TMTCR REDUNDANT	712	-10,53	-10	-20,53	-25	4,47	-35	14,47
MAGNETOMETER 1	713	-10,98	-10	-20,98	-20	-0,98	-40	19,02
MAGNETOMETER 1	714	-10,8	-10	-20,8	-20	-0,8	-40	19,2
MAGNETOMETER 1	715	-10,8	-10	-20,8	-20	-0,8	-40	19,2
MAGNETOMETER 1	716	-10,8	-10	-20,8	-20	-0,8	-40	19,2
MAGNETOMETER 1	717	-10,79	-10	-20,79	-20	-0,79	-40	19,21
MAGNETOMETER 1	718	-10,73	-10	-20,73	-20	-0,73	-40	19,27
MAGNETOMETER 2	719	-10,98	-10	-20,98	-20	-0,98	-40	19,02
MAGNETOMETER 2	720	-10,8	-10	-20,8	-20	-0,8	-40	19,2
MAGNETOMETER 2	721	-10,8	-10	-20,8	-20	-0,8	-40	19,2
MAGNETOMETER 2	722	-10,8	-10	-20,8	-20	-0,8	-40	19,2
MAGNETOMETER 2	723	-10,79	-10	-20,79	-20	-0,79	-40	19,21
MAGNETOMETER 2	724	-10,73	-10	-20,73	-20	-0,73	-40	19,27
LMP LCB	725	-11,13	-10	-21,13	-25	3,87	-45	23,87
LMP LCB	726	-11,05	-10	-21,05	-25	3,95	-45	23,95
LMP LCB	727	-11,05	-10	-21,05	-25	3,95	-45	23,95
LMP LCB	728	-11,05	-10	-21,05	-25	3,95	-45	23,95
LMP LCB	729	-11,05	-10	-21,05	-25	3,95	-45	23,95
LMP LCB	730	-11,03	-10	-21,03	-25	3,97	-45	23,97
TRITEL S	731	-11,14	-10	-21,14	-30	8,86	-40	18,86
TRITEL S	732	-11,07	-10	-21,07	-30	8,93	-40	18,93
TRITEL S	733	-11,07	-10	-21,07	-30	8,93	-40	18,93
TRITEL S	734	-11,07	-10	-21,07	-30	8,93	-40	18,93
TRITEL S	735	-11,07	-10	-21,07	-30	8,93	-40	18,93
TRITEL S	736	-11,03	-10	-21,03	-30	8,97	-40	18,97
MAGNETO-TORQUER -Z	737	-14,51	-10	-24,51	-30	5,49	-40	15,49
STRUCTURE +Z MLJ	800	-11,31	-10	-21,31	-30	8,69	-30	8,69
STRUCTURE -Z	900	-14,58	-10	-24,58	-30	5,42	-30	5,42
TMTCR PATCH -Z	901	-6,47	-10	-16,47	-100	83,53	-155	138,53
TMTCR PATCH -Z	902	-6,48	-10	-16,48	-100	83,52	-155	138,52
TMTCR PATCH -Z	903	-6,41	-10	-16,41	-100	83,59	-155	138,59
TMTCR PATCH -Z	904	-6,48	-10	-16,48	-100	83,52	-155	138,52
TMTCR PATCH -Z	905	-6,49	-10	-16,49	-100	83,51	-155	138,51
TMTCR PATCH -Z	906	-6,49	-10	-16,49	-100	83,51	-155	138,51
TMTCR BOX	907	-12,18	-10	-22,18	-25	2,82	-35	12,82
TMTCR BOX	908	-12,64	-10	-22,64	-25	2,36	-35	12,36
TMTCR BOX	909	-12,73	-10	-22,73	-25	2,27	-35	12,27
TMTCR BOX	910	-12,64	-10	-22,64	-25	2,36	-35	12,36
TMTCR BOX	911	-12,74	-10	-22,74	-25	2,26	-35	12,26
TMTCR BOX	912	-14,39	-10	-24,39	-25	0,61	-35	10,61
EPS BATTERY	913	-14,54	-10	-24,54	0	-24,54	-5	-19,54
EPS BATTERY	914	-14,58	-10	-24,58	0	-24,58	-5	-19,58
EPS BATTERY	915	-14,57	-10	-24,57	0	-24,57	-5	-19,57
EPS BATTERY	916	-14,57	-10	-24,57	0	-24,57	-5	-19,57
EPS BATTERY	917	-14,58	-10	-24,58	0	-24,58	-5	-19,58
EPS BATTERY	918	-14,55	-10	-24,55	0	-24,55	-5	-19,55
EPS BATTERY	919	-6,74	-10	-16,74	0	-16,74	-5	-11,74
EPS BATTERY	920	-6,74	-10	-16,74	0	-16,74	-5	-11,74
EPS BATTERY	921	-6,74	-10	-16,74	0	-16,74	-5	-11,74
EPS BATTERY	922	-6,74	-10	-16,74	0	-16,74	-5	-11,74
EPS BATTERY	923	-6,74	-10	-16,74	0	-16,74	-5	-11,74
EPS BATTERY	924	-6,74	-10	-16,74	0	-16,74	-5	-11,74

Figure 6.50: Passive Operative Cold Case Results 2

Throughout the old Phase-A and entire Phase-B design the thermal subsystem engineers tried to design the satellite in order to have a passive system. Unfortunately this solution was not possible due to the low temperature range of some components. In this passive operative analysis case as mentioned there are no problems regarding the maximum temperature range but unfortunately all components which suffered the extreme cold conditions in the previous two analyses also suffer in the passive operative case.

Let us analyze the various components during the 28 operative orbits in order to understand the entity and length of this range failure.

The components which most suffer the cold temperatures, as seen previously in the single mode analyses are the EPS batteries. The EPS batteries margined with a -5°C margin unfortunately are constantly under the allowable fail temperature and therefore are a big issue in ESEO's thermal control. The Gyro box instead stays inside the allowable fail temperature but does not satisfy the operative temperature when necessary. These two components are those who suffer the most due their very high minimum temperature limits. Analyzing the EPS graph its is very clear that a continuous active heater shall be necessary.

The reaction wheels only suffer slightly the cold and for a brief amount of time do not respect the minimum operative temperature limit. Unfortunately the reaction wheel are active during this time and therefore an increased error due to the temperature could lead to larger consequences which could lead to a failure. It can be clearly seen that the few orbits in the nadir pointing attitude heat the reaction wheels and then they slowly cool down.

Analyzing the residual components we can see that they do not respect their operative temperature limit by a small amount and in a limited amount of time. In this limited time most components are switched off and therefore seeing that their failure limits are respected these components do not create problems. For instance the ucam is only switched on when the satellite is in nadir pointing and this coincideds with its maximum temperature.

Having analyzed these results it becomes very clear that a heater must be modelled in order to satisfy the EPS batteries and gyro box. Considering that all negative

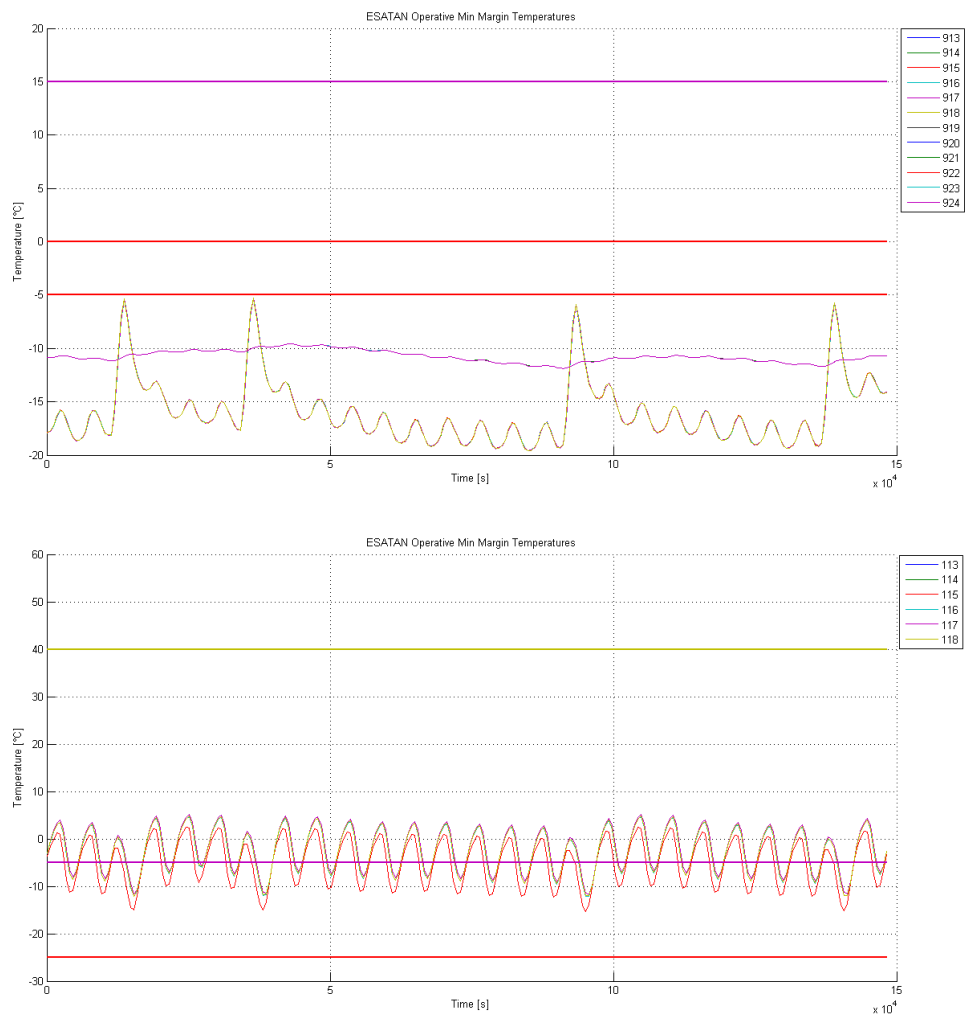


Figure 6.51: EPS Batteries (A) & Gyro Box (B) Heat Results

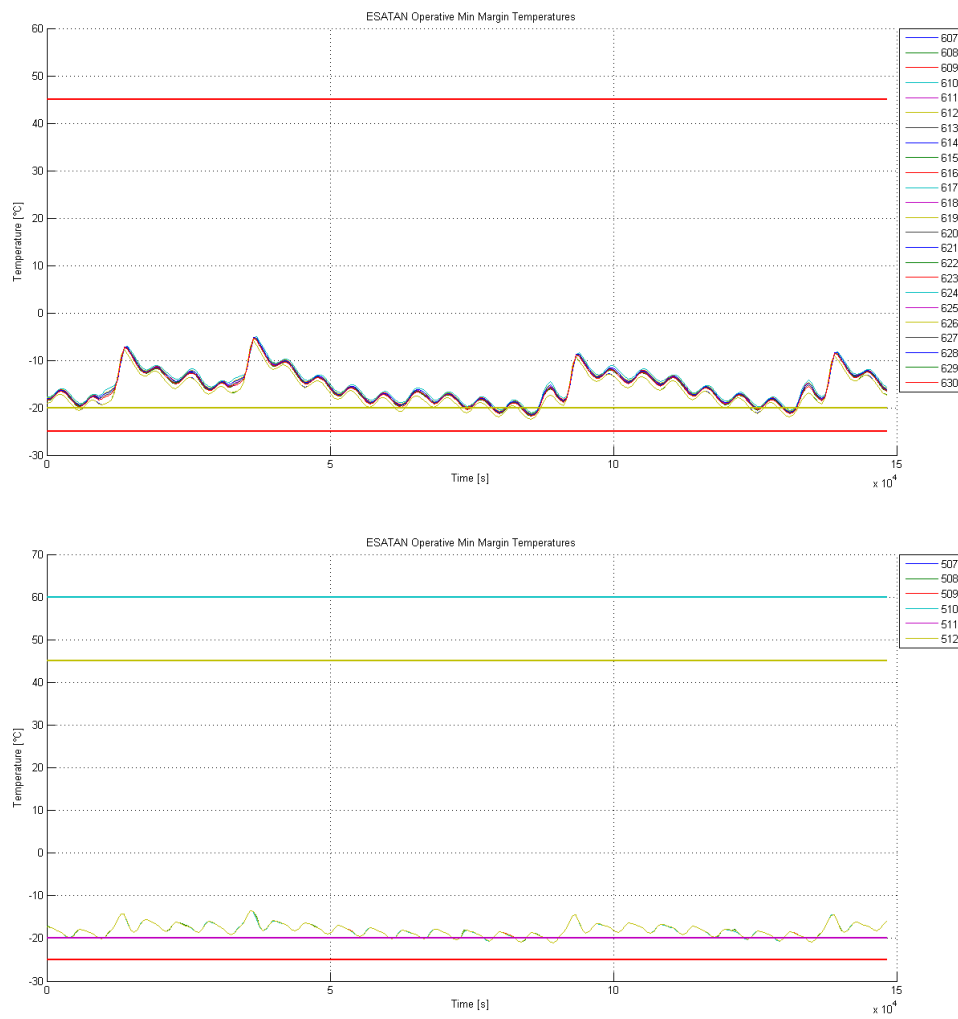


Figure 6.52: Reaction Wheels 1-4 (A) & Reaction Wheel +Y(B) Heat Results

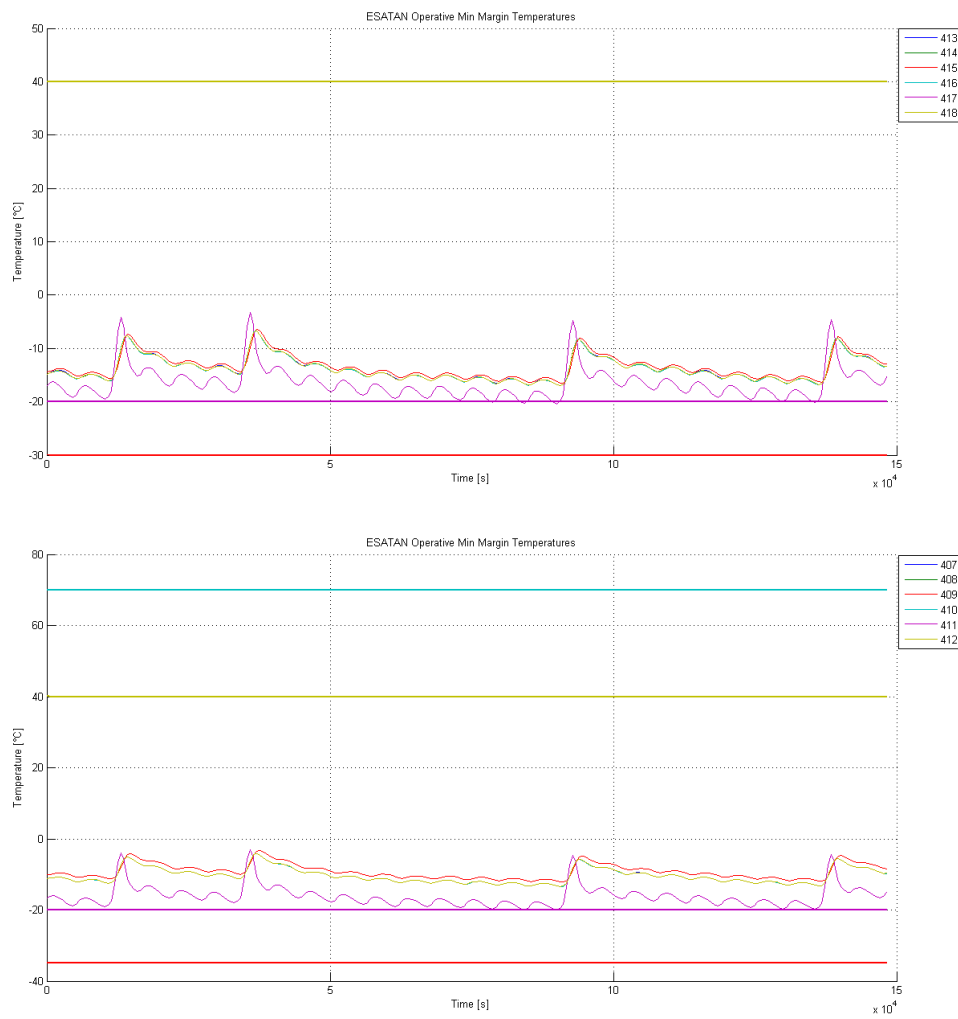


Figure 6.53: EPS PEB (A) & OBDH (B) Heat Results

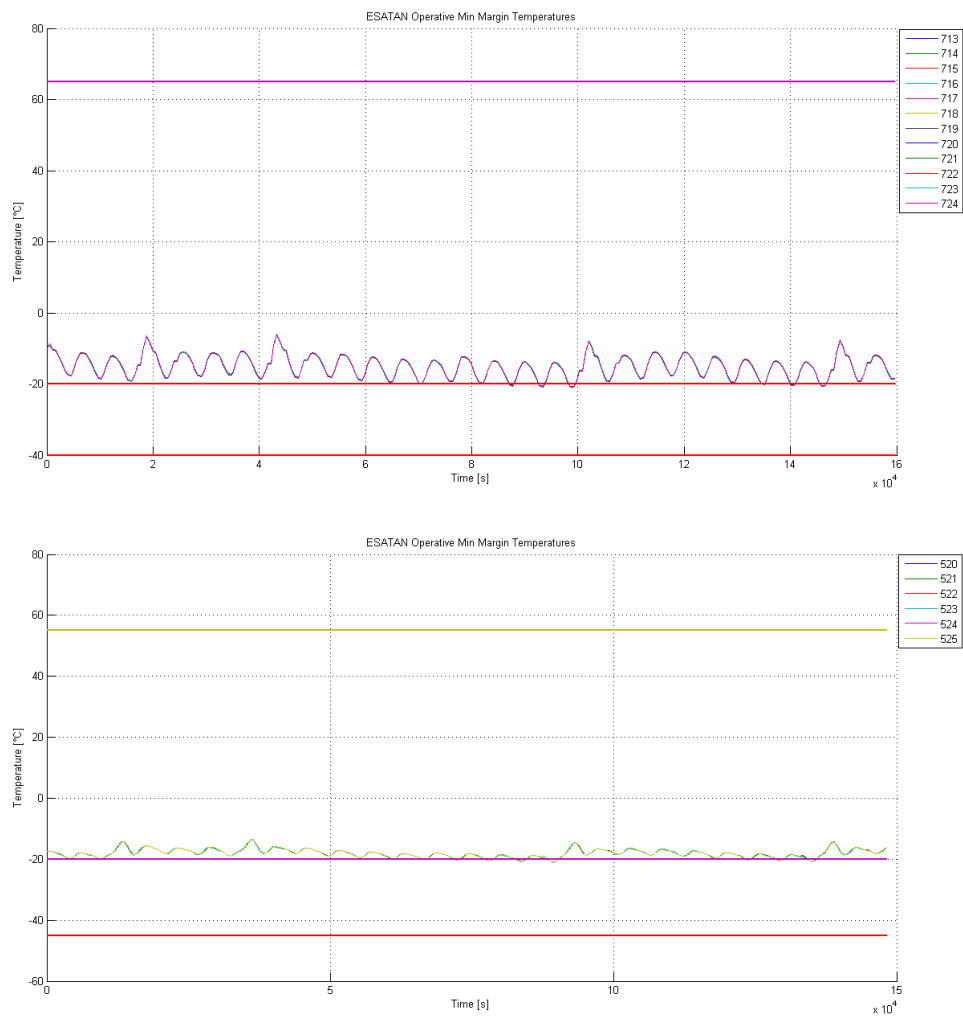


Figure 6.54: Magnetometer 1 & 2 (A) & Ucam (B) Heat Results

temperature peaks coincide one heater located close to the EPS batteries, in order to keep them inside their temperature ranges, could be sufficient to heat increase the temperature in those components which are very close to their margins.

4.3 Heater Modelling

Studying the previous passive analysis and iterating a the operative phase analysis case a heater was modelled. This heater was inserted inside the EPS batteries and was therefore considered as an extra dissipated power inside the EPS batteries. A heater usually works with a thermostat which switches on the heater if the temperature goes under a certain value and switches off the heater if the temperature rises above another thermal limit. The thermostat is useful in order not only to keep the temperature inside a minimum limit but also in order to avoid an excessive amount of power and make sure that due to the extra heat the component does not have a too high temperature increase which could lead to breaching the maximum temperature limit.

Unfortunately ESATAN does not have a thermostat option which introduces a certain dissipated heat only if a temperature limit is broken and therefore a heater had to be modelled manually. After a few iterations a heater was modelled with a nominal power of 30 W. A hypothetical time plot of the heater was calculated in order to analyze when the heater is switched off and led to the following results.

Analyzing the graph it is very clear that the heater unfortunately must almost constantly be on. Therefore the TCS will necessitate a large amount of power in order to keep ESEO inside its margins.

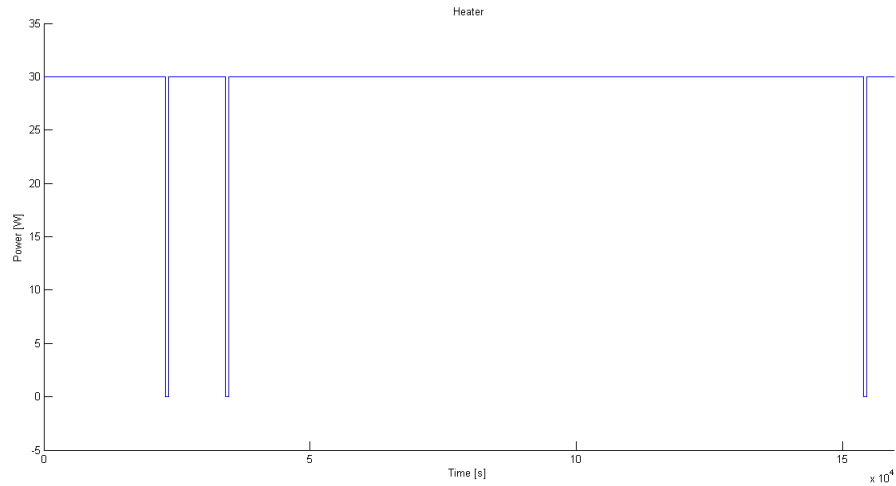


Figure 6.55: EPS Battery Heater

4.4 Active Thermal Results

Now that the heater has been modelled let us analyze the results obtained for those components which previously did not respect their temperature margins.

Having added a heater inside the EPS batteries brought the batteries inside the failure temperature range but not inside the operative temperature range. This is the EPS operative margin varies from 0°C to 15°C and considering a $\pm 5^{\circ}\text{C}$ margin the EPS batteries only have a 5°C range. Unfortunately the two attitude directions create a 10°C difference. Therefore considering the margins used and that the EPS batteries remain inside the failure margins the results can be considered acceptable but in further design phases and during thermal testing these components must be kept under attention.

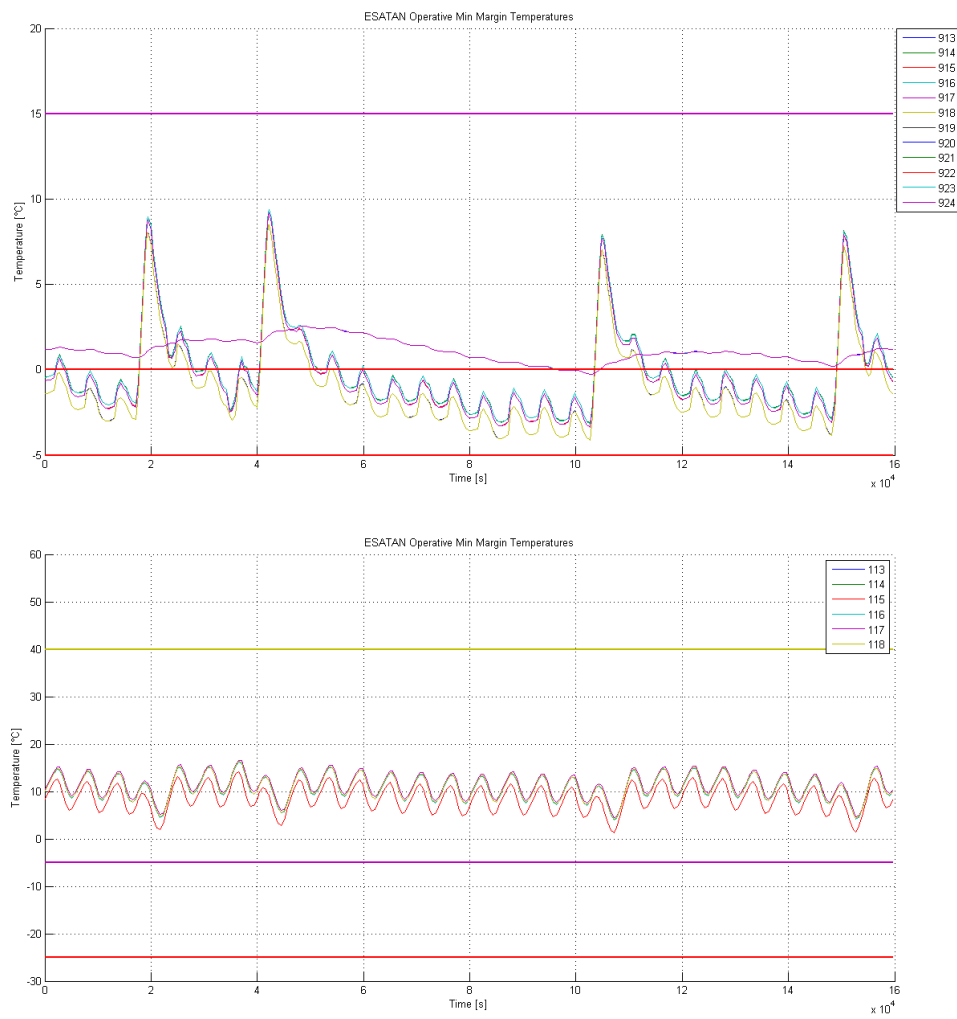


Figure 6.56: EPS Batteries (A) & Gyro Box (B) Heat Results

The heater inside the EPS batteries increases the median internal temperature of the satellite and therefore the temperature of all the other internal components slightly. This brings the gyro box back inside its operative thermal ranges.

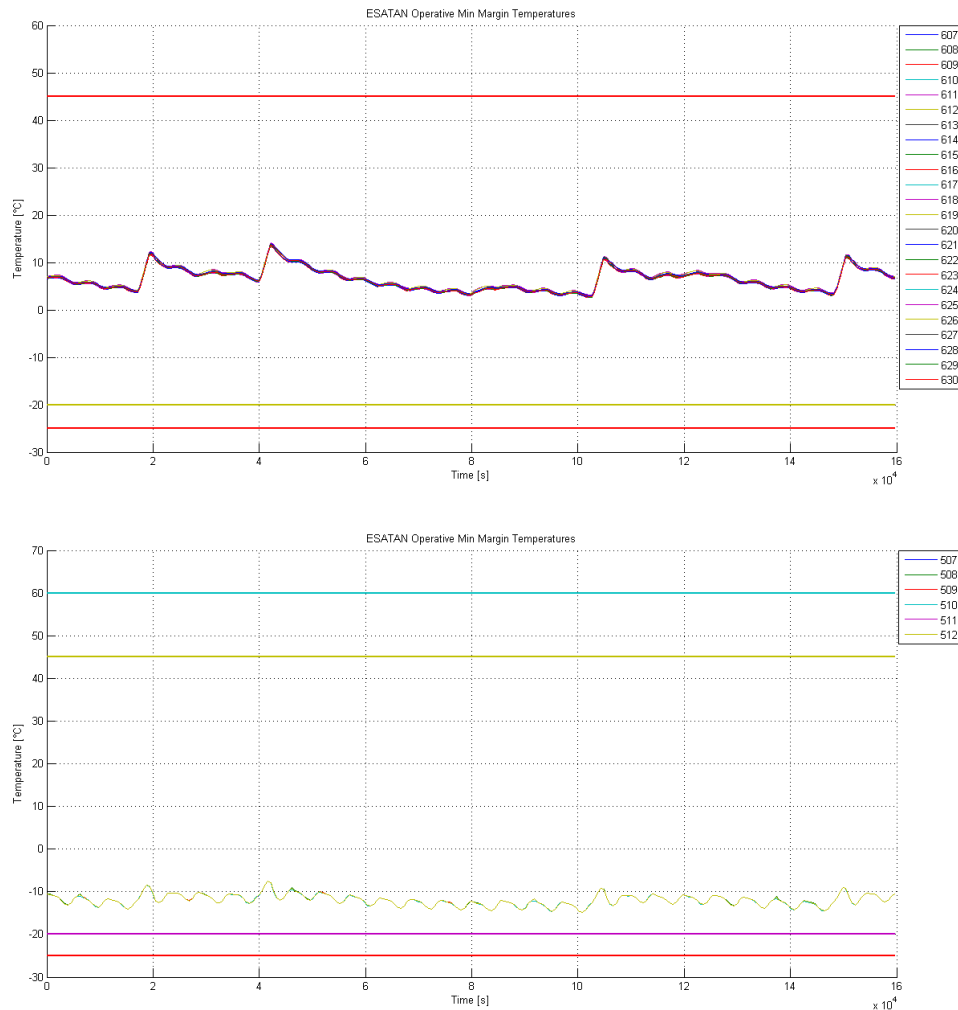


Figure 6.57: Reaction Wheels 1-4 (A) & Reaction Wheel +Y(B) Heat Results

Also the reaction wheels remain inside their operative margins together with all the other components which previously suffered the cold case. Even though the internal temperature of all components increases thank to the thermostat this does not significantly alter the maximum results of all the components.

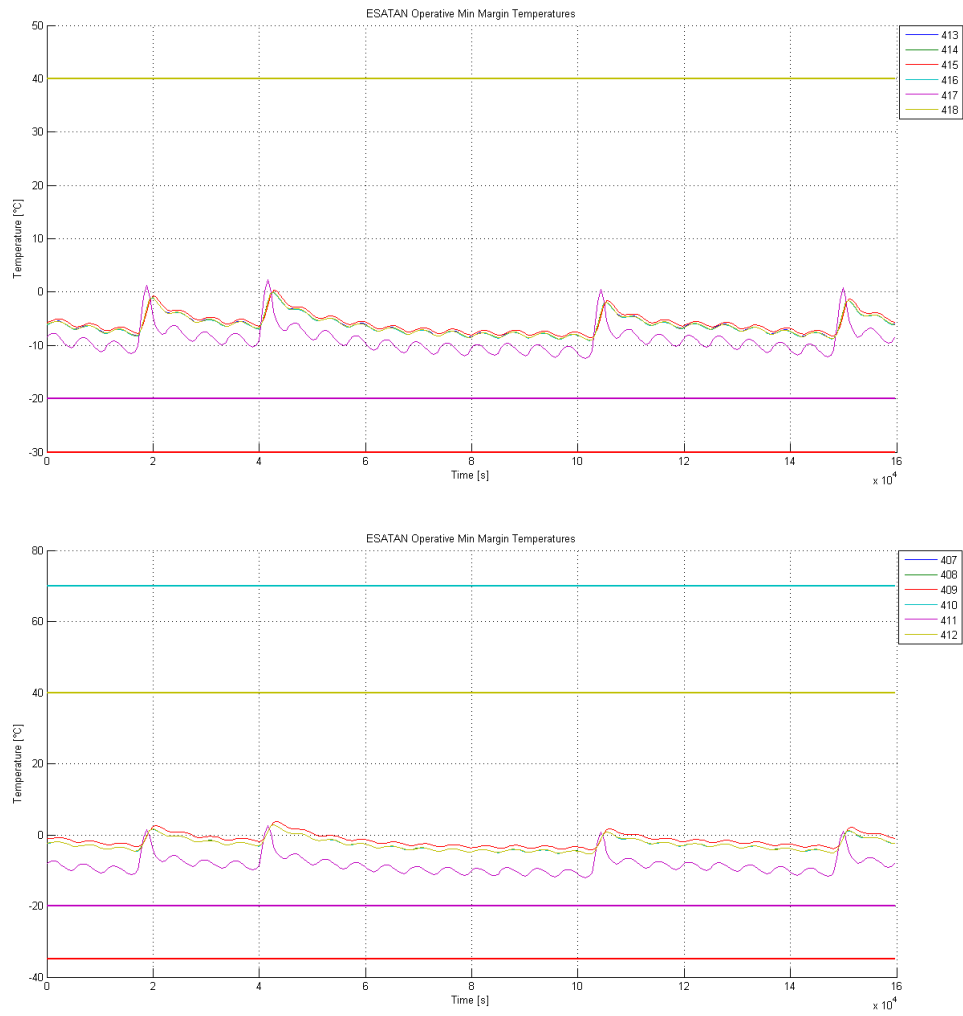


Figure 6.58: EPS PEB (A) & OBDH (B) Heat Results

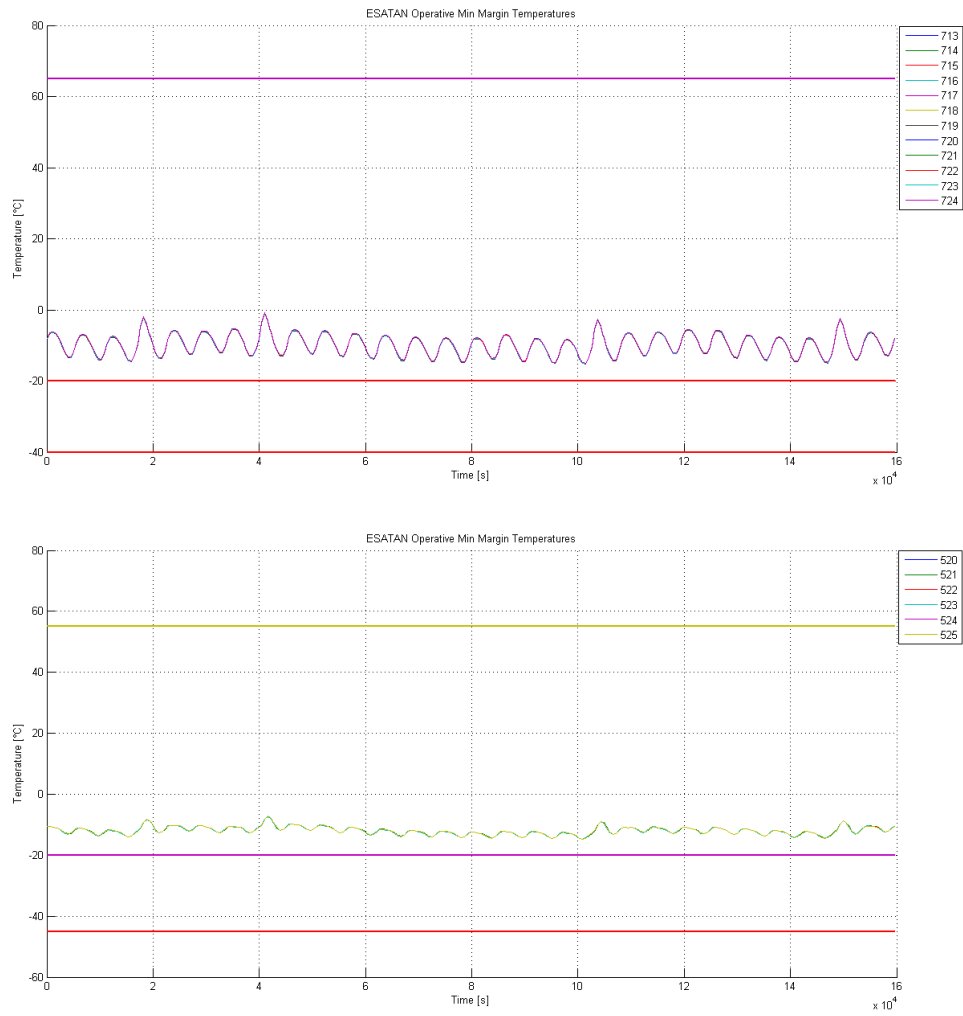


Figure 6.59: Magnetometer 1 & 2 (A) & Ucam (B) Heat Results

5 Margin Philosophy

All data used in previous models were nominal values of the various thermal characteristics of the model. Obviously these values are hypothetical and will never occur. Therefore in order to understand how the thermal subsystem results can vary two analyses were done. These two analyses consist in changing all thermal characteristics to 110 % and 90 % of their nominal value.

These two analyses are part of what is called the margin philosophy. In order to make sure that the thermal control system was not only designed to satisfy the nominal values of all thermal characteristics it is necessary to analyze how the TCS reacts to a variation of 10% to the thermal values. While analyzing all optical, thermal data each one had a intollerance which was well under 10 % but considering ECSS standards this value was kept as reference. It is obvious that the probability that all thermal and optical materials are at 110 % their nominal value is close to zero and therefore these margins should take into account all possibilities.

The characteristics which were margined are:

- Thermal Optical Values α, β
- Heater Power
- Component Heat Dissipations
- Conducitivity

Varying the thermal characteristics also is useful to understand how much the results vary based on these small variations and to get an idea of how stable the thermal control system is. In both analyses the active TCS model was margined and analyzed for the operative case, therefore in the 28 orbit configuration.

6 Margin Results

Obviously seeing that a precise margin philosophy is used the $\pm 5^{\circ}\text{C}$ margins are not necessary anymore. Instead we will have a variation of the temperature which will show the maximum temperature range that the components will most likely reach through their operative. Looking back on all previous analyses it can be noted that the lower temperature limit, the cold case, is that which most effects the TCS. The component which had the most problems in staying inside its temperature margins were the EPS batteries. It is therefore obvious that this component with the other components which suffered the cold case are the ones which must be reanalyzed. Analyzing therefore the 8 previous components which had problems with the cold case only the EPS batteries do not stay inside their operative temperature although they do stay inside their failure temperature range.

The three graphs below represent the thermal results of the EPS batteries for both nominal thermal values and margined thermal values.

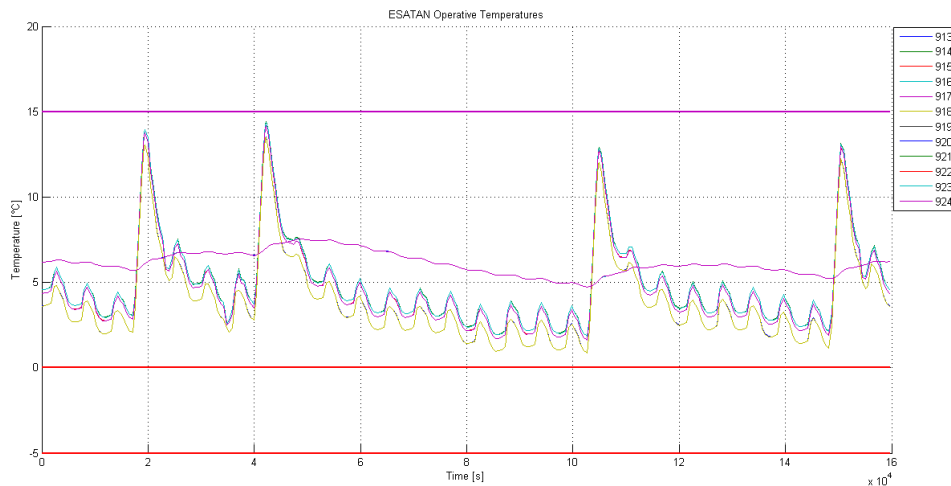


Figure 6.60: EPS Batteries Nominal Results

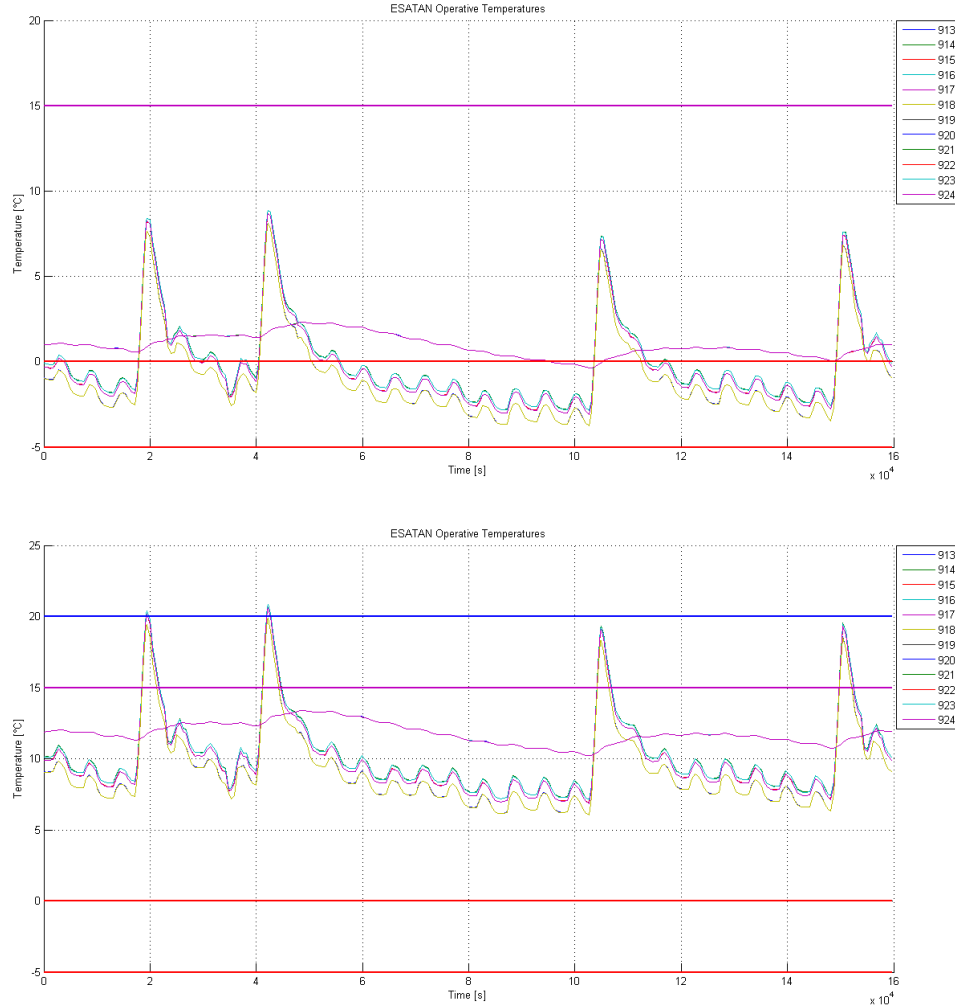


Figure 6.61: EPS Batteries 90% Margin (T) & 110% Margin (B) Results

The first graph shows that in case of nominal values the EPS batteries temperature remains inside the operative temperature margins. Analyzing the second graph representing the 90% margin case we note that this considers with a reduction in the temperature the EPS batteries register during their operative life. Comparing the -5°C margin graph of the EPS batteries previously used in the active analysis with the EPS results shown above it is very clear that the fixed margin previously used creates similar results compared to this new more accurate analysis. The third graph on the other hand refers to the 110% margin case which considers, opposite to the other lower margin, to

an increase in the median temperature of the EPS batteries. This is due to the fact that increasing the dissipated powers by 10% we have an excess heat which creates an increase in temperature.

There are two main causes which are responsible for the EPS batteries temperature exceeding the its limits. First up is the reduced temperature ranges the batteries have where the batteries unfortunately only have a 15-25°C range in which they can operate. The second cause results from the completely different thermal environments the satellite encounters in both Nadir & Sun Pointing. It is very clear that the Nadir-Pointing attitude (4 peaks) creates a large increase of temperature in the EPS batteries. The rotation to this new attitude unfortunately exposes the -Y structural panel to an increase in of heat flux from the sun. Unfortunately the EPS batteries are mounted on this structural panel and therefore an increase of temperature on the structural panel creates an increase of temperature for the EPS batteries.

7 Phase-A Minitan Results vs. Phase-B ESATAN Results

The initial Phase-A a design previously designed with MiniTAN due to the software's restrictions was composed of 50 thermal nodes. As explained previously MiniTAN is only a thermal solver and it does not calculate any thermal properties or the thermal fluxes which act on the system. In order to calculate the heat flux on all components a different software called SYSTEMA was used. The results obtained by this analysis are very similar to those obtained in the Phase-B model. Slight differences can be noted due to the different As an example here below are the results for the node 10 which corresponds to the +x structural panel.

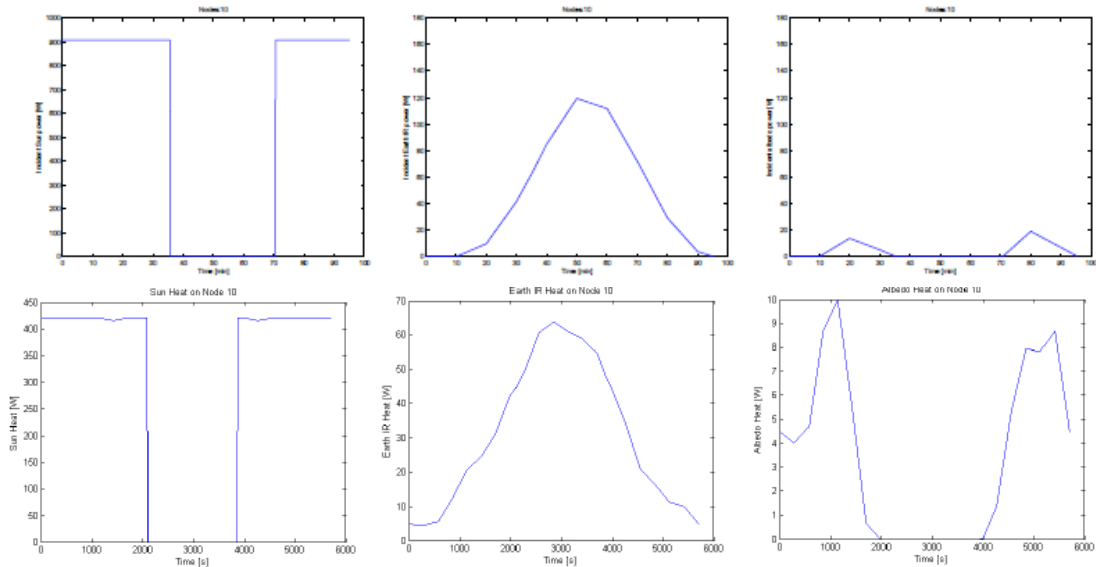


Figure 6.62: SYSTEMA(A) & ESATAN (B) NODE 10 Heat Flux Results

The similarity in results are not obtained for the thermal model. If we analyse the thermal results of the reduced MiniTAN model of the Phase-A design we can see that even though we have a cyclic temperature curve with a similar frequency the temperatures along the curve are very distant to the results obtained with ESATAN. The results obtained with MiniTAN and ESATAN of the +X Structural Panel, the EPS Batteries and the Reaction Wheels can be seen herebelow.

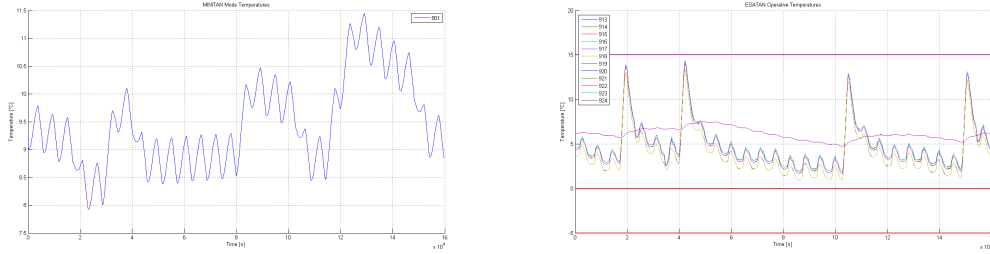


Figure 6.63: MiniTAN (A) & ESATAN (B) EPS Batteries Thermal Results

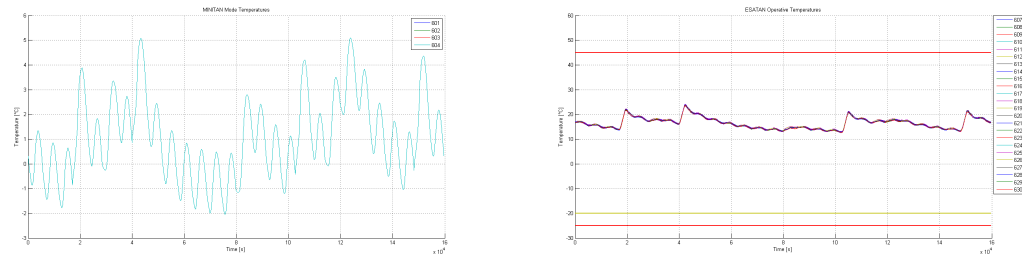


Figure 6.64: MiniTAN (A) & ESATAN (B) Reaction Wheel Thermal Results

In order to understand the difference in results the hypothesis assumed in the Phase-A design must be taken into consideration. In the results shown above used for the Phase-A design no internal radiative exchange was used. This therefore leads to the fact that hot components do not exchange heat by irradiation. This conservative hypothesis does not allow the satellite to balance its temperatures. Therefore the components attached to hot structural panels and which are more exposed to heat sources will have a higher temperature, because of conduction, while the components attached to cold panels not invested by heat sources will keep a low temperature due to the fact that their is no radiative heat exchange. This is why the structural panel has a higher temperature in the Phase-A design and the EPS Batteries have a lower temperature.

It is very clear that the Structural Panel which is subject to a lot of heat has a higher temperature in MiniTAN due to reduce heat exchagne, the EPS Battereis have a similar temperature due to the fact that they are on a reasonably exposed side of the satellite while the Reaction Wheels which are on cold side have a higher temperature in the Phase-B design in respect to the Phase-A design. Their must also be taken into account

that the Phase-B design has a significant rise in the median internal temperature due to the active thermal control subsystem which consists of heaters.

Chapter 7

Conclusions

The current model modelled with ESATAN is the endpoint of the Phase-B refinement design of the thermal control subsystem. The starting point of this model was a slim 50 node design with no internal radiative heat exchange modelled with MiniTAN. The new model increased the number of nodes to 176. By creating a geometrical representation of the satellite and using ESARAD to calculate all view factors the internal radiative heat exchange was calculated between all components and the external heat fluxes were recalculated, varified with the old model and optimized. The results obtained with the various analyses done on the thermal model brought to the conclusion that an active thermal subsystem must be used.

The active thermal model design was optimized in order to satisfy all components operative thermal ranges. These results were obtained for all components if we consider the nominal thermal characteristics. Unfortunately the data used and obtained from all the different datasheets were those relevant to the nominal value. Therefore in all initial analyses a $\pm 5^{\circ}C$ margin was used as ECSS standards suggest.

Once all preliminary analyses were done and a complete model was created the model was tested by using $\pm 10\%$ tollerance levels on all thermal characteristics such as thermo-optical data, conductivity, heat dissipations and heater power. This lead to margins which were amazingly similar to the ECSS standards proving their validity.

Analyzing every single component with these new margins lead to a model were all components remained inside their operative thermal ranges even when margined, except

for the EPS batteries. Analyzing these components closely it is clear that they have the least operative thermal range and are therefore the most sensible. Considering that the EPS batteries only have a 15°C operative temperature range from 0 to 15°C. It is therefore very important that this component shall be monitored the most during subsequent phases.

As mentioned before this model creation ends the Phase-B design of the ESEO satellite. The subsequent phase C/D is that of assembly, testing and validation of the entire satellite. The components and satellite model are created and tested in a laboratory in order to have experimental results which will be confronted with the modelled results. The satellite will be tested in a thermobaric chamber. In this phase therefore it will be necessary to see if the results obtained with the TCS ESATAN model are compatible with the experimental results.

The modelled results will never be identical to the experimental results due to various reasons. The first reason mentioned previously is due to the fact that the values used for the thermal model are nominal values but in obviously these values have a certain tolerance level. The other reason is due to the fact that using constant values for the thermal model does not take into account the fact that most thermal properties vary with the temperature and therefore not only were the values used defined for a reference temperature but they also vary with the temperature.

This difference between the results will have to be analyzed and based on this the experimental and mathematical model will be tweaked in order to have two similar results. In this way a full model will be created which truly represents how the satellite will react in real conditions. This new model will therefore be used to obtain results in the following thermal analyses. This thermal model will only be acceptable if the difference between the mathematical model and the experimental results less than average of 2°C with a standard deviation of 3°C.

Unfortunately due to budget issues the ESEO project ceased activity in June 2011 and this led to a stop in further projects. The C/D phase will not be brought forward.

Bibliography

- [1] Luca Canistro, *Progetto del sottosistema termico del satellite ESEO*.
Politecnico di Milano
- [2] David G. Gilmore, *Spacecraft Thermal Control Handbook, Volume I: Fundamental Technologies*.
The Aerospace Corporation Press El Segundo
- [3] John H. Lienard IV, John H. Lienard V *A Heat Transfer Textbook*.
Phlogiston Press, 3rd Edition, 2004
- [4] *ESATAN-TMS Workbench User Manual*.
ITP Engines UK Ltd. Whetstone, Leicester, UK 2009
- [5] *ESARAD User Manual: UM-ESARAD-024, Version 4.2*.
ALSTOM Power Technology Centre Whetstone, Leicester, UK 2001
- [6] John H. Henninger *Solar Absorptance and Thermal Emittance of Some Common Spacecraft Thermal-Control Coating*.
NASA Reference Publication 1121, 1984
- [7] *Spacecraft Thermal Control and Conductive Paints/Coatings and Services Catalog*.
AZ Technology, Inc., 7047 Old Madison Pike, Suite 300, Huntsville, AL 35806
<http://www.aztechnology.com/PDFs/materials-catalog.pdf>, 2008
- [8] *ESA Education - ESEO Mission*.
http://www.esa.int/esaMI/Education/SEM4DLPR4CF_0.html

[9] *HALA Thermally Conductive Gap Filler: TGF-C-SI.*

http://tuotteet.tibe.fi/documents/datasheets/HALA/EDBM_TGF-C-SI.pdf

[10] *Alfatec KERATHERM Thermal Materials.*

http://www.alfatec.de/fileadmin/Downloads/Kerafol/KERATHERM_interactive_guide_05_2010_english.pdf